МІНІСТЕРСТВО ОСВІТИ І НАУКИ УКРАЇНИ
ІВАНО-ФРАНКІВСЬКИЙ НАЦІОНАЛЬНИЙ
ТЕХНІЧНИЙ УНІВЕРСИТЕТ НАФТИ І ГАЗУ

РОЗВІДКА ТА РОЗРОБКА НАФТОВИХ І ГАЗОВИХ РОДОВИЩ

Науково-технічний журнал

Том 25, № 2
2025

ІВАНО-ФРАНКІВСЬК
2025

MINISTRY OF EDUCATION AND SCIENCE OF UKRAINE
IVANO-FRANKIVSK NATIONAL
TECHNICAL UNIVERSITY OF OIL AND GAS

PROSPECTING AND DEVELOPMENT OF OIL AND GAS FIELDS

Scientific and Technical Journal

Vol. 25, No. 2
2025

IVANO-FRANKIVSK
2025

ISSN 1993-9973
e-ISSN 2415-332X
УДК 622;550

Засновник та видавець:
Івано-Франківський національний технічний університет нафти і газу (ІФНТУНГ)

Рік заснування: 2001

Періодичність: двічі на рік

Ідентифікатор медіа: R30-01428
(Рішення Національної ради України з питань телебачення і радіомовлення № 3214,
протокол № 29 від 28 листопада 2024 року)

Журнал включено до категорії «Б» Переліку наукових фахових видань України
Технічні спеціальності: 133 – Галузеве машинобудування;
185 – Нафтогазова інженерія та технології
(Наказ Міністерства освіти і науки України № 1643 від 28 грудня 2019 року)
Геологічні спеціальності: 103 – Науки про землю
(Наказ Міністерства освіти і науки України № 409 від 17 березня 2020 року)

Журнал представлено в таких міжнародних наукометричних базах даних, репозитаріях та пошукових системах:
Національна бібліотека України імені В.І. Вернадського, Фахові видання України,
Crossref, Dimensions, Google Академія, German Union Catalogue of Serials (ZDB),
University of Oslo Library, Universitätsbibliothek Leipzig (UBL),
Open Ukrainian Citation Index (OUCI), Ulrichsweb Global Serials Directory, Litmaps

Адреса редакції:
Івано-Франківський національний технічний університет нафти і газу
76019, вул. Карпатська, 15, м. Івано-Франківськ, Україна
E-mail: nung@pdogf.com.ua
https://pdogf.com.ua/uk

ISSN 1993-9973
e-ISSN 2415-332X
UDC 622;550

Founder and publisher:
Ivano-Frankivsk National Technical University of Oil and Gas (IFNTUOG)

Year of foundation: 2001

Frequency: semi-annual

Media identifier: R30-01428
(Decision of the National Council of Television and Radio Broadcasting of Ukraine No. 3214,
Minutes No. 29 of November 28, 2024)

The journal is included in category "B"
of the List of scientific professional publications of Ukraine
Technical specialties: 0715 Mechanics and metal trades, 0716 Motor vehicles, ships and aircraft,
0724 Mining and extraction
(Order of the Ministry of Education and Science of Ukraine No. 1643 dated December 28, 2019)
Geological specialties: 0532 Earth sciences
(Order of the Ministry of Education and Science of Ukraine No. 409 dated March 17, 2020)

The journal is presented in the following international scientometric
databases, repositories and scientific systems:
Vernadsky National Library of Ukraine, Professional Publications of Ukraine,
Crossref, Dimensions, Google Scholar, German Union Catalogue of Serials (ZDB),
University of Oslo Library, Universitätsbibliothek Leipzig (UBL),
Open Ukrainian Citation Index (OUCI), Ulrichsweb Global Serials Directory, Litmaps

Editors office address:
Ivano-Frankivsk National Technical University of Oil and Gas
76019, 15 Karpatska Str., Ivano-Frankivsk, Ukraine
E-mail: nung@pdogf.com.ua
https://pdogf.com.ua/en

Редакційна колегія

Editorial Board

Зміст/Contents

О. Трубенко, Д. Федоришин, С. Федоришин
Можливості літолого-стратиграфічного розчленування геологічних розрізів
за даними спектрометрії природного гамма-випромінювання.....10
O. Trubenko, D. Fedoryshyn, S. Fedoryshyn
Possibilities of lithological and stratigraphic division of geological sections
based on natural gamma ray spectrometry 10

Н. Люта, Ю. Дорошенко, М. Пілецький
Про необхідність і доцільність перегляду та удосконалення методики розрахунку втрат
нафтопродуктів від випаровування за результатами розрахунково-порівняльного аналізу 22
N. Liuta, Yu. Doroshenko, M. Piletskyi
On the necessity and feasibility of revising and improving the methodology for calculating losses
of petroleum products from evaporation based on the results of calculation and comparative analysis 22

В. Харун, В. Попович, І. Петрик, З. Одосій
Кінематичний аналіз характеристик кривошипно-шківного верстата-гойдалки 36
V. Kharun, V. Popovych, I. Petryk, Z. Odosii
Kinematic analysis of the characteristics of a crank-pulley rocking machine 36

Ю. Волошин, В. Богославець, О. Марцинків, О. Куців, Б. Марцинків
До питання вибору оптимальних рецептур бурових розчинів в умовах HPHT обмежень 48
Yu. Voloshyn, V. Bohoslavets, O. Martsynkiv, O. Kutsiv, B. Martsynkiv
On the selection of optimal drilling fluid formulations under HPHT constraints 48

Ш. Ісмайлов, З. Мірзаєв, В. Іскендеров, Н. Ісмаїлов
Сучасні аналітичні методи оцінки технологічних показників у піщаних свердловинах 64
Sh. Ismayilov, Z. Mirzayev, V. Iskenderov, N. Ismayilov
Advanced analytical methods for evaluating technological indicators in sand-prone wells 64

ISSN 1993-9973, e-ISSN 2415-332X

Vol. 25, No. 2
2025

PROSPECTING AND DEVELOPMENT OF OIL AND GAS FIELDS

https://pdogf.com.ua/en

Received: 13.06.2025. Revised: 28.10.2025. Accepted: 08.12.2025. Published: 09.01.2026.

UDC 553.98.061.4

DOI: 10.63341/pdogf/2.2025.10

Possibilities of lithological and stratigraphic division of geological sections based on natural gamma ray spectrometry

Oleksandr Trubenko*

PhD in Geological Sciences, Dean
Ivano-Frankivsk National Technical University of Oil and Gas
76019, 15 Karpatska Str., Ivano-Frankivsk, Ukraine
https://orcid.org/0000-0003-3418-439X

Dmytro Fedoryshyn

Doctor of Geological Sciences, Professor
Ivano-Frankivsk National Technical University of Oil and Gas
76019, 15 Karpatska Str., Ivano-Frankivsk, Ukraine
https://orcid.org/0009-0004-5348-9564

Serhii Fedoryshyn

PhD in Geological Sciences, Associate Professor
Ivano-Frankivsk National Technical University of Oil and Gas
76019, 15 Karpatska Str., Ivano-Frankivsk, Ukraine
https://orcid.org/0009-0005-9274-7244

Abstract. Establishing the geological structure of complex sedimentary sections in oil- and gas-bearing areas of Ukraine, specifically their lithological and stratigraphic division, is quite challenging and often ambiguous when interpreting the sequence of sedimentary rock layers. The aim of the work was to study the possibility of lithological and stratigraphic division of a geological section based on the results of natural gamma-ray spectrometry in the interval of the boundaries between the Tournaisian and Visean deposits within the Plyskiv-Lysohorskyi outcrop of the crystalline basement of the Dnipro-Donets Basin. The methodology for studying the boundaries between the Tournaisian and Visean deposits was based on the results of the distribution of the concentration of radioactive isotopes of natural gamma radiation obtained directly during the drilling of exploration and prospecting wells. In addition, core material was taken from the Visean and Tournaisian stages of the Lower Carboniferous coal deposits, and its lithological and petrographic study was carried out by macroscopic description of core samples, preparation and description of thin sections, as well as X-ray structural and gamma-spectrometric analyses of the material composition of the sample collection. In general, the quantitative presence of natural radioactive elements was determined. Based on the results of these comprehensive geological and geophysical studies, it was established that the distribution of natural radioactive elements in the intervals of deposit occurrence depends on the lithological composition of the rocks and, accordingly, changes in the conditions of the sedimentation, which causes changes in the distribution of radioactive elements. Therefore, this particular feature of the structure can be used to trace the boundaries of lithotype distribution in horizons of different stratigraphic thicknesses. Considering that the radioactivity of polymictic rocks was characterised by a significant cumulative effect, and was caused by the increased radioactivity of the rock matrix skeleton and the clay material that fills the intergranular space. Therefore, it is advisable to determine clay content using gamma-ray spectrometry results based on the concentration of potassium-40 or gamma logging data. The introduction of such approaches not only facilitates the identification of boundaries between deposits but also enables the reconstruction of the physical and geological conditions under which the sedimentation of different lithotypes of rock was deposited

Keywords: lithotypes; reservoir; spectrometry; geological boundary; sedimentation

Suggested Citation: Trubenko, O., Fedoryshyn, D., & Fedoryshyn, S. (2025). Possibilities of lithological and stratigraphic division of geological sections based on natural gamma ray spectrometry. *Prospecting and Development of Oil and Gas Fields*, 25(2), 10-21. doi: 10.63341/pdogf/2.2025.10.

*Corresponding author

Introduction

The decline in hydrocarbon production from geological sections of exploration and appraisal structures was affected by both objective and subjective factors. One of these objective factors is the polymictic structure of terrigenous deposits in oil- and gas-bearing formations. Additionally, the reservoir rock matrix has a significant impact on the results of geophysical well logging (GWL). The study of such complex reservoir rocks using a standard GWL is difficult in some cases, particularly during the interpretation of gamma-ray logging (GR) and neutron methods. In most cases, when core material is available, the concentration of uranium, radium, thorium and potassium in rock is traditionally determined by chemical methods in laboratory conditions and usually in small volumes. Since chemical methods are labour-intensive and require significant costs and large amounts of chemical reagents, there is a need for alternative methods.

In particular, geophysical methods were proposed for determining radioactive elements in rock matrices, which allow for high-speed and unambiguous detection of radioactive elements, particularly uranium, thorium and potassium, in wells. In addition, spectrometry methods will allow the composition of complex structures to be determined in a lithological-stratigraphic section, and clayey and carbonate layers to be identified in intervals of polymictic coal deposits, followed by the selection of core material. Such studies contribute to the discovery of additional promising hydrocarbon accumulation sites within the Visean and Tournaisian deposits, which will make it possible to increase their reserves. In the process of oil exploration and development in the Dzhunhar basin, it was proposed to use natural gamma-ray spectral logging to assess reservoir productivity. It was the method of lithological identification of gamma-ray spectrometry that allowed for an increase in the accuracy of the distribution of formations along the geological section, to conduct an accurate interpretation of the formation lithology, and to assess the composition of the sedimentary environment.

The work of B. Shen *et al*. (2021) showed the possibility of using elemental logging in wells on the western edge of the Ordos Basin in the Changqing oil field and proved the presence of radioactive elements uranium, thorium, and potassium. The analysis of the principles of natural gamma ray and elemental logging measurement was performed to establish reference approaches for the separation of formations during drilling and to determine the formation lithology itself. In the article by W. Li *et al*. (2022), an approach was proposed for establishing the boundaries of sand reservoirs based on a created petrophysical distribution model with facies control. The model was created based on the volume of the sand body to identify excessively large sand bodies. This method allows to create a more realistic three-dimensional geological model of beach shoal sands in coastal areas. Their result shows that the property models better reflect the characteristics of the petrophysical distribution of the horizons only. A slightly different approach to lithology and reservoir identification was used by L. Xia *et al*. (2021), where a quantitative method was used to compare and distinguish a section with complex lithology in the Bohai Sea exploration area. The proposed method can realise the quantitative identification of reservoir lithology and effectively eliminate the deviations caused by many factors in lithology identification, thereby ensuring the accuracy of the separation of complex lithology sections.

The article by W. Wu *et al*. (2023) investigated the influence of Milankovitch cycles on sedimentation in fine-grained deep-water rocks of the lower Es3 subdivision of the FY1 well in the Dongying Basin (China). The authors identified stratigraphic cyclicity associated with precession and eccentricity using spectral analysis of geochemical and logging data. It was established that warm and humid climatic phases favoured the accumulation of organic matter, forming promising intervals for shale oil. In the work, the effectiveness of cyclostratigraphy for the accurate identification of productive zones in continental basins was confirmed. In the work of Q. Zhong *et al*. (2024), a reconstruction of the sedimentation process of fine-grained sedimentary rocks was carried out, studies were conducted that provide a benchmark for the classification of facies and characteristics of their distribution, and an assessment of optimal zones for shale oil reservoirs in graben lake basins was performed.

In the process of sedimentation, when sedimentation conditions change, radioactive elements are distributed, which is reflected in the pattern of changes in the mineral composition of rocks, as well as in the physical and geological conditions of their occurrence. The aim of the study was to substantiate and establish the possibility of using gamma spectrometry to assess the nature of the transition zone and trace the boundary between sediments on the example of the Visean and Tournaisian stages. Accordingly, the objective was to evaluate the possibility and informativeness of using natural gamma-ray spectrometry to establish the boundaries of the division between the Visean and Tournaisian deposits within the Plyskiv-Lysohorskyi outcrop of the crystalline basement of the Dnipro-Donetsk Basin axial zone.

Materials and Methods

Considering that the distribution of natural radioactive elements depends on the mineralogical composition of rocks and their physical and geological conditions during sedimentation, a study was conducted on the possibility of using gamma spectrometry to establish the transition zone and boundary between lithotypes using the example of the Visean and Tournaisian stages within the Plyskiv-Lysohorskyi outcrop of the crystalline basement (Fig. 1) of the Dnipro-Donets Basin.

The study of the geological structure and prospects for oil and gas content within the Plyskiv-Lysohorskyi outcrop is inextricably linked to oil and gas exploration in the northwestern part of the Dnipro-Donetsk Basin as a whole (Hrol & Lurie, 2021). The Plyskiv-Lysohorskyi outcrop of the crystalline basement extends along the

basin in a long ridge oriented latitudinally, measuring more than 50 km by 20 km (Lukin *et al.*, 2020). Its formation occurred under complex geological conditions, characterised by multidirectional movement of the basement blocks, which significantly influenced the development of the sedimentary complex (Lazaruk, 2012; Lazaruk, 2023). Within the Plyskiv-Lysohorskyi outcrop of the crystalline basement, the supersalt sedimentary complex almost completely inherits the tectonic structure of the crystalline basement. The Sofiika-Yaroshivka uplift zone can be traced here, within which there are separate Vasylivka, Sofiivka, Berezhivka, and Yaroshivka uplifts, and a whole series of small-amplitude closed and semi-closed domes can be distinguished.

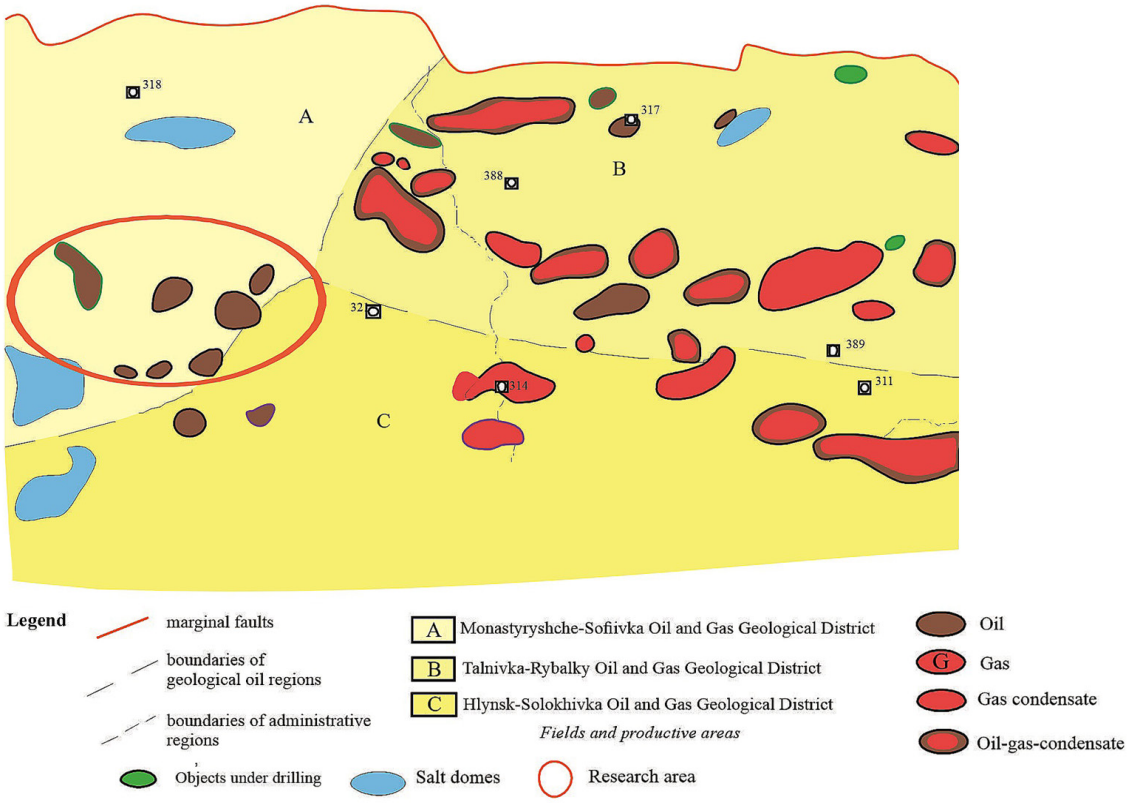

Figure 1. Overview map of the study area

Source: created by the authors with the use of M. Ivaniuta (1998)

To study the lithological and stratigraphic structure of wells drilled within the Plyskiv-Lysohorskyi outcrop of the crystalline basement, core material was taken from the Lower Visean and Tournaisian stages for lithological and petrographic studies, including a macroscopic description of samples, as well as preparation and description of thin sections (Bezrodna & Gozhyk, 2018), X-ray structural analysis of the material composition of the studied lithotypes (Danylchenko *et al.*, 2019), and evaluation of the results of gamma-spectrometric analysis (Vyzhva *et al.*, 2023) for the content of natural radioactive elements. A radiometric device, a spectrometer, was used to record radioactive emissions. It was used to study the spectral characteristics of radioactive radiation and determine the type and concentration of radionuclides (^{40}K, ^{235}U(Ra), ^{232}Th). The procedure for measuring instrumental spectra involves recording the number of pulses n during the exposure time t in the spectrometer channels and further calibration of its energy scale. The exposure time was selected taking into account the permissible pulse frequency error in the corresponding channels. During the interpretation of the obtained spectra, the radiation energy of charged particles and γ-quanta was determined by the position of the total absorption peaks on the energy scale, which is placed along the abscissa axis in accordance with the calibration data. It should be noted that in addition to the main lines of the source under study, secondary peaks may appear in the spectra, which arise as a result of side processes of interaction of radiation with the detector material and its shielding. In such cases, to accurately identify the peaks of total energy absorption, the spectrum under study was compared with the spectra of reference monoenergetic sources with similar energy characteristics (Vyzhva *et al.*, 2020).

To establish the transition zone between lithological rock types, GR and electrical methods were used. The GR method measured the intensity of radioactive radiation of rocks in wells using a γ-radiation indicator. Geiger-Muller counters or more efficient and modern scintillation counters were used as indicators. To determine the boundaries of the formation with an increased radioactive background with acceptable accuracy, we focused on the moment of the rise of the GR curve in the foot and its decline in the roof of

the formation boundaries. As for the electrical methods for determining the boundaries of formations and their thicknesses based on the apparent resistivity curves, they are based on the study of the distribution of artificial stationary and quasi-stationary electric fields in rocks. Typically, the resistivity of the environment surrounding a downhole device (probe) is determined by the observed values of the potential U, the potential difference ΔU, or the electric field strength E, created by a current source with a strength of I. To establish a relationship between the resistivity of the medium under study and the measured electric field characteristics (U, ΔU and E), the current strength I, and the geometric dimensions of the downhole probe, it was necessary to determine the potential value in the medium where the point source of current is located (Kurgansky & Tishayev, 2011).

The content of natural radioactive elements K, U(Ra), Th was determined within the collection of selected core material from the intervals of the Visean and Tournaisian deposits and compared with the data of GR and electrical methods. The lithological and petrophysical analysis focuses primarily on studying the lithological characteristics of rocks, as well as the physical and physicochemical processes that produce their physical properties, such as porosity, electrical conductivity, density, elasticity, etc. In addition, the analysis covers petrophysical parameters that describe the participation of rocks in geological and physical and chemical processes permeability, porosity coefficient, specific electrical resistance, elastic wave velocity, and others. In practice, the use of lithological and petrophysical methods makes it possible to divide rocks into strata, series and suites, to correlate simultaneously formed geological formations, and to identify promising areas for oil and gas exploration.

Results and Discussion

According to the results of the description of the thin sections, the lithological varieties of rocks had the following characteristics. Argillites could be divided into marly, red-coloured and chlorite-calcareous types according to the type of cement. The main part of the clayey material consisted of brown illite, sericite and sometimes hydrobiotite. The quartz content was 5-40%, quartzite – 5-20%, and chlorite – 1-3%. Alevrolitic argillite with remains of siliceous organisms was formed in a slightly acidic environment at shallow depths, where no coarse-grained material could reach. Alevrolitic argillite was carbonaceous, contained carbonised remains and was formed in coastal marshes. Monomictic sandstones consisted of well-sorted quartz fragments cemented by kaolinite, with rare calcite inclusions in the pores. This type of sandstone was mainly formed by semi-rounded fragments (75-85%) measuring 0.3-0.6 mm. Quartz predominated (60-63%), with quartzite (1-5%) and siliceous-clayey and sericite-clayey fragmental rock were also present. Fragments of orthoclase, oligoclase, occasionally colourless garnet, biotite and muscovite were noted. Polymict sandstones were mainly fine-grained, yellowish-greenish-grey in colour, and consisted of 80-85% fragmental material. The fragmentary material had the following composition: 25-50% quartz, other fragments were represented by quartzite, feldspar, as well as clayey-siliceous, quartzite-sericite, sericite-chlorite and clayey-sericite rock varieties. In addition, particles of orthoclase, oligoclase, albite, muscovite, biotite and chlorite were found in polymictic sandstones.

Rare were isolated grains of colourless garnet and zircon. Gravelites mainly consisted of fragments ranging in size from 3 to 8 mm (50-59%). The fragmental material was represented by limestones, marls, sandstones, siltstones and shales. Polymict gravelites consisted of fragments of quartz, quartzite, quartzite shale, chlorite argillites, limestones and, occasionally, fragments of effusive rocks. Limestones were grey with a pinkish tinge. The rock consisted mainly of calcite, dolomite, impurities of ferrous carbonate and a small amount of hematite-clay substance. As shown in Table 1, the distribution of radioactive elements in the rock types of the geological section within the Plyskiv-Lysohorskyi outcrop followed a general pattern, ranging from maximum values in argillites to minimum values in limestones, with a gradual change in siltstones and sandstones.

Table 1. Content of natural radioactive elements in the geological section of the Plyskiv-Lysohorskyi outcrop in the central part of the Dnipro-Donets Basin

Lithology	K, %	U(Ra), 10^{-4}%	Th, 10^{-4}%
Argillite	2.6-3.1	5.1-5.7	11.5-14.0
Siltstone	1.6-2.4	4.3-5.7	9.4-12.0
Monomictic sandstone	0.2-0.7	0.2-2.0	2.6-7.0
Polymict sandstone	2.5-2.7	2.7-3.7	5.0-8.6
Gravelite	0.6	1.3	2.1
Polymict gravelite	1.8	2.3	2.6
Siltite argillite	0.5-1.0	2.5-2.7	10.5-11.6
Carbonaceous silty argillite	0.3-0.68	4.7-6.5	16.5-25.7
Sandstone gravelly	0.2-0.4	1.5-1.6	4.5-14.0
Gravelite	0.2	0.7-0.8	5.0-5.6
Limestone	0.4-0.9	3.2-11.0	1.2-5.5

Source: developed by the authors

The content of radioactive elements (^{40}K, ^{235}U(Ra), ^{232}Th) did not vary depending on the structure of the geological section of the deposits. However, there was a significant difference between lithological types in terms of radioactive elements. Siltstone and carbonaceous argillites had significantly lower potassium content and higher U(Ra) and Th content compared to flinty argillite, which could be explained by the conditions of sedimentation, in particular, the transition from deep-sea to continental conditions of formation. The content of ^{40}K, ^{235}U(Ra), ^{232}Th in siltstones within different deposits of the outcrop had a similar concentration but lower values compared to argillites. In most cases, the radioactivity of sandstones varied depending on the mineralogical composition of the rock matrix and cement of the rock. Polymictic sandstones, due to the presence of feldspars and mica, were characterised by a significantly higher potassium content compared to ordinary sandstones. The content of ^{40}K, ^{235}U(Ra), and ^{232}Th in polymictic sandstones at different deposits remained almost unchanged. No significant differences in the content of radioactive elements were observed in gravel sandstones, gravelites and limestones. The only exception was limestones containing carbonaceous matter, which led to an increased content of ^{235}U(Ra).

Thus, lithological varieties of different mineralogical composition are distinguished by their content of naturally occurring radioactive elements. Changes in the distribution of radioactive elements ^{40}K, ^{235}U(Ra), and ^{232}Th mainly depended on the conditions of sedimentation, which made it possible to determine the transition zone and trace the boundary between stratigraphic horizons. Thus, the analysis and generalisation of lithological-stratigraphic varieties, particularly the aleurite-clayey strata, made it possible to characterise the section as comprising coarse-, medium-, and fine-laminated rocks with weakly developed rhythmicity, complicated by variable proportions of lithological types and the emergence of additional layers. It should be emphasised that these layers slightly disrupted the overall uniformity of the thickness; however, they did not constitute reference horizons (benchmarks) within the articulation zone of the identified strata.

In the examined lithological and stratigraphic section, no distinct boundary was identified between the Tournaisian and Visean strata (in particular, well-preserved basal conglomerates and other reference horizons, including angular unconformities). Consequently, the presence of various types of argillites made it difficult to visually subdivide the exposed thickness. In this context, the change in the lithological composition of the section was generally moderate, resulting from variations in the qualitative and quantitative characteristics of the rocks alongside significant changes in microrhythms. This was confirmed by experimental studies conducted on core samples obtained from the Tournaisian, transitional, and Visean rhythmites. The geological parameters obtained indicated small amplitudes of oscillatory movements and the gradual, impulsive development of transgressions and regressions induced by these movements (Iuras *et al.*, 2023). A considerable number of species of Tournaisian fauna were discovered in strata attributed to the Visean age. Given that floristic remains in submerged coastal areas rarely provided a reliable basis for age determination, the relative stability of the terrestrial biocenosis during transgressions facilitated the prolonged dispersion of such plant remains across different rock types (Stryzhak, 2021). This, in turn, further complicated the age determination of sedimentary rocks within thick geological sections of the Visean and Tournaisian deposits.

The upper part of the Tournaisian complex was characterised by several distinct mineralogical features. These included the widespread occurrence of kaolinite across various rock types, the formation of pyrite concretions of differing sizes and volumes, and the presence of rock layers containing siderite, other ferrous carbonates, and occasionally calcite. Lithologically, this interval exhibited a broad range of strata enriched with large carbonaceous plant remains, variegated layers with reddish and brownish hues indicative of oxidising environments typical of continental formations, and medium- to coarse-grained rocks (conglomerates, gravellite-like formations, gravels, and various sandstones) with quartz-kaolinite and quartz-carbonate-kaolinite cements, which defined the reservoir properties of the rocks. Additionally, layers of siliceous argillites and other siliceous formations were only sparsely distributed. These rocks typically exhibited elevated contents of radioactive elements adsorbed onto minerals such as kaolinite, iron hydroxides, and organic matter, as well as those localised in accessory minerals that enriched the weathering crust and its eroded products. Most of these rocks were defined by lenticular, cross-bedded, and coarse-bedded textures, as well as conglomeratic, regenerative structures, and features influencing the volumetric properties of lithotype porosity.

The lower part of the Visean complex was mineralogically distinguished by the widespread occurrence of cryptocrystalline chemogenic silica. This silica enriched various types of argillites, aleurolites, and other rocks, enhancing their strength and reducing porosity. Hydromica (and less commonly, montmorillonite) with elevated potassium content predominated, while kaolinite and kaolinite-bearing rocks played a subordinate role. Finely dispersed pyrite inclusions were common, and certain horizons showed enrichment in minerals such as sphalerite, barite, and chalcedony, suggesting episodic inflows of mineralised thermal waters into the basin. Horizons enriched in calcite were also noted. The aforementioned strata exhibited widespread accumulation of dispersed organic matter, fine carbonaceous detritus, rocks containing siliceous microfauna within silty argillites and siliceous argillites, and the presence of limestones and marls.

Most of the studied rocks were characterised by enrichment in radioactive potassium (^{40}K) and other elements, as well as by thinly laminated textures and conglomeratic, pelitic, and lepidoblastic structures (Selley, 2000). The transitional interval between the Tournaisian and Visean strata comprises interbedded sedimentary formations analogous

to the rocks of the corresponding stages. The principal lithological varieties identified in the geological section within the Plyskiv-Lysohorskyi outcrop, where the content of natural radioactive elements was determined, include: argillites; siliceous and carbonaceous argillite-aleurolites; aleurolites; monomictic and polymictic sandstones; gravelly sandstones; gravelites and polymictic gravelites; and limestones (Table 1). The concentrations of natural radioactive elements, such as potassium (K), uranium (U(Ra)), and thorium (Th), were measured using selected core material from both Visean and Tournaisian intervals and correlated with gamma-ray (GR) and electrical logging data.

Well 8. Core samples were taken from the interval 4,115-4,176 m. In the interval 4,130-4,160 m, the highest gamma activity recorded in the well interval was observed, averaging 20 μg/h, with gamma activity in thin interbeds reaching 40 μg/h. According to the results of lithological and petrophysical analysis, the rocks were mainly siltite-argillite. However, in the interval 4,115-4,132 m, siltite-argillite and siltstone with clay-siliceous cement of relatively deepwater origin were observed. In the lower part of the section, the siltite-argillite changes to fine-grained sandstone with organic matter residues. The content of radioactive elements varies within: K – 0.6-1.3%, U(Ra) – (2-3) × 10^{-4}%, Th – (8 - 12) × 10^{-4}%.

Below, in the interval 4,136-4,171 m, argillites and siltstones contained carbonised plant fragments and a significant amount of carbonised algae enriched with small and large crumbs. Accordingly, it could be assumed that they were formed in slightly acidic coastal shallow marsh conditions. The rocks were characterised by a low K content of 0.1-0.5%, an increase in U(Ra) of (10-15) – 10^{-4}%, and Th of (15-30) – 10^{-4}%. In the interval 4,171-4,176 m, colourful siltite-argillite changed into quartz and gravelly sandstones with kaolin-quartz cement. Content of radioactive elements: in variegated argillites: K – 0,1-0,6%, U(Ra) – 3 × 10^{-4}%, Th ~ (10-18) × 10^{-4}%. In sandstones and gravelly sandstones, the content of radioactive isotopes was respectively: K – 0.3%, U(Ra) – 1 × 10^{-4}%, Th – 5 × 10^{-4}%.

According to preliminary results, the boundary of the lithotype boundaries of the Tournaisian and Visean stages was predicted at a depth of 4,148 m. No changes in the recorded parameters were observed in this interval on the GR and SW curves (Fig. 1) or gamma-ray spectrometry. The transition from continental, coastal marsh, relatively shallow sedimentation conditions to deep-sea conditions (Lazaruk, 2022) can be traced by changes in the content of natural radioactive elements, namely, an increase in the content of radioactive potassium and a decrease in the content of U(Ra) and Th (Fig. 2).

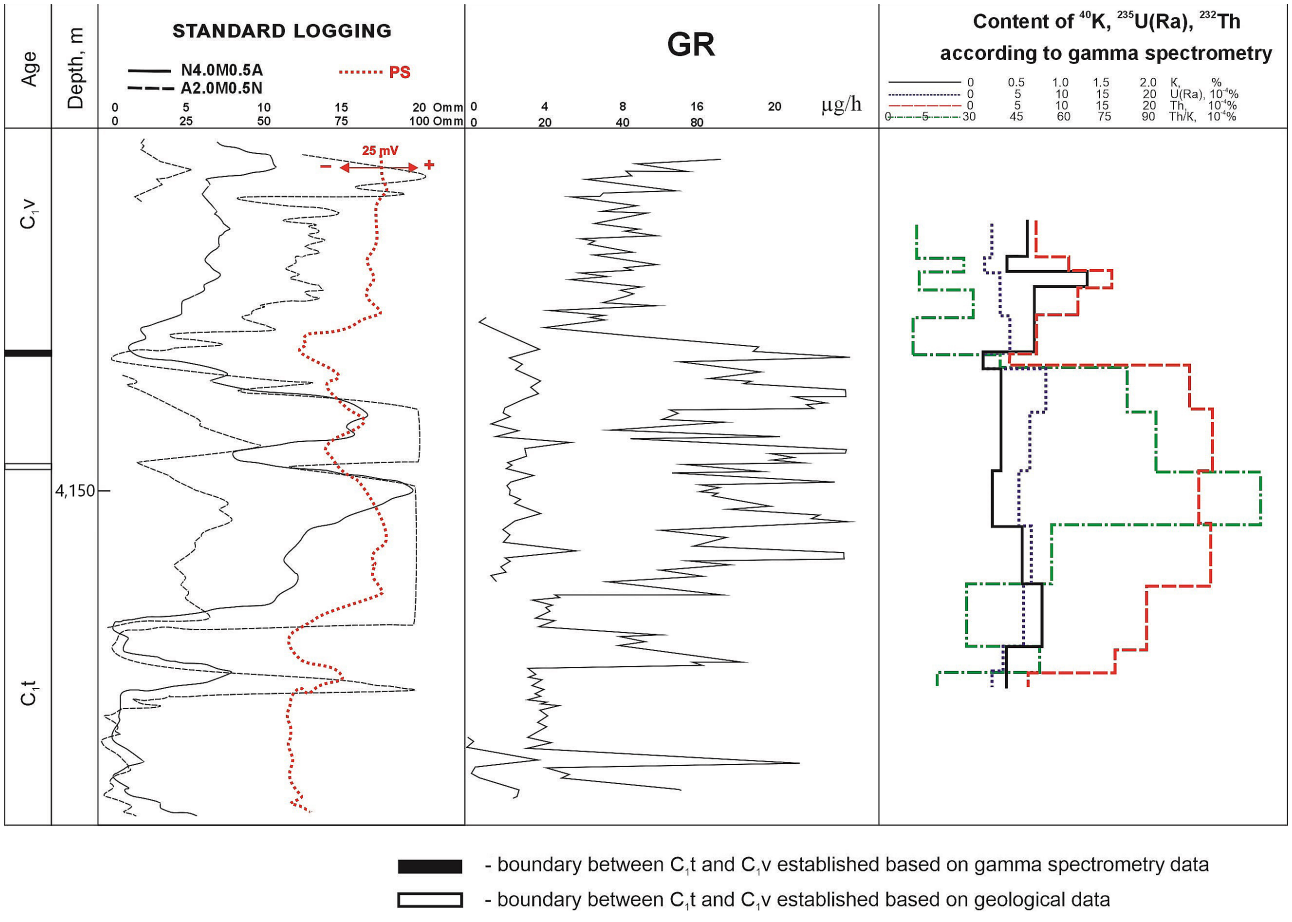

Figure 2. Well 8. The interval of exploration of depths 4,115-4,176 m

Source: made by the authors

The most informative parameter for studies of this type of rock was the relative value of Th/K. A sharp change in the value of this parameter was observed only at a depth of 4,136 m, which could already be attributed to the boundary between the Tournaisian and Visean deposits.

Well 4. The core was taken from the interval 4,041-4,100 m. As in the section of Well 8, the distribution of radioactive elements was caused by changes in the mineralogical composition of rocks and geochemical conditions of sedimentation processes. In the interval of 4,041-4,048 m, the rocks were represented by siltite-argillite with inclusions of isolated detrital fragments. They were characterised by a relatively high K content of (1-1.5)%, a decrease in U(Ra) of (2-4) to 10^{-4}%, and an increased content of siltstone containing carbon-emitting residues of various sizes, as well as small layers of carbonaceous siliceous argillite. The content of radioactive potassium decreased to 0.2-0.5%, U(Ra) and Th increased to (6-9) × 10^{-4}% and (27-30) × 10^{-4}%, respectively. Accordingly, these rocks were replaced by fine-grained sandstone with quartz kaolinite cement and small carbonised fragments with depth. The average content of radioactive potassium in the section was 0.2%, U(Ra) – 8 × 10^{-4}%, and Th – 30 × 10^{-4}%. In the interval 4,062-4,069 m, there was a multi-grained sandstone and gravel with quartz-alumina cement. The content of U(Ra) decreased sharply to 1.5 × 10^{-4}% and Th – 6 × 10^{-4}%.

At depths ranging from 4,069 m to 4,100 m, the sedimentation process was repeated. The upper interval of the lithological and stratigraphic section was represented by siltite-argillite with organic residues, while below it, there were colourful siltite-argillite, which sometimes contained hydrohematite impurities. Below the section, there are argillites, sometimes sandy siliceous, which turned into siltstone with quartz-clay cement enriched with scattered organic matter. These rocks were underlain by medium-grained and gravelly sandstone with kaolin-quartz cement and sulfide-quartz-barite cement. Accordingly, the content of radioactive elements in the above lithotypes was also changed. Thus, in the transition zone, there was a rhythmic nature of sedimentation processes. The transition from continental, coastal shallow-water sedimentation conditions to marine conditions was marked by an increase in the content of radioactive potassium, a sharp change in the Th/K ratio, which could be taken as the boundary of the transition from the Tournaisian to the Visean deposits (Fig. 3).

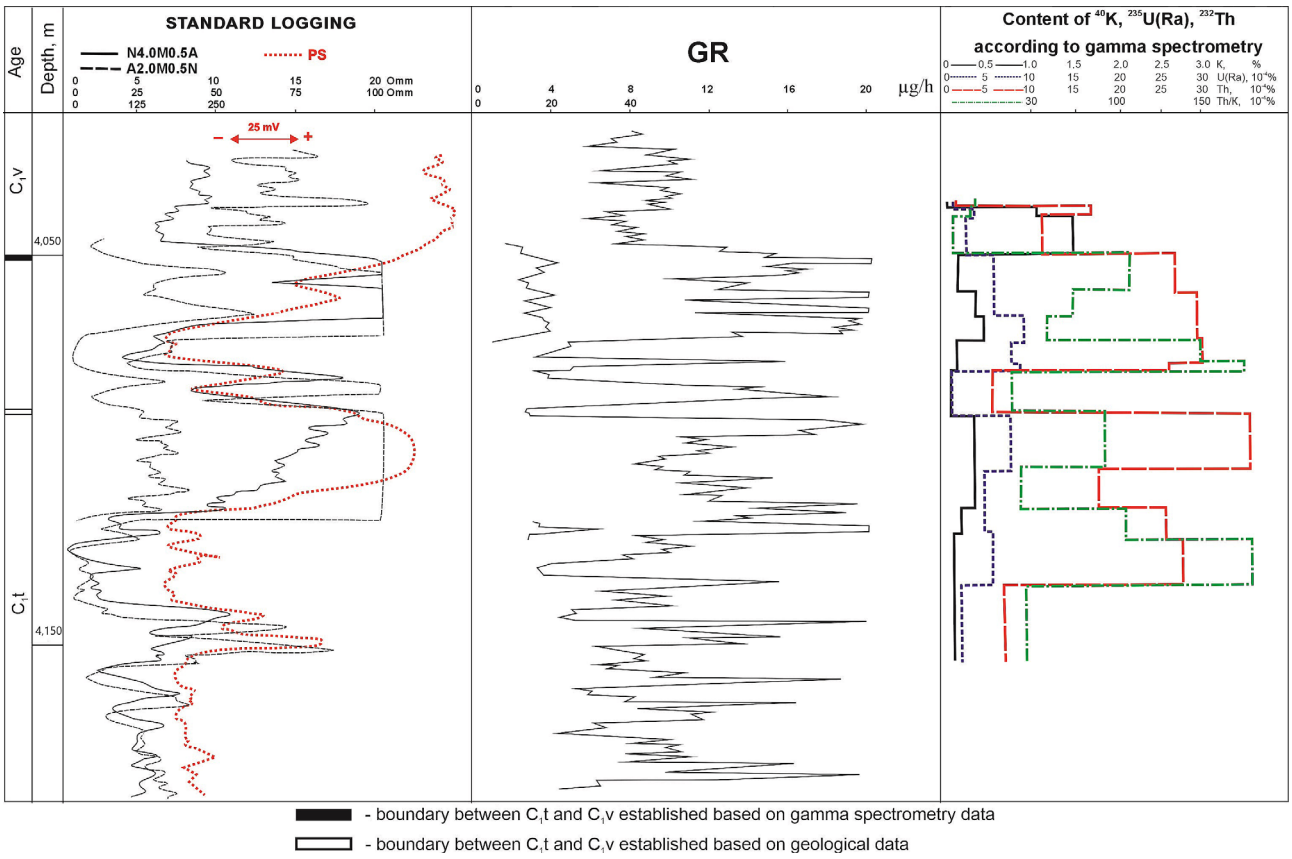

Figure 3. Well 4. The interval of exploration of depths 4,041-4,100 m

Source: made by the authors

Well 3. At depths of 4,759-4,767 m, the lithological and stratigraphic section consisted of siltite argillite with separate inclusions of carbonaceous material. Below, in the interval (4,767-4,770) m, there was silty-carbonaceous argillite with layers of limestone. The rock was characterised by average radioactivity values: K – 0.6-0.7%, U(Ra) –

(4-6) × 10^{-4}%, Th – (5-16) × 10^{-4}%. At depths of 4,919-4,936 m, the rock was represented by gravelly sandstones and gravelites with clayey-quartz kaolinite cement. They were characterised by a sharp decrease in potassium content – to (0.1-0.2)% and U(Ra) to 0.5 × 10^{-4}%, with an average thorium content of 9 × 10^{-4}% (Fig. 4). The change in lithological composition from coarse-grained gravelly sandstones to silty-clayey rocks with carbonaceous inclusions characterises the transitional thickness from Tournaisian to Visean deposits. The boundary between these layers was identified at a depth of 4,765 m and confirmed by a change in sedimentation conditions from marine and coastal to continental, which in turn was reflected in the distribution and abundance of natural radioactive elements.

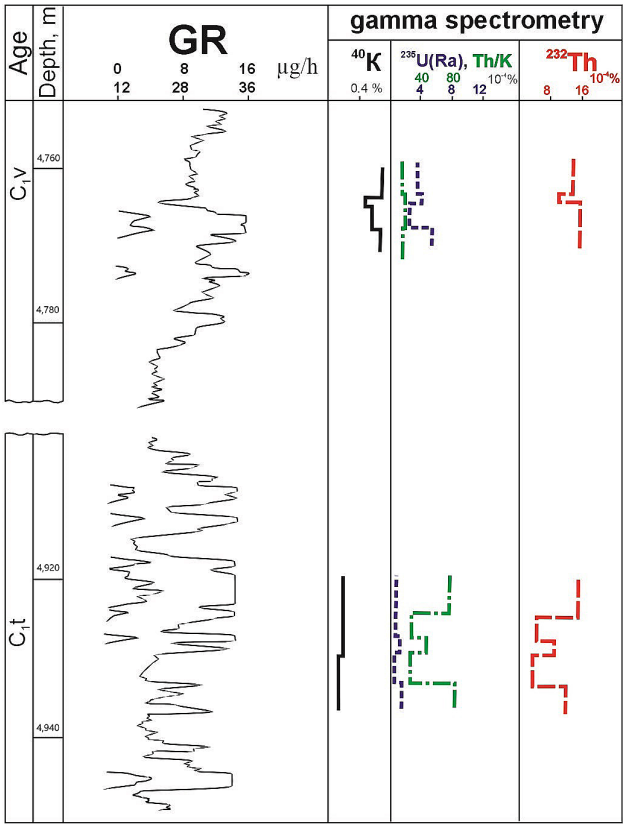

Figure 4. Well 3. The interval of exploration of depths 4,759-4,767 m

Source: made by the authors

Well 1. The rocks in the depth interval of 4,153-4,190 m were studied, with comparison of the results of the GR curve data and the distribution curves of K, U(Ra) and Th (Fig. 5). Comparing the radioactive parameter data, it was observed that the increased values of the GC method were characteristic of rocks in the depth interval of 4,117-4,212 m. No core was taken in the depth interval of 4,117-4,153 m. Starting from a depth of 4,153 m and down to 4,179 m, the rocks were represented by siltstone with some thin sandstone layers. These rocks were formed under marsh facies conditions, where the accumulation of organic matter sharply decreased due to the inflow of sandy-siltstone material from the shore. Below this section, gravelly sandstones with quartz-kaolinite cement were observed, which transitioned into gravels. The analysis of the K, U(Ra), and Th distribution curves and the GC diagram showed that the most abrupt change in sedimentation conditions occurred at a depth of 4,117 m. Below this level was a transitional rock stratum from the Visean to the Tournaisian deposits.

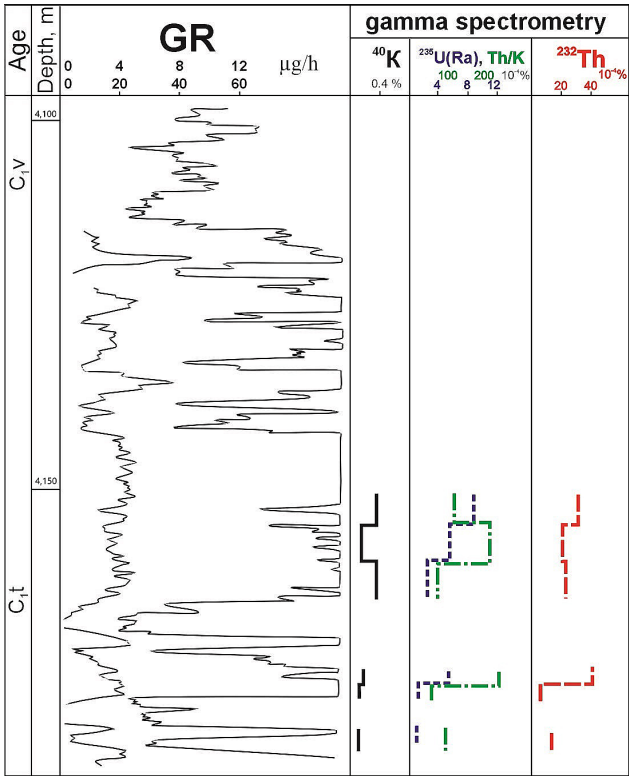

Figure 5. Well 1. The interval of exploration of depths 4,153-4,190 m

Source: made by the authors

Based on the fact that the Tournaisian rocks in the studied well sections within Plyskiv-Lysohorskyi outcrop were subcontinental and shallow, and the Visean rocks were marine, the boundaries between those stages could be taken by any coarse clastic rocks, any coarse fragmentary rocks that corresponded to short-term stages of intense erosion and faulting during tectonic impulses, the cover of the upper, light, gravelly or other sandstone in the Tuorniasian sequence that had kaolinite or quartz-kaolinite cement, indicating that the rocks were formed near the coastline separating the continent and the sea, the top of the upper red or variegated layer in the Tournaisian Formation marked the last shallowing, which led to the formation of rocks in an oxygenated (continental) environment, the top of the last upper Tournaisian layer of coal-bearing rocks (argillites rich in large carbonised plant remains, which were witnesses of the last bog regime, as well as by a geochemical parameter that indirectly characterised the predominantly acidic and alkaline conditions of sedimentation and separated strata formed in a substantially acidic

environment during the subcontinental period of the Tournaisian. It was distinguished from strata formed in a substantially alkaline marine environment of the early Visean. According to the above, such a feature was the content of natural radioactive elements (K, U(Ra), Th), which were determined and confirmed in rock samples from wells within the Plyskiv-Lysohorskyi outcrop.

Thus, by comparing the absolute values of natural radioactive elements, the upper limit of the subcontinental and continental acidic regime of sedimentation of siltstone and clayey rocks was traced, and significantly overlapped by marine rocks accumulated under alkaline conditions. Each of the above conventional indicators reflected a specific geological and stratigraphic process, and therefore naturally had a different stratigraphic position (Fedak & Koval, 2020). The difference in the location of these geological levels determined the thickness of the transitional unit that arose from the change in sedimentation regimes. Practical calculations and comparison with the descriptions of the grinds showed the effectiveness of the method proposed by the authors for diagnosing only polymictic sandstones. The actual discrepancy of the stratigraphic position of the boundary in terms of physical parameters depended on the amplitude of tectonic oscillatory movements in each specific structure (Vysochanskiy *et al*., 2022). The overall tectonic activity of the area, starting from the duration of the dominance of shallow and coastal sedimentation conditions, persisted until the continental regime was replaced by the marine regime (Stryzhak *et al*., 2020). The comparative position of the stratigraphic boundary of the Visean and Tournaisian stages within the Plyskiv-Lysohorskyi outcrop is shown in Table 2.

Table 2. The position of the stratigraphic boundary between the Visean and Tournaisian stages of the Pliskivsko-Lysogorsk protrusion in the central part of the Dnipro-Donets Basin

Well	Location of the boundary between the Visean and Tournaisian stages by depth, m				
	According to the logging data	According to the upper boundary of the coal bed	According to the upper boundary of the mottled rock	According to the clastic rock with kaolin	According to radiometry data
Well 8	4,148	4,135	4,150	4,132 sandstone	4,125
Well 4	4,070	4,058	4,080	4,060	4,050
Well 3	4,765	4,759	-	4,765 breccia	4,765
Well 1	4,162	4,153	-	4,157	4,120

Source: made by the authors

Each of these stratigraphic boundaries was legitimate. However, given the high relevance of the geochemical parameter, it was recommended to accept the boundary of the Visean and Tournaisian stages at depths where there was a sharp change in the content of natural radioactive elements, in particular radioactive potassium, as well as the Th/K ratio. Determining the thickness of the transition layer between stratigraphic horizons was also of great practical interest (Streltsova & Kruhlyk, 2020). Based on the patterns of tectonic movements, it was possible to predict the predominant nature of these movements at different stages of their development. In particular, a regularity was identified that the thicker the thickness of rocks formed during the change from a continental to a marine regime, the more reservoir rocks could be observed in the geological section.

The advantages of using GR in combination with conventional electrical logging techniques for predicting fractured zones in foundation rocks were discussed in the work of E.O. Amartey *et al*. (2016). The authors noted that gamma logging significantly improved the accuracy of identifying zones characterised by specific resistivity minima, which could also be caused solely by lithological factors. According to L. Ke *et al*. (2023), the study of continental deltaic deposits characterised by strong lateral heterogeneity, while identifying the boundaries of such reservoirs, was complicated by rapid changes in rock properties. Accordingly, the authors proposed a new workflow for the integrated study of 3D geomodelling of thin-layered reservoirs. This procedure demonstrated good ability to characterise thin interstitial reservoirs only in continental deltaic deposits.

Researcher L. Yemets (2024), based on the results of geological and technological studies using the Komyshnianske gas condensate field as an example, demonstrated the possibilities of rapid lithological and stratigraphic sectioning, identification of reference horizons, determination of the nature of reservoir saturation, and determination of hydrodynamic and technological characteristics of reservoirs for testing facilities. All of this allowed obtaining data on the well section, performing correlation, determining the required completion depth, identifying reference horizons by cuttings, assessing the hydrocarbon saturation of reservoir formations, formation pressures, and selecting the perforation interval. However, in conditions of limited information, complex geological structure and the absence of a complete set of logging studies, additional studies are mandatory.

According to V.B. Volovetskyi *et al*. (2024), an information and software system was developed for the operational analysis of geophysical logging data from underground gas storage wells. The developed information and software systems were used to accumulate, verify, correct and analyse geological and geophysical information. The data from the developed databases were used to automate the process of creating graphical geological materials for each well and for the underground gas storage facility (UGSF) as a whole.

The purpose of the systems was to provide an automated solution for various geological and technological tasks: systematisation, accumulation, processing of information, and its graphical and documented display. The developed information and software complex allows displaying the results of lithological analysis of geological sections of wells and correlation of these sections of UGSF wells. However, this complex required a large amount of initial information. The possibilities of using spectral GR to solve the problems of sequence stratigraphy were discussed in D. Šimíček & O. Bábek (2015), where they studied siliciclastic rocks showing moderately high total radioactivity and average concentrations of K, U and Th. Heavy minerals were predominantly U and Th and therefore tent to be concentrated in argillites and sandy-muddy facies, while sandstone and conglomerate facies had slightly higher K levels due to higher content of K-feldspars and mica.

Researcher S. Machulina (2022) noted that methodological approaches to detecting hidden cycling in carbonate deposits were based on a comprehensive analysis of the results of geophysical surveys of wells and laboratory studies of the core samples collected using a cable core sampler. For example, in terrigenous deposits, where cyclicity was manifested mainly through gradual changes in the grain composition of rocks, lithological, mineralogical, petrographic and facies-geotectonic methods were used to identify sedimentary cycles (cyclites). In contrast, in thick terrigenous-carbonate and carbonate strata, discrete boundaries between cycles were usually fixed by thin layers of clayey rocks or brecciated limestone with inclusions of other rocks. Such horizons were valuable references for correlation between wells. The most reliable identification of large sedimentation cycles in carbonate deposits was provided by data from geophysical methods of well logging, including radioactive, acoustic and electrical.

From the above approaches, it is clear that each of them allows solving certain specific tasks of studying geological sections. However, the position of the boundary between stratigraphic units is more clearly established comprehensively using logging data, the upper boundary of the coal bed, the upper boundary of the mottled rock, the debris rock with kaolin and radiometry data. Accordingly, the lithological and stratigraphic dissection of poorly studied geological sections based on natural gamma-ray spectrometry can be used to trace the boundaries of the interface between sediments not only of the Visean and Tournaisian stages, but also of other lithological and stratigraphic horizons within the oil- and gas-bearing areas of Ukraine and the world.

Conclusions

Comprehensive lithological, petrographic, X-ray diffraction and gamma-ray spectrometric studies established a close relationship between the mineralogical composition of rocks, geochemical conditions of sedimentation and the content of natural radioactive elements (^{40}K, U(Ra), Th) within the transition strata of the Tournaisian and Visean age of the Plyskiv-Lysohorskyi outcrop crystalline basement. The distribution of natural radioactive elements in the rocks of the geological section corresponds to their mineralogical features and sedimentation conditions. The highest concentrations were observed in argillites, especially in siltstone and coaliferous varieties, due to the increased content of organic matter, kaolinite and iron hydroxides. The lowest values were in limestone and gravelly sandstone. The Th/K ratio proved to be the most sensitive parameter for establishing the stratigraphic boundary between the Tournaisian and Visean deposits. Its sharp change allows for more accurate localisation of the boundary between marine and continental sedimentation conditions, especially within the transition strata.

The lithological and stratigraphic heterogeneity of the transitional thickness was manifested in the sharp alternation of different-grained sandstones, argillites, siltstones and gravel-like formations, with frequent inclusion of carbonised organic matter and flint layers. This change in lithotypes confirmed the oscillatory nature of the sedimentation regime, reflecting the alternation of transgressions and regressions. The chemical and mineralogical composition of rocks indicates a gradual transition from acidic, subcontinental (Tournaisian) to alkaline, marine (Visean) conditions of sedimentation. In particular, the Tournaisian rocks showed a wider distribution of kaolinite, siderite, pyrite nodules and flinty argillites, while the Visean rocks were enriched with chemogenic silica, hydro-mica and minerals of hydrothermal origin.

Gamma-ray spectrometry proved to be an effective method of stratigraphic dissection by recording not only the absolute content of radioactive isotopes, but also changes in their ratios. In particular, it made it possible to localise the transition zone between stratigraphic units in wells 1, 3, 4 and 8, where other methods (macroscopic description, GC, CS) did not reveal a clear boundary. The stratigraphic boundary between the Tournaisian and Visean deposits is diffuse and is usually not accompanied by typical reference horizons (e.g., basal conglomerates or angular unconformities). Its position can be determined only based on a multifactorial analysis: petrographic, geochemical, mineralogical and radiometric. Thus, the results of the study confirmed the feasibility of using gamma-ray spectrometry in combination with lithological and petrographic analysis as an effective tool for stratigraphic correlation in conditions of complex geological structure. This allows not only to localise the boundary between stratigraphic units, but also to assess the nature of changes in the sedimentary environment, which is important for predicting the oil and gas content of the area.

Acknowledgements

None.

Funding

None.

Conflict of Interest

None.

References

[1] Amartey, E.O., Akiti, T.T., Armah, T., Osae, S., & Agyekum, W.A. (2016). Integrating gamma log and conventional electrical logs to improve identification of fracture zones in hard rocks for hydrofracturing: A case study from Ghana. *Applied Water Science*, 7(3), 1091-1098. doi: 10.1007/s13201-016-0450-z.

[2] Bezrodna, I.M., & Gozhyk, A.P. (2018). *Petrophysics*. Kyiv: Kyiv University Publishing House.

[3] Danylchenko, S.M., Kuznetsov, V.M., & Protsenko, I.Y. (2019). *X-ray diffraction methods for the study of crystalline materials*. Sumy: Sumy State University.

[4] Fedak, I.O., & Koval, Y.M. (2020). Lithofacial zoning of producing horizons of oil and gas fields using artificial neural network. *Exploration and Development of Oil and Gas Fields*, 1, 96-105.

[5] Hrol, V., & Lurie, A. (2021). Criteria for assessment of hydrocarbon saturation of compact sand-aleurite rocks under DDB conditions. *Visnyk of V. N. Karazin Kharkiv National University, Series "Geology. Geography. Ecology"*, 54, 132-140. doi: 10.26565/2410-7360-2021-54-10.

[6] Iuras, S., Orlyuk, M., Levoniuk, S., Drukarenko, V., & Kruhlov, B. (2023). Unconventional shale gas potential of lower Visean organic-rich formations in Glynsko-Solohivskyi petroleum region. *Geodynamics*, 34(1), 80-96. doi: 10.23939/jgd2023.01.080.

[7] Ivaniuta, M.M. (Ed.). (1998). *Atlas of oil and gas fields of Ukraine* (Vol. 1). Lviv: Tsentr Yevropy.

[8] Ke, L., Ruan, F., Duan, T., Li, Z., Wang, X., & Zhao, L. (2023). Integrated geomodel accuracy enhancement based on embedded MPS geological modeling for thin interbedded reservoirs. *Energies*, 16(19), article number 6850. doi: 10.3390/en16196850.

[9] Kurgansky, V.M., & Tishayev, I.V. (2011). *Electrical and electromagnetic methods of well logging*. Kyiv: Kyiv University Publishing and Printing Center.

[10] Lazaruk, Y.G. (2022). Conditions of the formation of slide dislocations of the carboniferous of Dnieper-Donets Basin. In *Geological structure and mineral deposits of Ukraine: Abstracts of all-Ukrainian scientific conference* (pp. 360-364). Kyiv: NAS of Ukraine.

[11] Lazaruk, Y.H. (2012). Tectonic factors of oil and gas field formation in the northern slope of the Dnieper-Donets Basin. *Oil and Gas Industry*, 4, 8-11.

[12] Li, W., Li, S., Qu, Q., Zhang, H., Zhao, J., & Dou, M. (2022). A modeling approach for beach-bar sand reservoirs based on depositional mode and sandbody volume. *Minerals*, 12(8), article number 950. doi: 10.3390/min12080950.

[13] Lukin, O.Yu., Gafych, I.P., Goncharov, H.H., Makogon, V.V., & Prygarina, T.M. (2020). Hydrocarbon potential of Ukraine's subsoil and main directions of its development. *Mineral Resources of Ukraine*, 4, 28-38. doi: 10.31996/mru.2020.4.28-38.

[14] Machulina, S.O. (2022). New methodological techniques for studying cycling in carbonate sediments. *Scientific Collection "InterConf+"*, 22(113), 360-365. doi: 10.51582/interconf.19-20.06.2022.036.

[15] Selley, R.C. (2000). *Applied sedimentology* (2nd ed.). London: Academic Press.

[16] Shen, B., Li, Z., Wang, D., Ma, M., Meng, X., & Shi, X. (2021). Application of element logging and fitting gamma in formation identification. *Mud Logging Engineering*, 32(4), 33-36. doi: 10.3969/j.issn.1672-9803.2021.04.006.

[17] Šimíček, D., & Bábek, O. (2015). Spectral gamma-ray logging of the Grès d'Annot, SE France: An outcrop analogue to geophysical facies mapping and well-log correlation of sand-rich turbidite reservoirs. *Marine and Petroleum Geology*, 60, 1-17. doi: 10.1016/j.marpetgeo.2014.10.010.

[18] Streltsova, I.O., & Kruhlyk, V.M. (2020). Lithology and paleodepositional environment analysis of permian sediments in connection with oil and gas potential in the South-Khrestyshche area in the Dnieper-Donets Basin. *Collection of Scientific Works of the Institute of Geological Sciences of the National Academy of Sciences of Ukraine*, 13, 89-103. doi: 10.30836/igs.2522-9753.2020.213813.

[19] Stryzhak, L.I. (2021). *Lithogenesis and nature of reservoirs of deeply buried lower carboniferous terrigenous sediments of the central part of the Dnipro-Donetsk Basin*. (PhD dissertation, Institute of Geological Sciences of the National Academy of Sciences of Ukraine, Kyiv, Ukraine).

[20] Stryzhak, L.I., Aleksieienkova, M.V., & Stryzhak, V.P. (2020). Lithogenesis of terrigenous rocks and its influence on filtration-capacity properties of lower carbon reservoirs in the central part of the Dnieper-Donets Basin. *Collection of Scientific Works of the Institute of Geological Sciences of the National Academy of Sciences of Ukraine*, 13, 80-88. doi: 10.30836/igs.2522-9753.2020.220668.

[21] Volovetskyi, V.B., Romanyshyn, Y.L., Bugai, A.O., Altukhov, S.O., & Shchyrba, O.M. (2024). Development of information and software for automation and digitalisation of processing and analysing geological-geophysical data of underground gas storage wells. *Journal of Achievements in Materials and Manufacturing Engineering*, 126(2), 66-85. doi: 10.5604/01.3001.0054.9207.

[22] Vysochanskiy, I.V., Yakovlev, A.O., Samchuk, I.M., Volosnyk, Y.Y., Nekrasov, A.O., & Kupchinska, M.V. (2022). Conditions for the formation of non-anticlinal hydrocarbon traps in zones around salt stocks of the south-eastern part of the Dneper-Donetsk Depression. *Visnyk of V. N. Karazin Kharkiv National University, Series "Geology. Geography. Ecology"*, 56, 24-48. doi: 10.26565/2410-7360-2022-56-02.

[23] Vyzhva, S.A., Onyshchuk, V.I., Onyshchuk, I., & Shabatura, O.V. (2020). *Radioactive methods of geophysical research of boreholes*. Kyiv: Kyiv University Publishing and Printing Center.

[24] Vyzhva, S.A., Onyshchuk, V.I., Onyshchuk, I.I., & Shabatura, O.V. (2023). *Nuclear and geophysical methods of well research*. Kyiv: Kyiv University Publishing House.
[25] Wu, W., Zhang, L., Qiu, Y., Wang, G., & Yu, J. (2023). Milankovitch cycle of continental deep-water fine-grained sedimentary rocks in the lower submember of Es3 of Well FY1 in Dongying Sag and its significance for shale oil exploration. *Energy Exploration & Exploitation*, 41(6), 2140-2160. doi: 10.1177/01445987231181721.
[26] Xia, L., Zhao, Y., Hu, Y., Wang, J., Yuan, R., & Kan, L. (2021). Lithology identification method based on characteristic map of sensitive elements. *Mud Logging Engineering*, 32(4), 47-52. doi: 10.3969/j.issn.1672-9803.2021.04.009.
[27] Yemets, L. (2024). Application of geological and technological research data to correlate and clarify the structure of the Kamyshnya field. *Visnyk of the Lviv University. Series Geology*, 38, 178-184. doi: 10.30970/vgl.38.14.
[28] Zhong, Q., *et al*. (2024). Distribution characteristics and hydrocarbon significance of deep-water fine-grained sedimentary rocks in the steep-slope zone of a graben lake basin: A case study of Es_3^1 sub-member in the Jiyang Depression, Bohai Bay Basin, China. *Minerals*, 14(9), article number 882. doi: 10.3390/min14090882.

Можливості літолого-стратиграфічного розчленування геологічних розрізів за даними спектрометрії природного гамма-випромінювання

Олександр Трубенко

Кандидат геологічних наук, декан
Івано-Франківський національний технічний університет нафти і газу
76019, вул. Карпатська, 15, м. Івано-Франківськ, Україна
https://orcid.org/0000-0003-3418-439X

Дмитро Федоришин

Доктор геологічних наук, професор
Івано-Франківський національний технічний університет нафти і газу
76019, вул. Карпатська, 15, м. Івано-Франківськ, Україна
https://orcid.org/0009-0004-5348-9564

Сергій Федоришин

Кандидат геологічних наук, доцент
Івано-Франківський національний технічний університет нафти і газу
76019, вул. Карпатська, 15, м. Івано-Франківськ, Україна
https://orcid.org/0009-0005-9274-7244

Анотація. Встановлення геологічної будови складнопобудованих осадових розрізів нафтогазоносних територій України, а саме їх літолого-стратиграфічне розчленування, є доволі складним і часто неоднозначним у трактуванні послідовності нашарування товщ осадових порід. Метою роботи було вивчення можливості літолого-стратиграфічного розчленування геологічного розрізу за результатами спектрометрії природнього гамма-випромінювання в інтервалі границь розподілу турнейських та візейських відкладів, у межах Плисківсько-Лисогорівського виступу кристалічного фундаменту приосьової зони Дніпровсько-Донецької западини. Методика вивчення границь розподілу турнейських та візейських відкладів базувалася на результатах розподілу концентрації радіоактивних ізотопів природнього гамма-випромінювання, отриманих безпосередньо у процесі буріння пошукових і розвідувальних свердловин. Окрім цього з інтервалів візейського та турнейського ярусів нижньокам'яновугільних відкладів відібрано керновий матеріал, проведено його літолого-петрографічне дослідження шляхом макроскопічного опису зразків керну, виготовлення й опис шліфів, а також виконаний рентгено-структурний і гамма-спектрометричний аналізи речового складу колекції зразків. У цілому визначалась кількісна наявність природних радіоактивних елементів. За результатами таких комплексних геолого-геофізичних досліджень було встановлено, що розподіл природніх радіоактивних елементів у інтервалах залягання відкладів, залежить від літологічного складу гірських порід, і відповідно зміни умов процесу осадконагромадження, що обумовлює зміни в розподілі радіоактивних елементів. Тому саме ця особливість будови може бути використана для прослідковування границь розподілу літотипів у горизонтах різних стратиграфічних товщ. Враховуючи те, що радіоактивність порід поліміктового складу характеризуються значним сумарним ефектом показу і зумовлена підвищеною радіоактивністю скелету матриці породи і глинистого матеріалу, який заповнює міжзерновий простір. Тому визначення глинистості доцільно виконувати з використанням результатів гамма-спектрометрії за величиною концентрації калію-40 або за даними гамма каротажу. Впровадження таких підходів у процесі інтерпретації окрім виділення границь розподілу між відкладами також дозволяє встановлювати фізико-геологічні умови, у яких проходив процес осадконагромадження різних літотипів гірських порід

Ключові слова: літотипи; колектора; спектрометрія; геологічна границя; осадконагромадження

ISSN 1993-9973, e-ISSN 2415-332X

Vol. 25, No. 2 2025

PROSPECTING AND DEVELOPMENT OF OIL AND GAS FIELDS

https://pdogf.com.ua/en

Received: 28.05.2025. Revised: 17.10.2025. Accepted: 08.12.2025. Published: 09.01.2026.

UDC 622.692.4

DOI: 10.63341/pdogf/2.2025.22

On the necessity and feasibility of revising and improving the methodology for calculating losses of petroleum products from evaporation based on the results of calculation and comparative analysis

Nataliia Liuta

PhD in Technical Sciences, Associate Professor
Ivano-Frankivsk National Technical University of Oil and Gas
76019, 15 Karpatska Str., Ivano-Frankivsk, Ukraine
https://orcid.org/0000-0002-3321-0982

Yuliia Doroshenko*

PhD in Technical Sciences, Associate Professor
Ivano-Frankivsk National Technical University of Oil and Gas
76019, 15 Karpatska Str., Ivano-Frankivsk, Ukraine
https://orcid.org/0000-0002-7196-9383

Mykhailo Piletskyi

Postgraduate Student
Ivano-Frankivsk National Technical University of Oil and Gas
76019, 15 Karpatska Str., Ivano-Frankivsk, Ukraine
https://orcid.org/0009-0005-9885-2467

Abstract. The aim of the work was to analyse the regulatory framework for accounting for petroleum product losses in Ukraine. A comparative and empirical analysis of three methods for determining petroleum product losses from evaporation was carried out. Calculations were made of petrol standing losses in vertical steel tanks with a nominal volume of 1,000, 2,000 and 3,000 m^3 in different climatic zones of Ukraine. The impact of tank filling level and saturated vapour pressure on losses was assessed. A comparative analysis showed that the EPA and Konstantynov methods demonstrate a physically justified reduction in losses with an increase in the filling level, as well as high sensitivity to climatic conditions. For the VCT-3000 tank, the relative error between calculations for the middle and southern climatic zones according to the Konstantynov method is 6.9-10.6%, and according to the EPA method – 8.5-12.0%. For the VCT-2000, these figures are 5.9-9.3% (Konstantynov) and 6.9-10.5% (EPA), and for the VCT-1000, they are 6.9-10.6% and 8.5-12%, respectively. However, calculations using the standard methodology showed virtually zero sensitivity to the climate zone (relative error ~0.26%), which contradicts actual operating conditions and leads to potentially significant errors in the assessment of volatile organic compound losses. This indicates the need to revise the current Ukrainian standards, taking into account modern physicochemical evaporation models. Additionally, the influence of saturated petroleum product vapour pressure according to Reid on the amount of losses was analysed. The results of calculations for the middle and southern climatic zones showed that an increase in saturated vapour pressure from 50 kPa to 80 kPa causes an approximately 1.6-fold increase in losses for all types of tanks studied. This confirms the high sensitivity of physical and mathematical methods to the physical and chemical properties of petroleum products, in contrast to the normative approach, which does not take this parameter into account. The results obtained can be used to develop an adapted combined methodology that combines the accuracy of international standards with the simplicity of normative accounting

Keywords: petrol; standing losses; saturated vapour pressure; climate zones; tanks; regulatory document

Suggested Citation: Liuta, N., Doroshenko, Yu., & Piletskyi, M. (2025). On the necessity and feasibility of revising and improving the methodology for calculating losses of petroleum products from evaporation based on the results of calculation and comparative analysis. *Prospecting and Development of Oil and Gas Fields*, 25(2), 22-35. doi: 10.63341/pdogf/2.2025.22.

*Corresponding author

Introduction

The relevance of reviewing and improving the methodology for calculating petroleum product losses from evaporation is determined by factors that affect the efficiency of energy resource use, environmental safety, and economic costs. As stated in the study by G.C. Ribeiro *et al.* (2024), regular updating of regulatory documents should be considered a strategically important process that ensures the accuracy, reliability, and practical value of methods for assessing emissions from organic liquid storage tanks. This allows the document to remain an effective tool for environmental regulation, technological planning, and sustainable industrial development. Conducting a comparative analysis of existing methods is an important step in developing modern and scientifically sound standards that will optimise energy resource management in Ukraine.

International research confirms the scale of the problem. According to a study by G. You *et al.* (2024), the oil refining industry is one of the main sources of industrial emissions of volatile organic compounds (VOC). Based on the analysis of 76 samples from eight oil refineries, the authors determined that losses due to equipment leaks, storage tanks, wastewater treatment systems, and loading operations account for the majority of total emissions. In particular, emissions from storage tanks averaged 0.28 kg of VOC per tonne of refined oil, and total VOC losses at different plants ranged from 0.67 to 2.77 kg/t. Alkanes (ethane, propane, butane) and aromatic hydrocarbons (benzene, toluene) were the dominant components. This confirms that losses during storage in tanks are not only technically significant, but also have a significant environmental and regulatory dimension that needs to be taken into account in national methods for accounting and regulating losses.

A review of petrol loss calculation processes and the development of emission reduction technologies in the oil refining industry has highlighted a number of relevant issues. P. Orozco *et al*. (2023) describe the physical phenomena of petrol evaporation and their negative impact on the environment and human health. The article examines VOC emissions at various facilities (petrol stations, oil refineries), analyses standards and protocols for assessing losses in coastal reservoirs, and discusses the widespread application of these methods. It is emphasised that most studies are based on industry standards, and some of them take into account the uncertainty of measurements. In addition, the use of computational hydrodynamics methods to assess evaporation losses is described, which significantly enhances theoretical and experimental models in storage tanks. The article confirms the importance of modernising and refining national methods for calculating fuel losses during storage, aimed at reducing environmental risks, economic losses and improving regulatory control.

H. Rajabi *et al*. (2020) noted that during the storage of petroleum products in vertical tanks with floating or fixed roofs, hydrocarbons evaporate, leading to the formation of VOC in the air. These compounds are highly volatile, toxic and capable of forming a secondary pollutant such as tropospheric ozone, which has a negative impact on both human health and the environment. The study provides an overview of VOC emissions arising at various stages of oil processing and assesses the environmental impact of these emissions. An important aspect of the study was the creation of a global emissions inventory system, which provided a better understanding of the scale and sources of pollution and identified priority areas for regulating emissions and reducing environmental impact. This study was important for the development of environmental protection policies and practices, as it developed a comprehensive understanding of global VOC emissions from oil refining and helped in the search for more effective technologies to reduce these emissions. At the same time, tank losses account for a significant share of total VOC emissions at oil depots and fuel and energy complex enterprises.

Given global environmental challenges and Ukraine's international commitments to reduce industrial emissions, the issue of regulating and technically controlling VOC emissions has become particularly relevant (Law of Ukraine No. 2707-XII, 1992; Directive of the European Parliament and of the Council No. 2004/42/CE, 2004). At the same time, in order to harmonise national regulations with international standards and introduce best practices in the field of environmental protection, the regulation of industrial emissions is determined by Directive of the European Parliament and Council of the European Union No. 2010/75/EU (2010), which establishes requirements for integrated prevention and control of emissions.

In addition to the environmental impact, evaporation causes direct economic losses of fuel, which requires the implementation of effective technological solutions to minimise them. F. Beiranvand & H. Najibi (2021) emphasised the importance of reducing losses from the evaporation of volatile fuels, which is important from both an economic and environmental point of view. Evaporation leads to significant financial losses due to a reduction in fuel volume and also contributes to atmospheric pollution with harmful VOC, which can cause the formation of secondary pollutants, in particular tropospheric ozone. In addition, the accumulation of fuel vapours creates potential explosion hazards. The authors proposed an innovative approach using new mixtures of surfactants that effectively reduce evaporation, which highlights the relevance of developing and implementing technological solutions to minimise fuel losses in industry.

In accordance with the Instructions on the Procedure for Receiving, Transporting, Storing, Dispensing, and Accounting for Oil and Petroleum Products at Enterprises and Organisations in Ukraine (2008), during the storage of petroleum products, it is necessary to ensure proper accounting and control of losses. However, N.V. Liuta *et al*. (2020) noted that, unlike most developed countries, Ukraine lacks a clearly defined system for measuring, accounting for, and setting limits on petroleum product losses, particularly those resulting from evaporation during storage. The analysis of existing methods for regulating petroleum product losses showed that they do not sufficiently take into ac-

count the climatic and technological characteristics of different regions, which leads to inaccuracies in calculations and exceeding permissible losses.

The document Norms of Petroleum Product Losses During Their Reception, Storage, Dispensing, Transshipment and Transportation (2020) establishes the maximum permissible loss rates that occur during various stages of petroleum product circulation, in particular during transportation by road, rail, water and pipeline, as well as during storage. However, as noted in a study conducted by N.V. Liuta *et al*. (2020), the current methodology does not take into account a number of important factors that have a significant impact on the volume of losses, especially during the storage of petroleum products in tanks, and that it is precisely these factors ignored by the authors of the methodology that are often decisive in assessing losses from evaporation. In view of the above, the aim of this work was to justify the expediency of revising the current regulatory methodology for assessing petroleum product losses, taking into account a range of factors that actually influence the evaporation process, in order to ensure more accurate determination of such losses and improve the efficiency of their accounting and storage.

Materials and Methods

In order to identify areas for improvement in Norms of Petroleum Product Losses During Their Reception, Storage, Dispensing, Transshipment and Transportation (2020), it became necessary to conduct a scientific comparison with the methods of the United States Environmental Protection Agency (EPA) (AP-42 Chapter 7..., 2024) and Konstantynov (Lisafin & Liuta, 2018). The combined use of comparative and empirical analysis methods ensured an objective identification of differences in the approaches, parameters, calculations and regulatory aspects of these documents. Comparative analysis made it possible to compare the structure of calculation formulas, determine which factors are taken into account, and analyse the depth of scientific justification of each document.

Empirical analysis was performed based on calculations of losses for the same object (above-ground vertical cylindrical tanks (VCT) with a nominal volume of 1,000 m^3, 2,000 m^3 and 3,000 m^3) using three methods to verify the accuracy and reliability of the selected methods in practical examples. For the purpose of empirical analysis of standing losses, calculations were made for tanks with a nominal volume of 1,000 m^3 (one unit), 2,000 m^3 (one unit) and 3,000 m^3 (one unit), which were operated in the conditions of the middle and southern climatic zones. The analysis covered various tank filling levels – from minimum to maximum (Table 1), all months of the calendar year 2024, as well as the saturated vapour pressure of stored liquids in the range from 50 kPa to 80 kPa, and the geometric characteristics of the tanks. To calculate the losses of volatile fractions of petroleum products using the Konstantynov method and EPA standards, a number of initial data were taken into account. These include meteorological conditions, in particular the average monthly maximum and minimum air temperature, as well as barometric pressure on the date of calculation (Table 2).

Table 1. Main technical characteristics of the device

Nominal tank capacity, m^3	Tank diameter, m	Tank height, m	Minimum filling level, m	Maximum filling level, m
1,000	11.99	9.606	1	8
2,000	15.233	11.64	1	10
3,000	19.042	11.731	1	10.8

Source: created by authors based on V. Lisafin & N. Liuta (2018)

Table 2. Meteorological conditions in the central and southern climatic zones of Ukraine

Month	January	February	March	April	May	June	July	August	September	October	November	December
Middle zone												
Maximum air temperature, °C	5.4	1.8	4.9	11.9	17.6	20.3	22.1	22.1	17.7	11.8	8.1	8.2
Minimum air temperature, °C	0.8	-2.3	-1.5	3	7.8	10.7	12.5	11.5	8.9	6.3	4	2.9
Southern zone												
Maximum air temperature, °C	2.5	0.1	6.9	12.8	20.7	24.4	27.4	28	23	16.3	7.6	4.2
Minimum air temperature, °C	-0.1	-2.1	1.6	6.6	13.9	18.6	21.2	21.5	17.9	12.5	5	2.2

Source: created by the authors based on V.M. Lipinsky *et al*. (2003)

In addition, geographical parameters are important, in particular the geographical latitude of the reservoir location (47°37′N for the southern zone and 51°29′28″N for the middle zone). The geometric characteristics of the tank include its diameter, geometric height, and the level of liquid filling in the tank (filling height) (Table 1). The settings of the mechanical breathing valve, namely the excess pressure (2,000 Pa) and vacuum (250 Pa) at which it operates, must be taken into account. Among the physical and chemical characteristics of the petroleum product, its density (kg/m^3) and boiling point (40°C) are essential. Additionally, the review included the type and condition of the external surface of the tank (0.65), which affect the thermal regime and, accordingly, the intensity of evaporation.

Standing losses of petroleum products were calculated according to the EPA recommendations using the formula:

$$L_s = 365 \times V_V \times W_V \times K_E \times K_s, \quad (1)$$

where V_V is the volume of gas space in the tank; W_V is the vapour saturation; K_E is the gas space expansion coefficient; K_S is the saturated vapour ventilation coefficient. The vapour saturation is determined by the formula:

$$W_V = \frac{M_V \times P_{VA}}{R \times T_{LA}}, \quad (2)$$

where M_V is the molar mass of a mixture of hydrocarbon vapours; P_{VA} is the saturated vapour pressure at the average daily temperature of the surface layer of the liquid; R is the gas constant; T_{LA} is the average daily temperature of the surface layer of liquid. The average daily temperature of the surface layer of the liquid is determined by the formula:

$$T_{LA} = 0.44 \times T_{AA} + 0.56 \times T_B + 0.0079 \times \alpha \times I, \quad (3)$$

where T_{AA} is the average daily ambient temperature; T_B is the temperature of the liquid below the surface layer; α is the solar radiation absorption coefficient; I is the daily amount of solar radiation. The temperature of the liquid below the surface layer of the petroleum product is equal to:

$$T_B = T_{AA} + 6 \times \alpha - 1. \quad (4)$$

The saturated vapour pressure at the average daily temperature of the surface layer of the liquid C. de la Calle-Arroyo *et al*. (2021) recommend determining it using Antoine's formula:

$$P_{VA} = exp\left[A - \frac{B}{T_{LA}}\right], \quad (5)$$

where A and B are constant coefficients selected from reference literature depending on the type of liquid stored. The gas space expansion coefficient K_E for a known geographical location of the tank farm is determined by the following formula:

$$K_E = 0.0018[0.72 \times (T_{AX} - T_{AN}) + 0.28 \times \alpha \times I]. \quad (6)$$

If the geographical location of the tank farm is unknown, the gas space expansion coefficient is taken to be 0.04. The saturated vapour ventilation coefficient is equal to:

$$K_S = \frac{1}{1 + 0.053 \times P_{VA} \times H_{VO}}. \quad (7)$$

As part of calculating petroleum standing losses using Konstantynov's method, it is necessary to calculate the molar mass of petroleum vapours, the thermal conductivity coefficient of petrol at average temperature, the specific heat capacity of petrol, the density of petroleum products, the thermal conductivity coefficient of the petroleum product, the length of daylight hours, the transparency coefficient of atmospheric air, the intensity of solar radiation, the geometric characteristics of the gas space of the tank and the liquid surface in the tank, the amount of heat received from solar radiation by 1 m^2 of the wall limiting the gas space of the tank, determine the values of a number of heat transfer coefficients from graphs, simulate the temperature regime of the tank and petroleum product, the pressure of saturated vapours of the petroleum product, and the maximum and minimum partial pressures. The average mass content of petrol vapours in the gas-air mixture is calculated:

$$\sigma_m = \frac{P_{max} + P_{min}}{R(T_{gp.min} + T_{gp.max})}, \quad (8)$$

where P_{max}, P_{min} are the maximum and minimum pressure in the gas space of the tank; $T_{gp.max}$, $T_{gp.min}$ are the maximum and minimum temperature in the gas space of the tank; R is the universal gas constant. Volume of gas-air mixture released into the atmosphere:

$$\Delta V = V_{gp}\, ln\left(\frac{P_a - P_v - P_{min}}{P_a + P_n - P_{max}} \times \frac{T_{gp.max}}{T_{gp.min}}\right), \quad (9)$$

where V_{gp} is the volume of the gas space in the tank; P_a is the atmospheric pressure; P_v is the vacuum in the gas space in the tank; P_n is the excess pressure in the gas space in the tank. The saturated vapour pressure is determined using Rybakov's formula:

$$P_T = P_{S38} 10^{\frac{1,430}{T}}, \quad (10)$$

where P_{S38} is the saturated vapour pressure of petrol by Reid; T is the temperature of petroleum product vapours. Standing losses will be equal to:

$$M_{m.d.} = \Delta V \times \sigma_m. \quad (11)$$

To calculate petroleum product losses during storage in tanks, the following input parameters are used in accordance with the requirements of current regulations: the volume of petroleum products in the tank, its density at average temperature, the number of calendar days in the calculation month, as well as loss standards determined on the basis of daily product residues (Norms of Petroleum Product Losses..., 2020). The latter are formed on the basis of daily accounting data recorded in the petroleum product measurement log. These parameters are critical for ensuring the accuracy of loss calculations and further analysis of the efficiency of fuel and lubricant storage systems. Losses of petroleum products during storage in tanks are calculated:

$$M_{norm} = K \times V \times \rho, \quad (12)$$

where K is the loss rate based on the actual daily product balances according to the daily records specified in the petroleum product measurement log, %; V is the volume of petroleum product in the tank; ρ is the density of the petroleum product at average temperature. Another influential factor that must be indicated in the petrol quality certificate is the saturated vapour pressure according to Reid,

which is the approximate absolute vapour pressure of the petroleum product under study at a temperature of 37.8°C. The saturated vapour pressure of a petroleum product significantly depends on temperature. To model this dependence, the Rybakov formula (10) and the Antoine formula (5) were used in the compared methods. To evaluate the discrepancies between the results obtained using different methods, the relative error (discrepancy) was calculated using the formula:

$$\delta = \frac{x_1 - x_2}{x_1}, \quad (13)$$

where x_1 is the reference (or base) value; x_2 is the comparable value.

Results

There is a global practice of constantly updating and improving regulatory documents. In particular, as noted in their study by N. Stef & A. Ashta (2023), this is the continuously updated document AP-42 Chapter 7, Section 1 – organic liquid storage tanks (2024), designed to provide scientifically sound methods for calculating VOC emissions generated during the storage of organic liquids in industrial tanks. These methods are used in environmental reporting, planning of emission control measures, and environmental assessment. First published in 1968, it was the first edition of a collection of emission factors for air pollutants prepared by the U.S. Public Health Service, revised in 1972 and republished under the auspices of the EPA. Since then, this document has been regularly updated to take into account new scientific data, technological advances, and changes in regulatory requirements.

In order to systematise and gain a deeper understanding of approaches to assessing petroleum product losses from evaporation, this study conducted a comparative analysis of three common methods: the American EPA AP-42 method (Section 7), current Ukrainian standards (2020) and the Konstantynov engineering method. Table 3 summarises the main characteristics of each approach, including the type of document, purpose of application, scope, consideration of climatic factors, level of detail of parameters, calculation methods and practical relevance. The data presented made it possible to identify differences in the structure, purpose and accuracy of these methods, which is the basis for further analysis of their effectiveness in different conditions. The results of the comparative analysis of the three methods are presented in Table 3.

Table 3. Results of a comparative analysis of methods for calculating petroleum product losses due to evaporation from tanks

Criterion	AP-42 Chapter 7	Ukrainian standards	Konstantynov's methodology
Document type	Methodology for calculating VOC emissions	Regulatory document on loss accounting	Calculated engineering methodology
Main purpose	Environmental control of emissions	Regulation of permissible losses	Technical and economic accounting of losses
Developing organisation	U.S. EPA	Ministry of Economy of Ukraine	Transnefteprodukt Research Institute, USSR
Types of tanks	All types: fixed, floating, domed roofs	Mainly fixed roofs, some underground reservoirs	Vertical and horizontal steel tanks
Type of petroleum products	Organic liquids	Petrol, diesel fuel, fuel oil, kerosene, etc.	Petrol, diesel fuel, fuel oil
Climatic factors	The following must be taken into account: ambient temperature, temperature difference, wind	Autumn-winter and spring-summer periods are taken into account	Temperature of the surrounding environment, temperature difference, weather conditions (sunny, cloudy) are taken into account
Product parameters	Saturated vapour pressure, molar mass, density	Density, fuel type	Molar mass of vapours, thermal conductivity coefficient, specific heat capacity, density, thermal conductivity coefficient, saturated vapour pressure
Type of losses	Evaporation losses	Losses during storage, filling, draining, transportation	Evaporation losses
Calculation approach	Physical and chemical modelling of processes	Regulatory coefficients based on statistics	Semi-empirical formulas with corrections
Calculation methods	Analytical formulas + software (TANKS)	Tables and coefficients	Formulas with corrections (K_1, K_2, etc.)
Ease of application	High accuracy, requires software	The simplest option, easy to apply	Requires technical training, complex calculations, and software
Current relevance	Applicable in the United States, used globally	In Ukraine since 2020	Used in part in practice as an engineering basis in the post-Soviet space
Documentation purpose	Reporting emissions to environmental protection agencies	Accountancy, technological accounting	Project documentation, internal calculations of enterprises

Source: developed by the authors based on a comparison of V. Lisafin & N. Liuta (2018), Norms of Petroleum Product Losses During Their Reception, Storage, Dispensing, Transshipment and Transportation (2020), AP-42 Chapter 7, Section 1 – organic liquid storage tanks (2024)

Table 3 summarises the differences between the three approaches to estimating VOC losses during petroleum product storage. The EPA methodology is highly accurate due to physical and chemical modelling and the use of specialised software (e.g. TANKS), which makes it suitable for environmental monitoring and international reporting. At

the same time, Ukrainian standards are mainly focused on accounting and technological accounting of losses, are based on tabulated coefficients and are the easiest to implement in practice, although they are less accurate. Konstantynov's methodology, developed back in the Soviet period, remains relevant as an engineering basis due to semi-empirical formulas adapted to the real conditions of tank operation, but requires a high level of technical training and complex calculations. Comparative calculations were performed using the above-mentioned methodologies and standards. Table 4 presents the results of comparative calculations of evaporation losses from tanks with a nominal volume of 3,000 m^3, located in different climatic zones and for tank filling levels from a minimum of 1 m to a maximum of 10.8 m.

Table 4. Results of calculations of petrol losses due to evaporation during storage in an VCT-3000 tank at different filling levels

Level of petrol filling, m	The volume of petrol in the tank, m^3	Annual losses (Konstantynov method), kg/year		Annual losses (EPA method), kg/year		Calculation results based on storage loss rates according to Resolution of the Cabinet of Ministers of Ukraine No. 686 (2020)	
		Middle zone	Southern zone	Middle zone	Southern zone	Middle zone	Southern zone
10.8	3,076	5,261	6,502	5,962	7,644	8,272	8,315
9	2,566	12,254	14,697	13,954	17,476	6,892	6,929
8	2,278	16,005	18,954	18,214	22,567	6,127	6,159
7	1,994	19,689	23,061	22,373	27,457	5,361	5,389
6	1,709	23,292	27,021	26,420	32,143	4,595	4,619
5	1,424	26,789	30,812	30,319	36,594	3,829	3,849
4	1,139	30,127	34,387	34,010	40,739	3,063	3,080
3	854	33,205	37,638	37,361	44,423	2,298	2,310
2	570	35,759	40,280	40,046	47,246	1,532	1,540
1	285	36,775	41,188	40,812	47,672	766	770

Source: developed by the authors based on calculations

Analysis of the data in Table 4 revealed significant discrepancies in the results of calculating annual petrol losses depending on the methodology used. The EPA methodology showed the highest loss values, which clearly correlate with changes in climatic conditions: losses in the southern zone consistently exceeded the corresponding indicators for the middle zone. A similar trend, albeit with lower absolute values (by 20-30%), is recorded by the Konstantynov methodology. On the other hand, the standard method approved by Resolution of the Cabinet of Ministers of Ukraine No. 686 (2020) shows the opposite trend – as the tank filling level decreases, losses also decrease. This contradicts the physical nature of evaporation losses, which, as a rule, increase as the volume of fuel decreases due to an increase in the gas space above the liquid surface. The normative losses according to Resolution of the Cabinet of Ministers of Ukraine No. 686 (2020) are the smallest, and in the central and southern zones they differ insignificantly (less than 1%), which may indicate the limited sensitivity of this methodology to climatic factors. Table 5 presents the results of comparative calculations of evaporation losses from tanks with a nominal volume of 2,000 m^3 located in different climatic zones and for tank filling levels from a minimum of 1 m to a maximum of 10 m.

Table 5. Results of calculations of petrol losses due to evaporation during storage in an VCT-2000 tank at different filling levels

Level of petrol filling, m	The volume of petrol in the tank, m^3	Annual losses (Konstantynov method), kg/year		Annual losses (EPA method), kg/year		Calculation results based on storage loss rates according to Resolution of the Cabinet of Ministers of Ukraine No. 686 (2020)	
		Middle zone	Southern zone	Middle zone	Southern zone	Middle zone	Southern zone
10	1,823	4,664	5,628	5,084	6,274	4,933	4,959
9	1,640	6,842	8,153	7,464	9,114	4,440	4,463
8	1,458	8,958	10,558	9,768	11,816	3,947	3,967
7	1,276	11,019	12,865	12,008	14,401	3,453	3,471
6	1,094	13,023	15,076	14,177	16,872	2,960	2,975
5	911	14,955	17,182	16,261	19,217	2,467	2,480
4	729	16,791	19,159	18,230	21,401	1,973	1,984
3	547	18,474	20,946	20,019	23,352	1,480	1,488
2	365	19,860	22,383	2,146	24,871	987	992
1	182	20,394	22,844	21,921	25,193	493	496

Source: developed by the authors based on calculations

Analysis of the table showed that petrol losses based on the EPA methodology significantly exceed similar indicators based on the Konstantynov methodology and the normative methodology of Resolution of the Cabinet of Ministers of Ukraine No. 686 (2020). At a filling level of 10 m in the average climate zone, losses according to the EPA are approximately 9% higher than according to Konstantynov methodology and 3% higher than according to the standards. At the same time, Konstantynov methodology exceeds the standard losses by 5%. In the southern zone, the difference between the EPA and the Resolution is even more pronounced, amounting to 26.6%, and between the EPA and Konstantynov – 11.5%. There is also a significant difference between climatic zones: losses according to the EPA in the southern zone are 23.4% higher than in the average zone, while according to Konstantynov, this difference is about 20.7%, and according to the Resolution, only 0.5%, which confirmed the low sensitivity of the standard methodology to climatic factors. Table 6 presents the results of comparative calculations of evaporation losses from tanks with a nominal volume of 1,000 m³ located in different climatic zones and for tank filling levels from a minimum of 1 m to a maximum of 8 m.

Table 6. Results of calculations of petrol losses due to evaporation during storage in an VCT-1000 tank at different filling levels

Level of petrol filling, m	The volume of petrol in the tank, m³	Annual losses (Konstantynov method), kg/year		Annual losses (EPA method), kg/year		Calculation results based on storage loss rates according to Resolution of the Cabinet of Ministers of Ukraine No. 686 (2020)	
		Middle zone	Southern zone	Middle zone	Southern zone	Middle zone	Middle zone
8	903	4,472	5,530	4,935.7	6,283	2,432	2,445
7	790	6,491	7,906	7,174.7	9,021	2,128	2,139
6	678	8,409	10,115	9,296	11,562	1,824	1,834
5	565	10,240	12,183	11,312	13,934	1,520	1,528
4	452	11,973	14,107	13,209	16,127	1,216	1,223
3	339	13,572	15,852	14,945	18,093	912	916.9
2	226	14,938	17,301	16,400	19,678	608	611
1	113	15,670	17,982	17,099	20,281	304	306

Source: developed by the authors based on calculations

A comparative analysis of the results presented in Table 6 showed significant differences between the three methods of calculating petrol losses from evaporation. The EPA method gives values that are on average 9-10.5% higher than the Konstantynov method, which indicates its increased sensitivity to temperature and climatic factors, while the standard method showed significantly lower results – the largest deviations were observed at the minimum filling level (1 m), where the calculated losses according to the standards are only about 2% of the values obtained using engineering methods. Thus, the data in this table confirm the trends identified in the previous comparative tables: the standard approach provides simplicity of calculations, but is significantly inferior in accuracy, while the EPA and Konstantynov methods are more suitable for a reliable assessment of losses during the storage of petroleum products.

A comprehensive analysis of the data in Tables 4-6 showed that the two methods (EPA and Konstantynov) demonstrate a reduction in losses with an increase in the tank filling level, while the standard method approved by Resolution of the Cabinet of Ministers of Ukraine No. 686 (2020) shows the opposite trend. This is because the Konstantynov and EPA methodologies are based on the physical and chemical principles of liquid evaporation and take into account variable parameters, such as gas space volume, temperature and saturated vapour pressure. According to these approaches, an increase in the tank filling level is accompanied by a decrease in the volume of the vapour-gas phase, which leads to a reduction in VOC losses. In contrast, the regulatory methodology uses a simplified relationship, according to which losses are determined in proportion to the volume of petroleum products stored. This approach does not reflect the actual evaporation processes and leads to the opposite dynamics – an increase in calculated losses with an increase in the filling level. Table 7 presents a comparative calculation of the relative errors in determining petroleum product losses for tanks located in different regions of Ukraine using three methods in order to establish whether it is acceptable to ignore the geographical location of tanks with a nominal volume of 1,000 m³, 2,000 m³ and 3,000 m³ when determining the rate of petroleum product losses during storage in them.

Table 7. Relative errors in determining petrol losses from evaporation during storage in tanks, caused by differences in climate zones

Level of petrol filling, m	The volume of petrol in the tank, m³	Relative error caused by differences in climate zones, %		
		Results obtained using Konsantynov method	Results obtained using the EPA method	Results obtained using the standard method
VCT-3000				
10.8	3,076	10.6	12.4	0.262856
9	2,563	9.1	11.2	0.263364
8	2,278	8.4	10.7	0.262912
7	1,994	7.9	10.2	0.263258
6	1,709	7.4	9.8	0.263726
5	1,424	7.0	9.4	0.263076
4	1,139	6.6	9.0	0.263723
3	854	6.3	8.6	0.262638
2	570	5.9	8.2	0.260468
1	285	5.7	7.8	0.266979
VCT-2000				
10	1,823	9.4	10.5	0.258785
9	1,640	8.7	10.0	0.25946
8	1,458	8.2	9.5	0.259038
7	1,276	7.7	9.1	0.259943
6	1,094	7.3	8.7	0.25946
5	911	6.9	8.3	0.258785
4	729	6.6	8.0	0.260305
3	547	6.3	7.7	0.25946
2	365	6.0	84.1	0.257771
1	182	5.7	6.9	0.262839
VCT-1000				
8	903	10.6	12.0	0.264491
7	790	9.8	11.4	0.262443
6	678	9.2	10.9	0.262438
5	565	8.7	10.4	0.262433
4	452	8.2	9.9	0.262446
3	339	7.7	9.5	0.262438
2	226	7.3	9.1	0.262424
1	113	6.9	8.5	0.262467

Source: developed by the authors based on calculations

An analysis of the impact of climate zone and conditions on the results of petrol loss calculations also demonstrates a significant dependence of the results obtained using the physical and mathematical methods of Konstantynov and the EPA. For the VCT-3000 tank, the relative error between calculations for the middle and southern climate zones according to Konstantynov's method ranges from 6.9% to 10.6%, and according to the EPA method – from 8.5% to 12.0%, depending on the filling level. For the VCT-2000 tank, the relative error between calculations for the middle and southern climate zones according to Konstantynov method ranges from 5.9% to 9.3%, and according to the EPA method – from 6.9% to 10.5%, depending on the filling level. At the same time, for the VCT-1000 tank, the corresponding errors range from 6.9 to 10.6% and 8.5 to 12%. This indicates the high sensitivity of these methods to temperature factors that affect the intensity of evaporation. However, within the regulatory methodology in accordance with Resolution of the Cabinet of Ministers of Ukraine No. 686 (2020), the discrepancy between climate zones for all tanks is statistically insignificant – the relative error is approximately 0.26%, which indicates the actual indifference of the regulatory approach to the influence of climatic parameters. However, such a generalised assessment does not reflect the actual operating conditions of tanks in different regions and may lead to significant deviations from actual VOC losses. The results of comparative calculations of petroleum product losses, characterised by different saturated vapour pressure values according to Reid, are presented in the relevant tables. Table 8 shows the results of the study for the average storage zone.

Table 8. Results of research into the effect of saturated petroleum product vapour pressure on evaporation losses during storage (middle zone)

Pressure of saturated petrol vapours according to Reid, Pa	Losses of petroleum products from the tank VCT-1000, kg				Losses of petroleum products from the tank VCT-2000, kg				Losses of petroleum products from the tank VCT-3000, kg			
	Standard methodology		Methodology of Konstantynov		Standard methodology		Methodology of Konstantynov		Standard methodology		Methodology of Konstantynov	
	Filling level, m											
	1	8	1	8	1	10	1	10	1	10	1	10
50,000	304	2,432	12,160	3,415	493	4,935	20,394	4,664	766	7,658	28,695	6,495
60,000			14,461	4,102			24,211	5,590			34,021	7,759
70,000			16,795	4,823			28,036	6,549			39,307	9,048
80,000			19,168	5,586			31,870	7,548			44,548	10,369

Source: developed by the authors based on calculations

Analysing the data in Table 8, it should be noted that, according to Konstantynov's methodology, there is a clear dependence of the amount of petroleum product losses on the pressure of saturated petrol vapours: as the pressure increases, the losses increase significantly. In particular, when the saturated vapour pressure increases from 50 to 80 kPa, the calculated losses increase: for the VCT-1000 tank (H_{min} = 1 m) – from 12,160 kg to 19,168 kg, which is +57.6%, for the VCT-2000 tank (H_{min} = 1 m) – from 20,394 kg to 31,870 kg (+56.3%), for the VCT-3000 tank (H_{min} = 1 m) – from 28,695 kg to 44,548 kg (+55.3%). For all tank volumes and minimum fill level conditions, there is a steady increase in losses within the range of 55-58% when moving from the minimum to the maximum pressure considered. Analysis of the results for the maximum filling level (H_{max}) of the tanks also demonstrates a clear dependence of the amount of petroleum product losses on the saturated vapour pressure according to Konstantinov's method. With an increase in saturated vapour pressure from 50 kPa to 80 kPa, losses increase in all types of tanks: for the VCT-1000 tank from 3,415 kg to 5,586 kg, which is +63.6%, for the VCT-2000 tank, from 4,664 kg to 7,548 kg (+61.8%) for the VCT-3000 tank, from 6,495 kg to 10,369 kg (+59.6%). Thus, at maximum filling level, the increase in losses when the saturated vapour pressure of petrol increases by 30 kPa ranges from 59% to 64%, which is slightly higher than in the case of minimum filling level. This indicates the stable nature of the effect of saturated vapour pressure on the intensity of evaporation, even with a reduced volume of the vapour-gas phase. The standard method demonstrates complete insensitivity to this parameter: the loss values remain constant for each level of petroleum product filling, regardless of changes in saturated vapour pressure. Table 9 shows the results of a study of the effect of saturated vapour pressure according to Reid on petroleum product losses for the southern storage zone.

Table 9. Results of research into the effect of saturated petroleum product vapour pressure on evaporation losses during storage (southern zone)

Pressure of saturated petrol vapours according to Reid, Pa	Losses of petroleum products from the tank VCT-1000, kg				Losses of petroleum products from the tank VCT-2000, kg				Losses of petroleum products from the tank VCT-3000, kg			
	Standard methodology		Methodology of Konstantynov		Standard methodology		Methodology of Konstantynov		Standard methodology		Methodology of Konstantynov	
	Filling level, m											
	1	8	1	8	1	10	1	10	1	10	1	10
50,000	306	2,444	13,801	4,127	495	4,960	22,844	5,628	770	7,699	32,094	7,815
60,000			16,531	5,030			27,219	6,820			38,092	9,407
70,000			19,343	6,014			31,626	8,093			44,030	11,066
80,000			22,260	7,110			36,076	9,477			49,899	12,815

Source: developed by the authors based on calculations

Analysis of the results obtained using Konstantynov's method for the minimum tank filling level (H_{min}) in the southern climate zone also demonstrates an increase in petroleum product losses with an increase in saturated petrol vapour pressure for the VCT-1000 tank from 13,801 kg (at 50 kPa) to 22,260 kg (at 80 kPa), which is +61.3%, for the VCT-2000 tank from 22,844 kg to 36,076 kg (+57.9%), for the VCT-3000 tank from 32,094 kg to 49,899 kg (+55.5%). In all cases, there is an increase in losses within the range of 55-61%, which is consistent with the results obtained for the average climate zone. For the maximum filling level (H_{max}), there is also a significant increase in losses, namely for the VCT-1000 from 4,127 kg to 7,110 kg, which is +72.2%, for VCT-2000 from 5,628 kg to 9,477 kg (+68.3%), for VCT-3000 from 7,815 kg to 12,815 kg (+64.0%). The increase in losses at maximum filling levels ranges from 64% to 72%, which is due to the influence of higher temperatures in the southern climate zone, which contribute to more intense evaporation. As in the previous case (Table 7), the standard methodology remains insensitive to changes in saturated vapour pressure, demonstrating fixed loss values regardless of the physical and chemical characteristics of the fuel. As shown in Tables 8 and 9, a change in the saturated vapour pressure of petroleum products according to

Reid from 50 to 80 kPa causes an increase in the calculated values of petroleum product losses from small breaths by approximately 1.6 times for all tanks studied.

Discussion

Continuous updating and revision of the document is a necessary and systematic process aimed at ensuring its scientific validity, technical relevance, and compliance with current environmental requirements, as noted by G. Xing *et al*. (2023). The EPA regularly reviews the document, taking into account both scientific advances and practical changes (AP-42 Chapter 7..., 2024). In particular, updates are prompted by the emergence of new experimental data, refinement of the physicochemical properties of liquids, development of evaporation models, and the need to consider factors such as temperature, solar radiation, and air flows. An additional reason is the introduction of modern storage technologies: the modernisation of tanks, the improvement of seals, the use of inert gases and vapour recovery systems require a review of emission factors. Changes in climatic conditions also play an important role, in particular the rise in average temperatures and the emergence of extreme weather events that alter evaporation dynamics. The EPA also continuously verifies the accuracy of methodologies, updates calculation factors and adapts approaches to modern monitoring tools. Finally, an important source of change is feedback from users: industrialists, scientists, environmentalists and the public, which contributes to the openness and relevance of the document.

The study by H. Yang *et al*. (2024) provided important empirical data on VOC emissions from tanks with internal floating roofs, allowing for a deeper understanding of the main factors affecting petroleum product losses through evaporation. The authors pointed to the significant influence of parameters such as temperature, wind speed, tank design and sealing quality, confirming the need to take these factors into account when developing loss calculation methods. In particular, the use of secondary sealing and pontoons significantly reduces VOC emissions, indicating the advisability of introducing more detailed and comprehensive correction factors into the calculation models. In addition, the identified negative correlation between the height of the liquid in the tank and the intensity of emissions emphasises the need to take into account variable operating conditions, which are often ignored in traditional methods. The use of infrared imaging as a tool for rapid and accurate detection of leak sources demonstrates the promise of implementing the latest technological monitoring tools to improve the accuracy of loss estimates. Overall, the results of the study indicate the need to revise existing approaches to calculating petroleum product losses, taking into account multifactorial influences, which will improve the accuracy of forecasts and enable the development of effective measures to minimise environmental and economic losses.

I.M. Babić (2023) investigated methods for reducing evaporation losses in oil and petroleum product storage tanks using the example of a warehouse in Požega (Serbia). The paper analyses the impact of tank design features and operating conditions on evaporation levels and proposes measures to optimise storage in order to minimise VOC losses. The results of the study highlight the importance of applying technological and organisational measures to reduce the environmental and economic impact of evaporation losses from tanks. The article by X. Kong *et al*. (2025) is devoted to the numerical modelling of evaporation and oil vapour emission processes during the loading of oil into railway tankers using the Volume of Fluid method. The study covers a wide range of aspects, including the impact of ambient temperature, wind speed, tank geometry and fill level on VOC emissions. The modelling was carried out taking into account various scenarios, allowing the effectiveness of different emission reduction measures to be assessed.

The results of a study by M.R. Raazi Tabari *et al*. (2020) confirmed the importance of considering ambient temperature, wind speed, and tank design features when assessing VOC losses. The authors found that the highest emission rates were observed in the summer, particularly in July, when air temperature and wind speed reached their maximum values, indicating a significant influence of meteorological factors on evaporation intensity. In addition, a comparison of tanks with external and internal floating roofs showed that the former account for more than 98% of total VOC emissions, while the latter account for only 2%, demonstrating the significant role of tank design in determining losses.

C. Wu *et al*. (2022) combined numerical modelling and aerodynamic experiments to study the spread of oil vapours after spillage from tanks, focusing on the relationship between the evaporation of petroleum products from tanks and the level of fire safety. The authors showed that under certain conditions – in particular, high fire barriers, windward position of tanks and multiple spill sources – vapour concentrations can reach or exceed the lower explosive limit. Thus, the paper demonstrates for the first time the practical relationship between evaporation intensity and explosion risk, which is important for the development of effective fire safety measures in tank farms.

Another issue was investigated by M. Farzaneh-Gord *et al*. (2011), who analysed how the absorption capacity of the paint coating of crude oil storage tanks affects their temperature and, accordingly, losses in tropical climates. It turned out that when the absorption coefficient increases to 90%, annual losses increase to 200%. Similar conclusions were obtained in the publication by N.V. Liuta *et al*. (2020), which studied this problem in Ukraine. According to their data, if the solar radiation absorption coefficient of a reservoir increases from 0.3 to 0.9, this leads to an increase in petroleum product losses by approximately 40%. Thus, the results of independent studies conducted in different climatic zones indicate the need and expediency of taking into account the geographical location of reservoirs when determining the volume of losses during storage.

In their study, S.V. Boichenko & N.H. Kalmykova (2020) conducted a systematic cause-and-effect analysis of the process of petrol evaporation from horizontal

tanks using an Ishikawa diagram, which makes it possible to clearly identify the factors causing losses. The authors draw attention to the significant influence of the physical and chemical characteristics of fuel (volatility, saturated vapour pressure), ambient temperature, tank design features and operating modes on the intensity of evaporation. It has been established that the main causes include technological "breathing" losses during filling and emptying, losses due to the capillary effect in the gaps of the seals, as well as insufficient sealing and organisational shortcomings in product accounting. In addition, the economic (reduced fuel quality, shorter engine life), environmental (pollution of the atmosphere with toxic hydrocarbons) and technical consequences of such losses were assessed. The authors consider a combined approach to be the most effective measure: the introduction of both methods for accurate leak accounting (quantitative determination of losses) and organisational and technical measures for sealing and monitoring the condition of tanks. Thus, the results of S.V. Boichenko & N.H. Kalmykova (2020) emphasise the expediency of updating the methods for calculating petroleum product losses due to the need to integrate a multifactorial approach that includes the design, operational, and chemical-physical properties of fuel.

One of the compelling arguments in favour of improving calculation approaches for determining petroleum product losses is the work of A. Ahmed Alwaise *et al.* (2023), which analyses the impact of the physical properties of petroleum products on the volume of losses in vertical tanks. The authors focused on the specific gravity and volatility of products such as kerosene and gas oil, investigating changes in losses when the density (0.750-0.820 t/m^3) of samples in a volume of 1,000 m^3 varied. It was found that losses can fluctuate up to 5 m^3 per 1,000 m^3 when physical properties change. In view of this, the researchers recommend periodically checking the physical and chemical parameters of products to update the methods for calculating losses, which will reduce the discrepancies between theoretical estimates and actual values. In the context of improving existing methods, this study highlights the need to introduce correction factors or update input parameters in accordance with the actual properties of petroleum products, which will avoid systematic errors in loss calculations.

In developing the topic of the impact of operating parameters on petroleum product losses, it is also worth paying attention to the work of S. Andalucia (2023), which conducted multi-variant calculations of petroleum product losses from evaporation in two fixed-roof tanks at the SA Field PT X Prabumulih facility. The author analyses the impact of parameters such as petroleum product temperature, ambient temperature and gas space volume in the tank, establishing that an increase in free space directly correlates with an increase in oil evaporation. The economic consequences of these losses are also assessed: large volumes of losses lead to significant financial losses for the enterprise. Thus, the results of these studies also confirm the need and expediency of revising the current regulatory methodology, taking into account a complex of factors that actually influence the evaporation process. N. Kapilan *et al.* (2025) investigated the loss of petroleum products through evaporation from tanks under laboratory conditions, simulating different evaporation surface areas and petroleum product temperatures. The results confirmed that petroleum product losses increase with time, surface area and temperature.

Scientific research and practical experience in calculating petroleum product losses during storage in vertical tanks indicate an objective need for a systematic update of current regulatory approaches. The summary shows that the accuracy of loss assessment significantly depends on taking into account a wide range of factors: temperature regime, wind speed, saturated vapour pressure, gas space volume, tank design characteristics, sealing efficiency, etc. Ignoring these parameters in simplified regulatory methods leads to significant discrepancies with the results of physical and mathematical models and experimental observations. Particular attention should be paid to the introduction of correction factors, regular updating of input parameters in accordance with actual operating conditions, and the use of modern monitoring tools. In addition, the results of the analysis confirm the advisability of harmonising the regulatory framework with international standards. This will ensure high accuracy of calculations, compliance with environmental requirements, and increase the efficiency of VOC loss management. In this context, the development of an integrated methodology that combines scientific validity, adaptability to real operating conditions, and compliance with modern international approaches is particularly relevant.

Conclusions

In summary, a systematic review of the current regulatory framework in Ukraine regarding the accounting of petroleum product losses during storage in vertical tanks is required. The analysis revealed a number of limitations in the current Ukrainian regulatory framework. This methodology does not take into account a number of important factors, including the design features of tanks, climatic conditions, the properties of stored products, the degree of tank filling, the level of sealing, etc. A comparative analysis of the results obtained using different methodologies revealed significant discrepancies. Calculations showed that physical and mathematical methods (Konstantynov and EPA) are highly dependent on climatic conditions: for VCT-1000, VCT-2000 and VCT-3000 tanks, the relative error between the northern and southern climatic zones ranges from 5.9% to 12%. In contrast, the standard method practically does not take climatic differences into account (error of about 0.26%), which can lead to inaccuracies in the assessment of VOC losses in different regions.

A comparative analysis of the results obtained using different methods revealed significant discrepancies. In particular, two methods (EPA and Konstantynov), which are based on the physical and chemical principles of liquid evaporation and take into account variable parameters (gas space volume, temperature, saturated vapour

pressure), show a decrease in losses with an increase in the tank filling level. In contrast, the standard method uses a simplified relationship, where losses are proportional to the volume of petroleum products stored, which leads to the opposite trend – an increase in losses with an increase in the filling level. It has also been established that an increase in the saturated vapour pressure of petroleum products from 50 to 80 kPa increases the calculated losses by almost 1.6 times for all tanks studied. Further research will focus on developing a scientifically sound, technologically adapted and environmentally oriented methodology for determining and standardising petroleum product losses during storage in tanks.

Acknowledgements
None.

Funding
None.

Conflict of Interest
None.

References
[1] Ahmed Alwaise, A., Alrashedi, M.A., Mohammed, A.E., Ibrahim, A.I., Habeeb, O.A., Saleh, S.H., Abdulqader, M.A., & Hussein, O.A. (2023). The effect of physical properties of lost petroleum quantities in vertical tanks at (NRC) Baiji. *Energy Exploration & Exploitation*, 42(2), 685-691. doi: 10.1177/01445987231220961.

[2] Andalucia, S. (2023). Calculation of evaporation loss in tank Y and tank Z at SA field PT X Prabumulih. *Journal of Earth Energy Engineering*, 12(1), 19-27. doi: 10.25299/jeee.2023.11934.

[3] AP-42 Chapter 7, Section 1 – organic liquid storage tanks. (2024). Retrieved from https://surl.li/vzkcbb.

[4] Babić, I.M. (2023). Reduction of evaporation losses in oil and oil derivatives storage tanks: A case study for warehouse in Požega, Serbia. *Thermal Science*, 27(3(B)), 2455-2464. doi: 10.2298/TSCI220923172B.

[5] Beiranvand, F., & Najibi, H. (2021). Decrease in evaporative loss of volatile fuels using new mixture of surfactants. *Petroleum Science and Technology*, 39(23-24), 1139-1156. doi: 10.1080/10916466.2021.1986067.

[6] Boichenko, S.V., & Kalmykova, N.H. (2020). Cause and consequence analysis of losses of petroleum products in the tank park. *Science-Intensive Technologies*, 46(2), 218-223. doi: 10.18372/2310-5461.46.14810.

[7] de la Calle-Arroyo, C., López-Fidalgo, J., & Rodríguez-Aragón, L.J. (2021). Optimal designs for Antoine Equation. *Chemometrics and Intelligent Laboratory Systems*, 214, article number 104334. doi: 10.1016/j.chemolab.2021.104334.

[8] Directive of European Parliament and Council of the European Union No. 2010/75/EU "On Industrial Emissions (Integrated Pollution Prevention and Control)". (2010, November). Retrieved from https://surl.li/leuwtl.

[9] Directive of the European Parliament and of the Council No. 2004/42/CE "On the Limitation of Emissions of Volatile Organic Compounds Due To the Use of Organic Solvents in Certain Paints and Varnishes and Vehicle Refinishing Products and Amending Directive 1999/13/EC". (2004, April). Retrieved from https://eur-lex.europa.eu/legal-content/EN/TXT/?uri=CELEX%3A32004L0042.

[10] Farzaneh-Gord, M., Nabati, A., Rasekh, A., & Saadat-Targhi, M. (2011). Effects of outer surface paint color on crude oil evaporative loss from the Khark Island storage tanks. *Brazilian Journal of Petroleum and Gas*, 5(3), 123-137. doi: 10.5419/bjpg2011-0013.

[11] Instructions on the Procedure for Receiving, Transporting, Storing, Dispensing, and Accounting for Oil and Petroleum Products at Enterprises and Organisations in Ukraine. (2008, May). Retrieved from https://zakon.rada.gov.ua/laws/show/z0805-08#Text.

[12] Kapilan, N., Premnath, K., Varshitha, D., Nayak, S., & Sunil, S. (2025). Laboratory simulation studies on evaporative fuel loss from storage tanks. *BIO Web of Conferences*, 172, article number 01004. doi: 10.1051/bioconf/202517201004.

[13] Kong, X., Huang, W., Li, X., Xia, P., Zhou, N., Zhang, C., Ge, Y., Zhou, Y., & Chai, X. (2025). Numerical simulation of oil evaporation and emission loss in loading oil into railway tankers based on a VOF method. *Energy Sources, Part A: Recovery, Utilization, and Environmental Effects*, 47(1), 3093-3115. doi: 10.1080/15567036.2025.2454527.

[14] Law of Ukraine No. 2707-XII "On the Protection of Atmospheric Air". (1992, October). Retrieved from https://zakon.rada.gov.ua/laws/show/2707-12#Text.

[15] Lipinsky, V.M., Dyachuk, V.A., & Babichenko, V.M. (Eds.). (2003). *Climate of Ukraine*. Kyiv: Raevsky Publishing House.

[16] Lisafin, V., & Liuta, N. (2018). *Design and operation of oil and petroleum product storage facilities*. Ivano-Frankivsk: Ivano-Frankivsk National Technical University of Oil and Gas.

[17] Liuta, N.V., Doroshenko, Y.I., & Kuchera, N.M. (2020). Study of the impact of surface condition of a vertical steel tank on evaporation losses using the EPA methodology. In *Tendances scientifiques de la recherche fondamentale et appliquée: Collection de papiers scientifiques "ΛΟΓΟΣ"* (pp. 96-102). Strasbourg: Plateforme Scientifique Européenne. doi: 10.36074/30.10.2020.V1.29.

[18] Norms of Petroleum Product Losses During Their Reception, Storage, Dispensing, Transshipment and Transportation. (2020, August). Retrieved from https://zakon.rada.gov.ua/laws/show/686-2020-п#Text.

[19] Orozco, P., Pugliese, V., Gonzalez-Quiroga, A., & Arango, A. (2023). Technological advances for estimating and reducing gasoline evaporation losses in the petroleum industry. In *2023 IEEE Colombian Caribbean conference (C3)* (pp. 1-6). Barranquilla: IEEE. doi: 10.1109/C358072.2023.10436276.

[20] Raazi Tabari, M.R., Sabzalipour, S., Peyghambarzadeh, S.M., & Jalilzadeh Yengejeh, R. (2020). Determining the emission rates of volatile organic compounds and modeling their dispersion from the petroleum and chemical storage tanks of the largest oil terminal in the southwest of Iran. *Journal of Advanced Environmental Health Research*, 8(4), 269-280. doi: 10.22102/jaehr.2021.251979.1187.

[21] Rajabi, H., Mosleh, M.H., Mandal, P., Lea-Langton, A., & Sedighi, M. (2020). Emissions of volatile organic compounds from crude oil processing – global emission inventory and environmental release. *Science of The Total Environment*, 727, article number 138654. doi: 10.1016/j.scitotenv.2020.138654.

[22] Resolution of the Cabinet of Ministers of Ukraine No. 686 "On Approval of the Norms of Petroleum Product Losses During Their Reception, Storage, Dispensing, Transshipment and Transportation". (2020, August). Retrieved from https://zakon.rada.gov.ua/laws/show/686-2020-п#Text.

[23] Ribeiro, G.C., de Barros Gallo, A., Fossa, A.J., Pereira, E.G., & dos Santos, E.M. (2024). Standardization and benchmark initiatives for emission reduction in the petroleum industry. *REM: International Engineering Journal*, 77(4). doi: 10.1590/0370-44672023770125.

[24] Stef, N., & Ashta, A. (2023). Dynamics in environmental legislation. *International Review of Law and Economics*, 76, article number 106170. doi: 10.1016/j.irle.2023.106170.

[25] Wu, C., Huang, W., Chen, F., Xu, X., Li, X., & Wang, X. (2022). Analysis of oil vapor diffusion after oil spill from tank group based on wind tunnel experiment and numerical simulation. *Petroleum Science and Technology*, 42(3), 303-320. doi: 10.1080/10916466.2022.2134894.

[26] Xing, G., Zhang, Y., & Guo, J. (2023). Environmental regulation in evolution and governance strategies. *International Journal of Environmental Research and Public Health*, 20(6), article number 4906. doi: 10.3390/ijerph20064906.

[27] Yang, H., Ren, B., Huang, Y., Zhang, Z., Hu, W., Liu, M., Zhao, H., Jiang, G., & Hao, Z. (2024). Volatile organic compounds (VOCs) emissions from internal floating-roof tank in oil depots in Beijing: Influencing factors and emission reduction strategies analysis. *Science of The Total Environment*, 916, article number 170222. doi: 10.1016/j.scitotenv.2024.170222.

[28] You, G., Lu, S., Jin, Z., Ren, J., Sun, R., Li, J., Hou, W., & Xie, S. (2024). Emission factors and source profiles of volatile organic compounds in the petroleum refining industry through on-site measurement from multiple refineries. *Environmental Science & Technology Letters*, 11(3), 230-236. doi: 10.1021/acs.estlett.4c00036.

Про необхідність і доцільність перегляду та удосконалення методики розрахунку втрат нафтопродуктів від випаровування за результатами розрахунково-порівняльного аналізу

Наталія Люта

Кандидат технічних наук, доцент
Івано-Франківський національний технічний університет нафти і газу
76019, вул. Карпатська, 15, м. Івано-Франківськ, Україна
https://orcid.org/0000-0002-3321-0982

Юлія Дорошенко

Кандидат технічних наук, доцент
Івано-Франківський національний технічний університет нафти і газу
76019, вул. Карпатська, 15, м. Івано-Франківськ, Україна
https://orcid.org/0000-0002-7196-9383

Михайло Пілецький

Аспірант
Івано-Франківський національний технічний університет нафти і газу
76019, вул. Карпатська, 15, м. Івано-Франківськ, Україна
https://orcid.org/0009-0005-9885-2467

Анотація. Метою роботи було проаналізувати нормативну базу обліку втрат нафтопродуктів в Україні. Здійснено компаративний і емпіричний аналіз трьох методик визначення втрат нафтопродуктів від випаровування. Виконано розрахунки втрат бензину від «малих дихань» у вертикальних сталевих резервуарах номінальним об'ємом 1 000, 2 000 та 3 000 м^3 у різних кліматичних зонах України. Проведено оцінку впливу рівня заповнення резервуара та тиску насичених парів на втрати. Порівняльний аналіз виявив, що методики EPA та Константинова демонструють фізично обґрунтоване зменшення втрат при підвищенні рівня наливу, а також високу чутливість до кліматичних умов. Для резервуара РВС-3000 відносна похибка між розрахунками для середньої та південної кліматичних зон за методикою Константинова становить 6,9-10,6 %, а за методикою EPA – 8,5-12,0 %. Для РВС-2000 ці показники становлять 5,9-9,3 % (Константинова) та 6,9-10,5 % (EPA), а для РВС-1000 – 6,9-10,6 % і 8,5-12 % відповідно. Натомість розрахунки за нормативною методикою показали практично нульову чутливість до кліматичної зони (відносна похибка ~0,26 %), що суперечить реальним умовам експлуатації й призводить до потенційно значних похибок в оцінці втрат летких органічних сполук. Це свідчить про необхідність перегляду чинних українських норм з урахуванням сучасних фізико-хімічних моделей випаровування. Додатково проаналізовано вплив тиску насичених парів нафтопродукту за Рейдом на величину втрат. Результати розрахунків для середньої та південної кліматичних зон показали, що зростання тиску насичених парів від 50 кПа до 80 кПа спричиняє збільшення втрат приблизно в 1,6 рази для всіх досліджуваних типів резервуарів. Це підтверджує високу чутливість фізико-математичних методик до фізико-хімічних властивостей нафтопродуктів, на відміну від нормативного підходу, який не враховує цей параметр. Отримані результати можуть бути використані для розробки адаптованої комбінованої методики, що поєднує точність міжнародних стандартів із простотою нормативного обліку

Ключові слова: бензин; малі дихання; тиск насичених парів; кліматичні зони; резервуари; нормативний документ

ISSN 1993-9973, e-ISSN 2415-332X

Vol. 25, No. 2
2025

PROSPECTING AND DEVELOPMENT OF OIL AND GAS FIELDS

https://pdogf.com.ua/en

Received: 15.07.2025. Revised: 03.11.2025. Accepted: 08.12.2025. Published: 09.01.2026.

UDC 622.276.53.054

DOI: 10.63341/pdogf/2.2025.36

Kinematic analysis of the characteristics of a crank-pulley rocking machine

Viktor Kharun*

PhD in Technical Sciences, Associate Professor
Ivano-Frankivsk National Technical University of Oil and Gas
76019, 15 Karpatska Str., Ivano-Frankivsk, Ukraine
https://orcid.org/0000-0003-1422-6003

Vasyl Popovych

PhD in Technical Sciences, Associate Professor
Ivano-Frankivsk National Technical University of Oil and Gas
76019, 15 Karpatska Str., Ivano-Frankivsk, Ukraine
https://orcid.org/0000-0003-2438-8532

Ivan Petryk

PhD in Technical Sciences, Associate Professor
Ivano-Frankivsk National Technical University of Oil and Gas
76019, 15 Karpatska Str., Ivano-Frankivsk, Ukraine
https://orcid.org/0000-0003-0863-5476

Zinovii Odosii

PhD in Technical Sciences, Professor
Ivano-Frankivsk National Technical University of Oil and Gas
76019, 15 Karpatska Str., Ivano-Frankivsk, Ukraine
https://orcid.org/0000-0003-0914-2489

Abstract. Oil production enterprises in Ukraine mainly use traditional balance drives, which have proven their reliability over many years of operation. New drive schemes, in terms of efficiency, require a comparative assessment of their characteristics with balance drives. For the purpose of comparative analysis and calculation of the kinematic parameters of the crank-pulley drive, which was operated at the Oil and Gas Production Department Okhtyrkanaftogaz of the Public Joint Stock Company Ukrnafta from 1993 to 2021, the paper presents the development of its mathematical model. For this purpose, geometric dependencies were used to calculate the length of the rope, which acts as a flexible link, and, accordingly, the displacement of the rod suspension. By differentiating the displacement graph, the corresponding kinematic characteristics were obtained – velocities and accelerations, which are components for calculating the moment of resistance forces reduced to the crank of the executive mechanism. The coefficients of mean square deviation calculated for traditional sucker-rod pumping units and crank-pulley drives allowed a comparative assessment of their balancing quality. Their characteristics were compared based on the load of the executive mechanism using a typical static dynamogram, since the accepted rotation speed of the crankshaft of sucker-rod pumping unit is less than 8 rpm. It was determined that the root mean square deviation of the torque of the crank-pulley drive was 9.47 kN×m, which is 33.6% less than that of a traditional balancing drive. Using a developed mathematical model, which employs the vector contour method, a system of linear equations was obtained to determine the dependence of the rotation angle φ_2 of the lower crossbar, to which the rope is attached, and the rotation angle φ_3 of the movable pulley on the rotation angle φ_1 of

Suggested Citation: Kharun, V., Popovych, V., Petryk, I., & Odosii, Z. (2025). Kinematic analysis of the characteristics of a crank-pulley rocking machine. *Prospecting and Development of Oil and Gas Fields*, 25(2), 36-47. doi: 10.63341/pdogf/2.2025.36.

*Corresponding author

the crank. It has been established that the movable pulley changes its direction of movement twice per revolution of the crank of the executive mechanism, which may be the cause of accelerated wear of the drive rope

Keywords: root mean square deviation; downhole rod pump unit; mathematical model; pump drive; reduced torque

Introduction

During 1993-2021, the Oil and Gas Production Department (OGPD) Okhtyrkanaftogaz of the Public Joint Stock Company (PJSC) Ukrnafta operated sucker-rod pumping units with a crank-pulley drive, which were later decommissioned due to the complexity of their maintenance. Most commonly, these sucker-rod pumping units are designed with a double-arm balancer. There are many types of executive mechanisms based on this design, which differ in the length of the front and rear arms (beams) of the balancer and other geometric dimensions. Despite the long period of use of such drives, researchers are working on improving their design methods.

J. Wang *et al.* (2025) proposed a new design scheme for the executive mechanism of a double-arm balancing drive by sequentially optimising both their kinematic and dynamic characteristics. The effectiveness of the new design was compared by calculating the root mean square value of the torque. Researchers J. Xu *et al.* (2022) improved the method of balancing a downhole rod pumping unit (DRPU) equipped with a double-arm balancer drive. The modified design of the executive mechanism, due to the placement of secondary balancing counterweights rotating at double angular velocity, made it possible to avoid changing the sign of the crank torque, which reduced the energy consumption of the drive electric motor.

Z.W. Gao & S. Jia (2024) conducted a review of methods for modelling and controlling balance drives and their mathematical models. It was determined that comparisons of the effectiveness of different methods should be based on comparisons with a reference mathematical model. Scientists A. Malyar & S. Cieslik (2023) developed mathematical models of a balance drive to calculate the process of changing the capacity of cosine capacitors to compensate for reactive power in the starting and steady states of an electric drive of DRPU. As a result, the change in the sign of the crankshaft torque was compensated by adjusting the capacitance of the capacitors.

In the publication by A.M. Aliyev & S.Y. Aliyeva (2023), the mathematical model of the DRPU was expanded in terms of modelling the processes of downhole equipment, in particular the stress-strain state of the valve assembly of a well pump. The influence of friction forces on the deformation and destruction of rods was determined, taking into account the kinematics of the rod string. The geometry of the DRPU drive usually includes several of the most common types of drives (sucker-rod pumping units) such as: traditional double-arm or single-arm balance drives with counterweights placed on cranks, called sucker-rod pumping units, long-stroke drives, which are used for significant lengths of well pump stroke (GE Oil & Gas, n.d.).

The situation is no different in Ukrainian fields. According to research by V.V. Savchuk (2016), ten oil fields were developed at the Dolyna Naftogaz Oil and Gas Production Company with an operational fund of 392 production wells, with an average depth of 2,700 metres. All major fields are in the late stages of development, which is characterised by high water cut – over 86%. More than 70% of wells are operated using balance drives. For wells with high oil flow rates, the use of non-balancing long-stroke DRPU drives (Weatherford, n.d.) is proposed, the design of whose executive mechanisms differs from that of balancing drives. In addition, the search for a replacement for the balancing drive with other executive mechanism schemes, for example, through the use of a hydraulic drive, continues. To determine the technical condition of DRPU equipment, the most common method remains the dynamographic method, which is constantly being improved. Based on this method, models are being developed for diagnostics, taking into account the actual dynamic level of fluid in the well in order to determine the energy of the oil and gas reservoir for selecting the necessary operating modes of sucker-rod pumping units (Zhang *et al*., 2021).

Analysis of scientific research allows to conclude that analytical calculations according to the developed mathematical models of traditional balance drives can be used as a basis for comparing the kinematic and dynamic characteristics of other drive schemes. Given the originality of the design of the crank-pulley drive executive mechanism and the absence of publications by Ukrainian researchers that theoretically confirm the advantages or highlight the disadvantages of such a drive scheme for DRPU, the purpose of this study was to calculate the kinematic parameters of the developed mathematical model for comparative evaluation with similar balance drives.

Materials and Methods

The structural diagram of the unbalanced crank-pulley drive of a well rod pump (DPCP) is shown in Figure 1. The DPCP operates as follows. Crank 1 rotates at an angular velocity ω_1 around the standpipe O and drives the tension pulley 2, which is covered by rope 3 thrown over the guide pulley 4. At point E, the rope is attached to the rod suspension 5, and at O_2 to a fixed link. Crank 1 has an L-shape, with a guide pulley hinged to one end, at A, and crank counterweights located at the other end, deflected by an angle α, at point B. When the crank rotates around the stand O, it pushes the tension pulley 2, which begins to move the rope 3, simultaneously rotating at an angular velocity ω_2. The movement of the rope is transmitted to the guide pulley 4, which rotates around the stand O_1 at an angular velocity ω_3, changing the direction of the rope's movement to vertical and, thus, the rod suspension E together with the rod string performs a translational movement, which is transmitted to the plunger of the deep well pump 7, which is located

in the pump-compressor pipe string 8. The weight of the rod string and the liquid above the plunger of the deep well pump is balanced by counterweights 9 located on the crank. During the operation of the rocker machine, the plunger 7 of the deep pump performs a reciprocating motion, moving from the extreme lower to the extreme upper position. The stroke of the plunger h is defined as the difference in the displacement of the rod suspension between its two extreme positions, which are defined by E_0 and E' (Fig. 2).

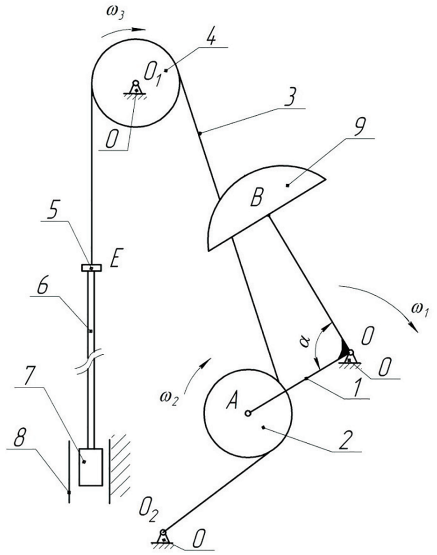

Figure 1. Structural diagram of DPCP

Note: 0 – fixed link (frame to which other moving links are attached); 1 – crank; 2 – tension (moving) pulley; 3 – rope; 4 – guide pulley; 5 – rod suspension; 6 – rod string; 7 – deep well pump plunger; 8 – tubing string (TS); 9 – crank counterweights
Source: developed by the authors based on Osnastka NPP (2001)

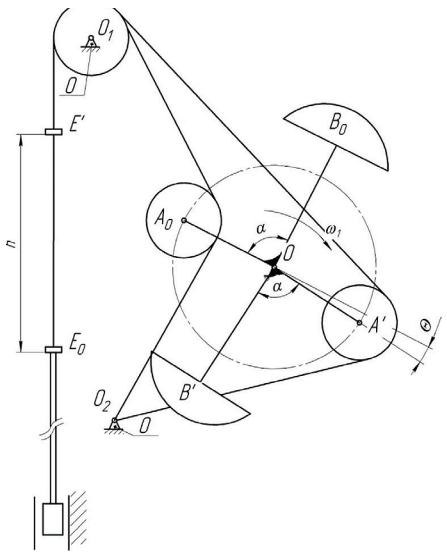

Figure 2. Extreme positions of the DPCP executive mechanism

Source: developed by the authors based on Osnastka NPP (2001)

The dimensions of the links are selected in such a way that between the extreme positions of the crank, which are determined by the lengths of segments OA_0 and OA', an angle of misalignment Q is formed, which allows the average speed of the rod suspension to be redistributed – reducing its value for the working stroke (upward movement of the rod suspension). This angle is calculated using the formula:

$$\theta = 180 \times \frac{k_v - 1}{k_v + 1}, \quad (1)$$

where k_v – crank average speed variation coefficient.

$$k_v = \frac{V_{up}}{V_d}, \quad (2)$$

where V_{up}, V_d – average speed of the rod suspension for its upward and downward movement. To compare the capabilities of this drive with traditional sucker-rod pumping unit, a mathematical model was created (Fig. 3), which was used to calculate the kinematic characteristics. For ease of reading the diagram, the part of the crank with counterweights is not shown.

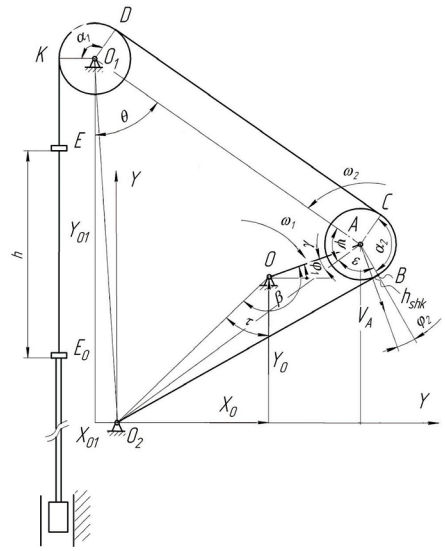

Figure 3. Calculation scheme of the executive mechanism
Source: developed by the authors

The displacement of the rod suspension h is calculated as the difference in rope length between its lower and upper extreme positions (E):

$$S_k = l_k - l_{k0}, \quad (3)$$

where l_k, l_{k0} – the, rope length in the arbitrary and initial (extreme) position of the crank:

$$l_k = O_2B + BC + CD + DK + KE, \quad (4)$$

where O_2B – the length of the rope between the standpipe and point B where the rope contacts the movable pulley.

$$O_2B = \sqrt{O_2A^2 - AB^2}, \quad (5)$$

where $AB = r_{shk}$ – the radius of the moving pulley. The length of the rope between A and B at the point where it attaches to the pulley is variable and depends on the position of the crank OA:

$$O_2A = \sqrt{(X_O + X_A)^2 + (Y_O + Y_A)^2}, \quad (6)$$

where X_O, Y_O – the projection of coordinate O on axes X and Y; $X_A = rkr \times \cos(\varphi_1)$ – the projection of crank length r_{kr} on axis X; $Y_A = r_{kr} \times \sin(\varphi_1)$ – the projection of crank length r_{kr} on axis Y; φ_1 – the crank rotation angle, calculated relative to the positive direction of axis X. Length of rope covering the movable pulley on the arc BC:

$$BC = r_{shk} \times \alpha_2, \quad (7)$$

where α_2 – the angle of rope coverage of the movable pulley.

$$\alpha_2 = \frac{3}{2} \times \pi - \varepsilon - \psi, \quad (8)$$

where $\varepsilon = \tan^{-1}\left(\frac{O_2B}{r_{shk}}\right)$; $\psi = \cos^{-1}\left(\frac{O_2A^2 + O_1A^2 - O_1O_2^2}{2 \times O_2A \times O_1A}\right)$, where $O_1O_2 = \sqrt{X_{01}^2 + Y_{01}^2}$. The length of the rope between points DC is equal to the length:

$$A = \sqrt{(Y_{O1} - Y_A)^2 + (X_O + X_A)^2}. \quad (9)$$

Length of rope covering the guide pulley:

$$DK = (\pi - \theta) \times r_{shk1}, \quad (10)$$

where r_{shk1} – the radius of the fixed pulley. The length of the rope in the initial position is calculated according to Figure 2, when point A of the crank is in such a position that the length of the rope l_k is minimal. By performing numerical differentiation of this graph, the dependence of the rod suspension speed is obtained, which is a component for calculating the reduced moment acting on the crankshaft. However, a special feature of this executive mechanism is that the DPCP drive contains a movable pulley 2, which changes the direction of its rotation several times during one revolution of the crankshaft, so this must be taken into account when constructing a mathematical model. To determine the dependence of the angular velocity of the movable pulley on the angle of rotation of the crank 1, the vector contour method was used, the calculation scheme of which is shown in Figure 4.

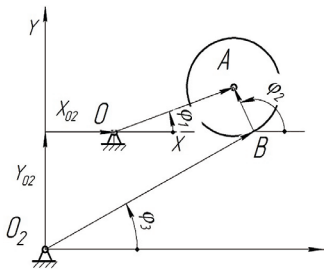

Figure 4. Vector contour for determining the kinematic parameters of a moving pulley

Source: developed by the authors

Equation of a vector contour:

$$\vec{l}_{OA} = \vec{X}_{O2} + \vec{Y}_{O2} + \vec{l}_{O2B} + \vec{l}_{AB}. \quad (11)$$

Projections on the axis to determine the unknowns φ_2 – the angle of rotation of the moving pulley and φ_3 – the angle of rotation of the rope:

$$\begin{cases} l_{OA} \times \cos\varphi_1 = -X_{02} + l_{O2B} \times \cos\varphi_3 + l_{AB} \times \cos\varphi_2 \\ l_{OA} \times \sin\varphi_1 = -Y_{02} + l_{O2B} \times \sin\varphi_3 + l_{AB} \times \sin\varphi_2 \end{cases}. \quad (12)$$

Solving the system of equations (12) allows obtaining the dependence of the angle of rotation φ_3 of the lower crossbar to which the rope is attached at O_2 and the angle of rotation φ_2 of the movable pulley. Differentiating equation (12) with respect to time t, the expressions for determining the angular velocities ω_2 and ω_3 are found:

$$\begin{cases} -l_{OA} \times \sin\varphi_1 \times \omega_1 = -l_{O2B} \times \sin\varphi_3 \times \omega_3 - l_{AB} \times \sin\varphi_2 \times \omega_2 \\ l_{OA} \times \cos\varphi_1 \times \omega_1 = l_{O2B} \times \cos\varphi_3 \times \omega_3 + l_{AB} \times \cos\varphi_2 \times \omega_2 \end{cases}. \quad (13)$$

The power of the drive motor depends on the shape of the torque curve acting on the drive crankshaft. Therefore, the next task was to determine the reduced torque acting on the crankshaft, taking into account the placement of crankshaft counterweights on it, which is determined according to the equation:

$$M_{zv}^0(\varphi_1) = M_F(\varphi_1) + M_{kr}(\varphi_1) + M_{pr}(\varphi_1), \quad (14)$$

where $M_F(\varphi_1)$ – the moment reduced to a crank from the force of useful resistance acting at the point of suspension of the rods; $M_{kr}(\varphi_1)$ – the moment created by the mass of the crank; $M_{pr}(\varphi_1)$ – the moment created by the masses of crank counterweights.

$$M_{zv}^0(\varphi_1) = F_{ko} \times \frac{V_E}{\omega_1} \times \cos\alpha_1 + \left(G_{shk} + \frac{1}{2} \times G_{kr}\right) \times \times l_{OA} \times \cos\varphi_1 + G_{bpr} \times l_{spr} \times \cos(\varphi_1 - \alpha), \quad (15)$$

where F_{ko} – the force of useful resistance acting on the bar suspension; V_E – the speed of the point of application of the force of useful resistance; ω_1 – the angular velocity of the crank; α_1 – the angle between the direction F_{ko} and velocity V_E; G_{shk} – the pulley weight; G_{kr} – the crank weight; G_{bpr} – the weight of counterweights; l_{spr} – the distance to the centre of mass of the counterweights; α – the angle between crankshaft beams. The components of the combined moment of resistance forces are shown in Figure 5.

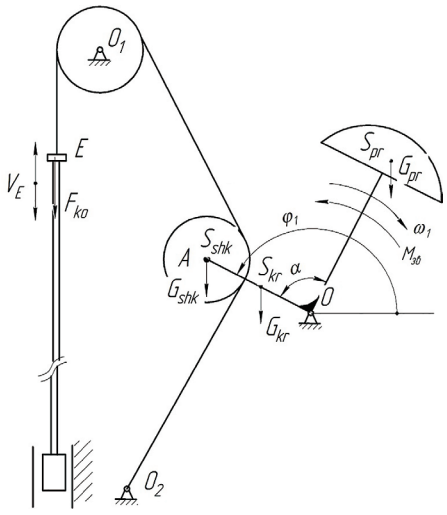

Figure 5. Components of the combined moment of resistance forces

Source: developed by the authors

In this case, the value of the useful resistance force is calculated taking into account the displacement of the rod suspension in accordance with the calculation scheme developed above (Fig. 3) for the upward (16) and downward (17) movement of the rod suspension:

$$\begin{cases} F_{ko} = \left(F_{min} + (F_{max} - F_{min}) \times \frac{S_E}{\lambda_1}\right) \times S_E \le \lambda_1 \\ F_{ko} = F_{max} \times \lambda_1 \le S_E < H; \end{cases} \quad (16)$$

$$\begin{cases} F_{ko} = \left(F_{max} - (F_{max} - F_{min}) \times \frac{H - S_E}{\lambda_1}\right) \times S_E \ge H - \lambda_2 \\ F_{ko} = F_{min} \times S_E < H - \lambda_2, \end{cases} \quad (17)$$

where H – stroke E of the rod suspension. For a dynamic dynamogram, the values F_{min} and F_{max} are calculated taking into account the acceleration of point E of the rod suspension:

$$\begin{cases} F_{min}^{d} = F_{min} \times a_E \\ F_{min}^{d} = F_{max} \times a_E, \end{cases} \quad (18)$$

where a_E – the acceleration of the rod suspension. The criterion for comparing the efficiency of balancing the DRPU drives is the coefficient of the root mean square deviation of the torque, which is calculated using the formula V.R. Kharun *et al*. (2021):

$$\sigma_M = \sqrt{\frac{\int_0^{2\pi} M_{zv^2} \times d\varphi_1}{2 \times \pi}}, \text{ H×m}, \quad (19)$$

where M_{zv} – the crank-reduced moment of resistance forces; φ_1 is the crank rotation angle.

Results and Discussion

Further on, a comparative analysis of the developed mathematical model of the DRPU crank-pulley drive with known analogues is presented, and its kinematic, dynamic and energy characteristics are considered in order to evaluate the efficiency and quality of the drive balancing. The manufacturers of the DPCP drive have determined that the unique geometry of this executive mechanism allows it to consume 1.5 times less electricity compared to a traditional balance drive (Osnastka NPP, 2001). However, these drives have not found wide application. The most widely used balancing drive in the world, the sucker-rod pumping unit, continues to be used in oil fields, accounting for more than 80% of oil production. To compare the capabilities of the drive with traditional sucker-rod pumping units, a mathematical model was created.

A similar mathematical model of a sucker-rod pumping unit with a crank-pulley drive, in which the crank with a drive pulley located on it is positioned with a certain eccentricity relative to another crank on which balancing counterweights are installed, was developed by researchers J. Xu *et al.* (2024). The drive scheme of these authors differs from the one considered in this article in that the counterweights are located on separate cranks, the axis of rotation of which coincides with the axis of rotation of the cranks with a movable pulley, but is located at a certain distance. This made it possible to improve the balance of the drive. In this mathematical model, the displacement of the rod suspension is determined by calculating the change in the length of the rope driven by the movable pulley, similar to the article presented, but the kinematics of the movable pulley is not taken into account. The researchers tested the prototype in the field, which allowed them to conclude that this design reduced the power of the drive motor by 80%, reduced the weight of the drive by 25%, and saved more than 50% of electricity. Thus, the advantage of such drives over traditional sucker-rod pumping units has been determined.

The mathematical model of the DPCP developed in this publication made it possible to determine the displacement of the rod suspension according to formula (3), determining the difference in rope lengths for the upper and lower positions of the rod suspension, similar to the model by J. Xu *et al*. (2024). However, it differs in the rope direction scheme from the drive (moving) pulley to the guide pulley, and this model additionally takes into account the kinematics of the moving pulley. The first kinematic characteristic that makes it possible to evaluate the correctness of the mathematical model is the displacement of the rod suspension. An example of constructing graphs of the dependence of the displacement of point E – the rod suspension – on the angle of rotation of the crank for different stroke lengths is shown in Figure 6.

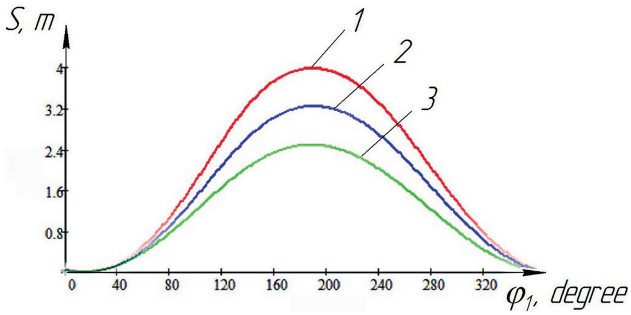

Figure 6. Stroke graphs for different plunger stroke lengths

Note: 1 – 4 m; 2 – 3 m; 3 – 2.5 m

Source: developed by the authors

The graph showing the dependence of the displacement of the suspension point of the rods on the angle of rotation of the crank is used by researchers to compare the differences between the proposed models of new executive mechanisms of DRPU drives and traditional balance drives. The authors J. Shao *et al.* (2021) developed an DRPU drive using a gear rack mechanism to transfer motion to the rod suspension. To confirm the difference in the movement of the rod suspension, they constructed a graph of the movement of the rod suspension of their proposed drive, along with a graph of a traditional sucker-rod pumping unit.

Displacement graphs are used not only to compare the performance of new drive models, but also to select the most efficient design for existing balance drives. B. Wang (2021) proposed an improved DRPU balance drive scheme with dynamic balancing tracking. The advantages of this scheme, compared to balance drives, were determined using displacement, velocity, and acceleration

graphs of the rod suspension point. Similarly, in this work, three displacement graphs of the rod suspension were constructed, which made it possible to evaluate the nature of displacement changes for different stroke lengths.

The developed mathematical model made it possible to compare the nature of the displacement change of the rod suspension. For this purpose, a comparison was made with a traditional balance drive with a rod suspension stroke of 3 m (Fig. 7). The maximum displacement of the rod suspension is 3 m, while for a traditional sucker-rod pumping unit, the crank rotation angle is 187°, and the desaxial angle is 7°, while in the DPCP drive, the rotation angle is 189°, i.e., the desaxial angle is increased to 9°. The desaxial angle characterises the duration of the working and idle strokes. Increasing the duration of the working stroke, during which the maximum load is applied to the rod suspension, allows for a more even distribution of the load on the drive.

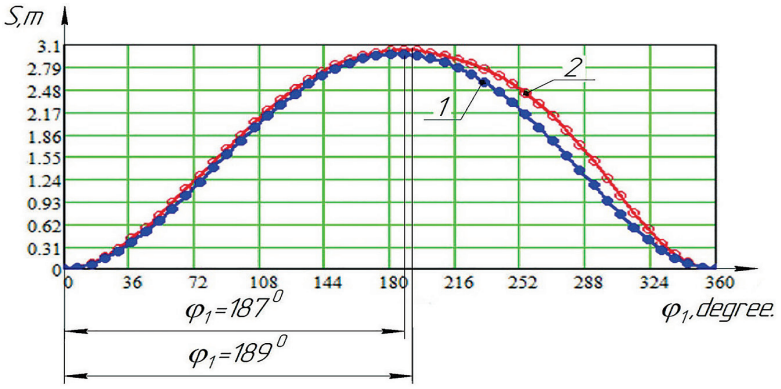

Figure 7. Rod suspension movement graphs for a stroke length of 3 m
Note: 1 – traditional balance drive; 2 – drive with DPCP
Source: developed by the authors

The dependence of the speed of the rod suspension can be obtained by differentiating the displacement, which can be done using analytical methods, as used by A.M. Aliyev & S.Y. Aliyeva (2023) and J. Wang *et al.* (2025), or numerical methods (Han *et al.*, 2025). Figure 8 shows the graphs of the speed of the rod suspension of a traditional balance drive and a crank-pulley drive, constructed by numerical differentiation of the displacement graphs, for the same crank rotation speed of 6.5 rpm.

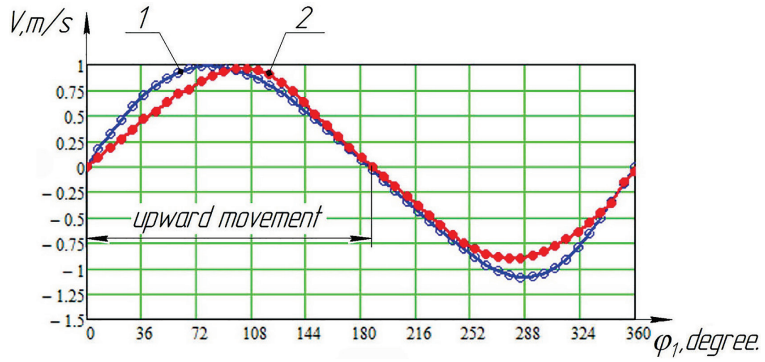

Figure 8. Rod suspension speed charts for a stroke length of 3 m
Note: 1 – traditional balance drive; 2 – drive with DPCP
Source: developed by the authors

Comparing speed graphs shows the advantages of new designs over traditional balance drives. From the analysis of these graphs (Fig. 8), it can be concluded that for a traditional sucker-rod pumping unit, the maximum speed value corresponds to 0.99 m/s for the upward stroke of the rod suspension and 1.08 m/s for the downward stroke. Accordingly, for a crank-pulley drive, the speed value for upward movement will be 0.96 m/s, which is close to the traditional value, but for downward movement it reaches 0.9 m/s. That is, for the DPCP drive, the difference in speeds for upward and downward movement will be smaller. Since the power at the rod suspension point is the product of speed and useful resistance force, the smaller the speed fluctuation, the lower the power consumption of the drive. Figure 9 shows the acceleration graphs of the suspension point of the rods of a traditional balance drive and a DRPU crank-pulley drive. Acceleration is a component of inertial force, which can be calculated using formula (18).

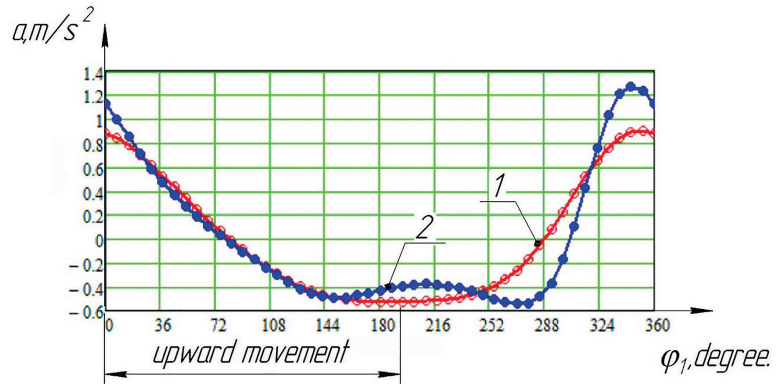

Figure 9. Acceleration graphs for rod suspension for a stroke length of 3 m

Note: 1 – traditional balance drive; 2 – drive with DPCP
Source: developed by the authors

Comparing the graphs, it can be seen that for the crank-pulley drive, the acceleration value is 20% lower at the beginning of the rod suspension's upward movement, but when the crank rotates by 22°, it actually equals the acceleration of a traditional balance drive. Also, at the end of the second phase of movement, when the rod suspension moves down, the acceleration value is also 26% lower than that of a traditional balance drive, which increases when the crank rotates from 324° to 360°. The developed mathematical model allows calculating the angular velocity of the moving pulley and the lower crossbar (Fig. 10), to which a rope is attached at point O_2 (Fig. 3).

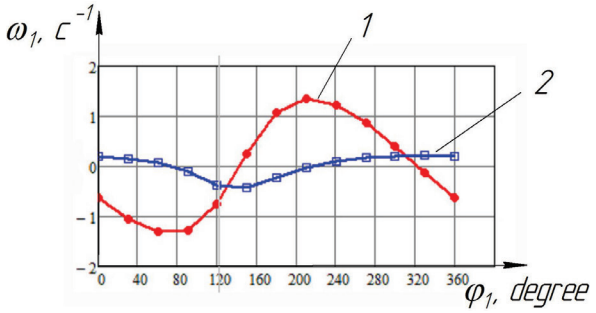

Figure 10. Angular velocities of the moving pulley 1 and the lower crossbar 2

Source: developed by the authors

Analysing the graphs, it can be noted that the angular velocity of the moving pulley changes the direction of its rotation twice per crank revolution and reaches 1.3 rad/s. Since the drive pulley is in contact with the rope, the movement of which is transmitted to the rod suspension, the change in the direction of movement leads to a similar change in the direction of the friction force, and this can cause increased rope wear. In formula (15), the effective resistance force F_{ko} is a mechanical characteristic (dynamogram) that shows how the force acting on the rod suspension changes depending on the displacement of point E of the rod suspension. The graph of this force is the basic component for balancing the sucker-rod pumping unit (Takacs & Kis, 2021).

In the work of R. Zhang *et al*. (2021), a study was conducted on the influence of the condition of the downhole pump on the shape of surface and downhole dynamograms. It was noted that the shape of the dynamogram depends on the dynamic level of fluid in the well, the presence of gas, rod breakage, high or low plunger seating of the deep well pump, and other conditions of deep well equipment. F.C. de Oliveira & O.J. Romero (2024) modelled dynamograms to evaluate the strategy for optimising production processes in DRPU oil production. These researchers compared dynamograms with a theoretical (static) dynamogram, which does not take into account the dynamic loads caused by the acceleration and vibration of the links.

A dynamic dynamogram (Fig. 11, curve 2), which takes into account the acceleration of the rod suspension (18), has a certain effect on the shape of the torque, as noted in the studies by G. Takacs & L. Kis (2021), so this must be taken into account in order to achieve a better balance of the balance drive. Scientists note that traditionally, most researchers do not take into account the influence of inertial forces on the torque of the crankshaft. Figure 11 shows a static dynamogram that was modelled for the design of a rod string, taking into account the deformation of the rods and the pump-compressor pipe string when they are subjected to the load from the weight of the fluid (Fig. 11, curve 1) according to formulas (16-17) and a dynamic dynamogram, using the formula (18).

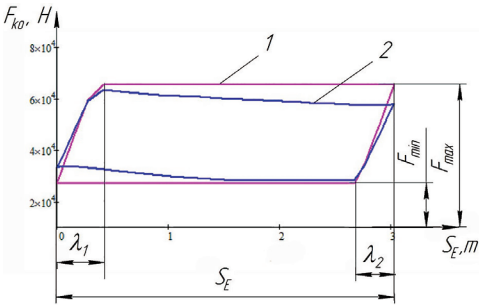

Figure 11. Typical dynamograms

Note: 1 – static; 2 – dynamic
Source: developed by the authors

For both dynamograms, it is possible to identify characteristic sections where the maximum load F_{max} acts, caused by the rod suspension perceiving the static load of the rod string and the fluid above the plunger, and the minimum load F_{min}, the main component of which is the weight of the rod string. During the transfer of load from the pump-compressor pipe column to the rod column, they are deformed by an amount λ_1 during the upward movement of the rod suspension and reverse deformed by an amount λ_2 during its downward movement. Since, according to Figure 9, the acceleration graphs of the balance and crank-pulley drives practically coincide in the phase of the rod suspension's upward movement, when the maximum load is applied to the drive, and most authors use a static dynamogram for kinematic analysis, it was decided to calculate the torque of the crank shaft using a static dynamogram.

Authors Z.W. Gao & S. Jia (2024) conducted a comparative analysis of the works of researchers who studied intelligent methods of controlling DRPU. It is noted that most of them focused on controlling the drive motor (52%) and the well fluid pumping system (34%), respectively. The main works concerned increasing the efficiency of the installation as a whole (31% of scientific publications) and reducing the power of the electric motor (28% of works), 16% on controlling the torque of the electric motor, 12% on the speed of pumping fluid from the well, and 13% on controlling the speed of rotation of the electric motor shaft. These findings are confirmed by researchers T.A. Aliev *et al.* (2022), who conducted early diagnostics of the technical condition of the DRPU equipment and controlled the drive electric motor using frequency converters.

The authors B. Ahmedov *et al.* (2023) claim that when switching from a balanced pump unit to an unbalanced one, the efficiency coefficient (EC) decreases from 83.4% to 65%. Similarly, researchers A. Malyar & M. Malyar (2025) combined the optimisation of the DRPU, choosing the torque of the crank and the delivery coefficient of the deep well pump as the optimisation criteria. Other scientists, D. Feng *et al.* (2022), created a parametric model of a balance drive and optimised it by developing a neural network in which one of the optimisation factors was the torque of the crankshaft. Therefore, in the presented DPCP model, this parameter was selected for the study, the graph of which was obtained as the result of two torques reduced to the crank – from the force of useful resistance $M_F(\varphi_1)$ and the moment of crank counterweights $M_{pr}(\varphi_1)$. The graphs of these moments, which are included in formula (15), calculated for the crank-pulley drive are shown in Figure 12.

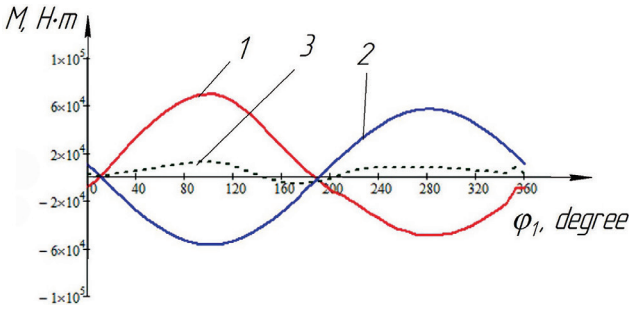

Figure 12. Moment graphs

Note: 1 – $M_F(\varphi_1)$; 2 – $M_{pr}(\varphi_1)$; 3 – $M_{zv}(\varphi_1)$
Source: developed by the authors

As can be seen from the analysis of the graph of the resulting torque $M_{zv}(\varphi_1)$, when the crank rotates from 0 to 150°, the torque is positive, from 150° to 205° it is negative, and from 205° to 360° it is positive again. Thus, the crank-pulley drive scheme cannot avoid a change in the sign of the torque, which is a negative factor in the operation of the drive. The same conclusion was reached by B. Ahmedov *et al.* (2021), who studied the balancing of the DRPU unbalanced drive and noted the presence of a negative part of the torque, which leads to shocks in the gear transmission of the reducer, increased wear and tear, and tooth breakage. As a result, it is impossible to completely eliminate this phenomenon, so efforts should be made to limit the magnitude of the negative torque by means of high-quality balancing.

The presence of a negative torque component was also noted by scientists in the work of G. Takacs & L. Kis (2021), which additionally investigated the influence of inertial forces and provided recommendations for improving balance, taking into account the position of the centre of mass of the counterweights, which leads to a reduction in both the negative part and the amplitude of the torque. It was noted that the traditional method of optimising torque, which consists of equalising its maximum values for the upward and downward movement of the suspension rods, does not ensure minimum power consumption of the drive motor. It is more expedient to use its root mean square deviation, and the smaller it is, the lower the required rated power of the motor.

Researchers A. Malyar & S. Cieslik (2023) noted that the negative part of the torque is the cause of the variable load of the DRPU drive, it is practically impossible to avoid this part, and it leads to the emergence of reactive power of the electric motor. The developed methodology made it possible to compensate for reactive power in the starting and steady-state modes of the electric drive. Comparative graphs of the crankshaft torque are presented in Figure 13, and the values of the root mean square deviation coefficients are given in Table 1.

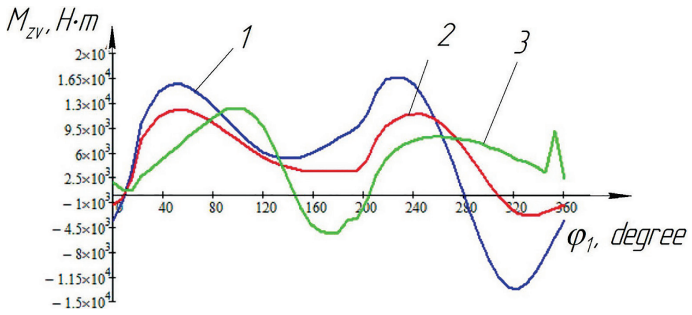

Figure 13. Graphs of combined moments of DRPU drives

Note: 1 – improved balance drive with a movable pulley; 2 – traditional balance drive; 3 – crank-pulley drive
Source: developed by the authors based on current research and V.R. Kharun *et al*. (2021)

According to comparative calculations, an improvement in balancing was obtained for the crank-pulley drive (Table 1), since the root mean square deviation coefficient decreased by 33.6% compared to the traditional balance drive. And, therefore, in accordance with the above considerations, this led to an increase in the efficiency of the entire DRPU. The results of the calculations are summarised in Table 1.

Table 1. Comparison of drive balancing quality assessment

Type of drive DRPU	Value σ_M, kN×m	Reduction of the root mean square deviation coefficient, %
Traditional balance UP12T-3-5500	14.26	-
The UP12T-3-5500-based balancer drive equipped with a movable pulley	10.54	26.1
Crank-pulley DPCP	9.47	33.6

Source: developed by the authors based on current research and V.R. Kharun *et al*. (2021)

It should be noted that although the calculation of the DPCP balance resulted in graph 3 with different values of the maximum moment during the upward movement of the rod suspension (crank rotation angle of 97°) and downward movement (rotation angle of 250°), the quality of its balancing is better (the root mean square deviation coefficient is 9.47 versus 14.26), which is consistent with the conclusions of G. Takacs & L. Kis (2021). The analysis of the root mean square deviation coefficient of the reduced moment of the crank shaft can be used in the development of adaptive control algorithms based on artificial intelligence, which was proposed by the author O. Turchyn (2025) for automatic regulation of the operating modes of the DRPU. Thus, the results of modelling and comparative analysis confirm the feasibility of using a crank-pulley drive, since the proposed mathematical model allows for an adequate description of kinematic and dynamic processes, improves the quality of balancing, reduces torque fluctuations, and creates the conditions for increasing the energy efficiency and reliability of the pump unit.

Conclusions

The developed mathematical model and comparative assessment calculations of balancing quality showed that the speed characteristics of the crank-pulley drive's executive mechanism allow it to operate with better performance than traditional balance drives, since the speed for the downward stroke of the suspension is 0.9 m/s compared to 1.08 m/s for a traditional balance drive, which is 20% less. The comparison of the displacement graphs of the rod suspension of a traditional balance drive and a crank-pulley drive should be performed relative to the extreme position of the rod suspension. One of the advantages of the latter is a larger desaxial angle, which has been increased to 9°, allowing for a reduction in the deviation of the speed and acceleration of the rod suspension point from its average value.

At the beginning of the stroke of the balance drive rod suspension, the acceleration exceeds the DPCP value by 20%, but when the crank rotates 22° relative to the extreme position, it evens out and practically coincides with the acceleration of the DPCP drive. At the end of the downward stroke of the rod suspension, which corresponds to a crank rotation angle of 324° to 360°, the acceleration of the balance drive again exceeds the value by 26%. This indicates that the dynamic characteristics of the DPCP drive are also better. Using a mathematical model, it has been determined that the operation of this drive is accompanied by a change in the direction of rotation of the drive pulley, twice per crank rotation its angular velocity reaches 1.3 rad/s. Accordingly, this negatively affects the durability of the flexible link – the rope, since the change in the direction of rotation leads to a change in the sign of the contact stresses at the point of contact between the rope and the pulley. A comparative analysis of traditional balance drives and new DRPU executive mechanism schemes can be carried out using a typical static dynamogram, since the acceleration graphs of the balance drive rod suspension and the DPCP drive coincide in the upward movement phase of the rod suspension when the maximum load is applied to the drive.

Intelligent control methods for rod pump units aimed at improving the efficiency of the DRPU oil extraction process

are mainly focused on controlling the characteristics of the drive motor – torque and shaft rotation speed. The torque of the drive motor, through the drive gear ratio, is related to the torque of the crankshaft, so by comparing the root mean square torque deviation coefficient, more efficient drives can be selected. In the study, the root mean square deviation coefficient of the DPCP drive is 9.47 kN/m, which is 33.6% less than in the balance drive, so it can be argued that the crank-pulley drive has better balancing performance.

The negative value of the crankshaft torque negatively affects the operation of the drive gearboxes and, for a well-balanced drive, is 12 kN×m and manifests itself at the end of the rod suspension stroke downwards during the crankshaft rotation angle from 280° to 360°, while for the crank-pulley drive it is significantly lower, amounting to 5 kN×m, and manifests itself at the end of the rod suspension stroke upwards during the crank rotation from 150° to 205°. Thus, based on the research conducted, it can be noted that the kinematic characteristics of the DPCP drive are better compared to traditional balance drives. Considering the significant service life of these drives, from 1993 to 2021, at the OGPD Okhtyrkanaftogaz PJSC Ukrnafta, it would be advisable in the future to conduct a technical assessment of the reasons for their problematic operation in order to further improve the design of unbalanced drives.

Acknowledgements

The authors express their sincere gratitude to Mykolai Chepula, former technical director of Osnastka NPP, who was involved in the manufacture of crank-pulley drives, for his assistance in obtaining information materials on these drives and providing ideas for writing this publication. Also, Oleksii Fesenko, Head of Technical Service at OGPD Okhtyrkanaftogaz PJSC Ukrnafta, for his assistance in evaluating the operational capabilities of sucker-rod pumping units with crank-pulley drives.

Funding

None.

Conflict of Interest

None.

References

[1] Ahmedov, B., Hajiyev, A., & Mustafayev, V. (2021). Estimation of the equality of the beamless sucker-rod oil pumping unit by the value of the consumption current. *Nafta-Gaz*, 9, 571-578. doi: 10.18668/NG.2021.09.01.

[2] Ahmedov, B., Khalilov, I., & Hajiyev, A. (2023). Evaluation of the energy efficiency of the new model of sucker-rod pumping unit. *Machine Science*, 2, 28-39. doi: 10.61413/DOVZ1701.

[3] Aliev, T.A., Guluyev, G.A., Rzayev, A.H., Aliyev, Y.G., Rezvan, M.H., Yashin, A.N., & Khakimyanov, M.I. (2022). Ways to increase the efficiency of sucker rod pump units in oil production. *Journal of Engineering Research and Sciences*, 1(3). doi: 10.55708/js0103001.

[4] Aliyev, A.M., & Aliyeva, S.Y. (2023). Influence of mechanical factors on the performance and aging process of oil pump jack. *Nafta-Gaz*, 12, 776-785. doi: 10.18668/NG.2023.12.03.

[5] de Oliveira, F.C., & Romero, O.J. (2024). Development of the Rodsim numerical simulator for the study of a sucker rod pump, comparing the Gibbs (1963) and Lea (1990) models. *Latin American Journal of Energy Research*, 11(1), 12-23. doi: 10.21712/lajer.2024.v11.n1.p12-23.

[6] Feng, D., Qi, Y., Yu, Y., & Zhu, H. (2022). Neural network-based beam pumper model optimization. *Computational Intelligence and Neuroscience*, 2022(1), article number 8562387. doi: 10.1155/2022/8562387.

[7] Gao, Z.-W., & Jia, S. (2024). Modeling and control for beam pumping units: An overview. *Processes*, 12(7), article number 1468. doi: 10.3390/pr12071468.

[8] GE Oil & Gas. (n.d.). *Lufkin beam pumping units*. Retrieved from https://www.geoilandgas.com/oilfield/artificial-lift-well-performance-services/lufkin-beam-pumping-units.

[9] Han, X., Zhao, P., Zhao, X., & Zi, B. (2025). Review on machine learning-based approaches for the kinematic analysis and synthesis of mechanisms. *Frontiers of Mechanical Engineering*, 20, article number 11. doi: 10.1007/s11465-025-0827-5.

[10] Kharun, V.R., Senchishak, V.M., Popovych, V.Ya., & Shostakivskyi, I.I. (2021). Comparative evaluation of the executive mechanism of beam pumping unit drive equipped with a long-stroke column. *Oil and Gas Power Engineering*, 2(36), 57-67. doi: 10.31471/1993-9868-2021-2(36)-57-67.

[11] Malyar, A., & Cieslik, S. (2023). Calculation of processes in the electric drive of the sucker-rod pumping unit with reactive power compensation. *Energies*, 16(23), article number 7782. doi: 10.3390/en16237782.

[12] Malyar, A., & Malyar, M. (2025). Optimization of pump jack electric drive operation taking into account reservoir flow rate. *Technology Audit and Production Reserves*, 1(81), 75-78. doi: 10.15587/2706-5448.2025.322457.

[13] Osnastka NPP. (2001). *Crank-sheave drive of the sucker-rod pump PKSh56-120-4: Non-counterbalanced pumping unit with crank-shtave converting mechanism. Passport*. Kramatorsk: Osnastka NPP.

[14] Savchuk, V.V. (2016). Oil production with high content of sand, asphaltenes and wax using special pump constructions. *Scientific Bulletin of Ivano-Frankivsk National Technical University of Oil and Gas*, 1(40), 20-29.

[15] Shao, J., Ding, K., & Wang, D. (2021). Kinematics analysis of incomplete gear and rack pumping unit. *Journal of Physics*: *Conference Series*, 2095, article number 012090. doi: 10.1088/1742-6596/2095/1/012090.

[16] Takacs, G., & Kis, L. (2021). A new model to find optimum counterbalancing of sucker-rod pumping units including a rigorous procedure for gearbox torque calculations. *Journal of Petroleum Science and Engineering*, 205, article number 108792. doi: 10.1016/j.petrol.2021.108792.
[17] Turchyn, O. (2025). Introduction of neural network technologies to optimise the control of the operating modes of a sucker-rod pump installation. *Machinery & Energetics*, 16(1), 32-42. doi: 10.31548/machinery/1.2025.32.
[18] Wang, B. (2021). Dynamic strength analysis of the key components of the beam-type pumping unit with dynamic tracking balance. *Fracture and Structural Integrity*, 15(57), 291-299. doi: 10.3221/IGF-ESIS.57.21.
[19] Wang, J., Guo, Q.-Y., Fu, C.-L., Dai, G., Xia, C.-Y., & Qian, L.-Q. (2025). A novel optimization scheme for structure and balance of compound balanced beam pumping units using the PSO, GA, and GWO algorithms. *Petroleum Science*, 22(3), 1340-1359. doi: 10.1016/j.petsci.2025.01.007.
[20] Weatherford. (n.d.). *Long-stroke pumping unit*. Retrieved from https://www.weatherford.com/products-and-services/production-and-intervention/artificial-lift-systems/reciprocating-rod-lift-systems/pumping-units/long-stroke-pumping-unit/.
[21] Xu, J., Li, W., & Meng, S. (2022). Kinematic and dynamic simulation analysis of modified conventional beam pumping unit. *Energies*, 15(15), article number 5496. doi: 10.3390/en15155496.
[22] Xu, J., Wang, W., Li, W., Zhu, Q., & Lu, H. (2024). Kinematic and dynamic analysis of eccentric balanced positive torque pumping unit. *Machines*, 12(4), article number 240. doi: 10.3390/machines12040240.
[23] Zhang, R., Yin, Y., Xiao, L., & Chen, D. (2021). A real-time diagnosis method of reservoir-wellbore-surface conditions in sucker-rod pump wells based on multidata combination analysis. *Journal of Petroleum Science and Engineering*, 198, article number 108254. doi: 10.1016/j.petrol.2020.108254.

Кінематичний аналіз характеристик кривошипно-шківного верстата-гойдалки

Віктор Харун

Кандидат технічних наук, доцент
Івано-Франківський національний технічний університет нафти і газу
76019, вул. Карпатська, 15, м. Івано-Франківськ, Україна
https://orcid.org/0000-0003-1422-6003

Василь Попович

Кандидат технічних наук, доцент
Івано-Франківський національний технічний університет нафти і газу
76019, вул. Карпатська, 15, м. Івано-Франківськ, Україна
https://orcid.org/0000-0003-2438-8532

Іван Петрик

Кандидат технічних наук, доцент
Івано-Франківський національний технічний університет нафти і газу
76019, вул. Карпатська, 15, м. Івано-Франківськ, Україна
https://orcid.org/0000-0003-0863-5476

Зіновій Одосій

Кандидат технічних наук, професор
Івано-Франківський національний технічний університет нафти і газу
76019, вул. Карпатська, 15, м. Івано-Франківськ, Україна
https://orcid.org/0000-0003-0914-2489

Анотація. Нафтовидобувні підприємства в Україні переважно використовують традиційні балансирні приводи, які впродовж багатьох років експлуатації підтвердили свою надійність. Нові схеми приводів, з точки зору ефективності, потребують проведення порівняльної оцінки їх характеристик з балансирними приводами. З метою порівняльного аналізу та розрахунку кінематичних параметрів кривошипно-шківного приводу, який експлуатувався в Нафтогазовидобувному управлінні «Охтирканафтогаз» Публічного акціонерного товариства «Укрнафта» з 1993 по 2021 рр., у роботі наведено розробку його математичної моделі. Для цього використано геометричні залежності, які дозволили розрахувати довжину канату, який виступає гнучкою ланкою, і відповідно, переміщення штангової підвіски. Диференціюючи графік переміщення отримано відповідні кінематичні характеристики – швидкості та пришвидшення, які виступають складовою для розрахунку моменту сил опору, зведених до кривошипа виконавчого механізму. Коефіцієнти середньоквадратичного відхилення, розраховані для традиційних балансирних верстатів-гойдалок та кривошипно-шківного приводу, дозволили провести порівняльну оцінку якості їх зрівноваження. Порівняння їх характеристик проведено за навантаженням виконавчого механізму типовою статичною динамограмою, оскільки прийнята швидкість обертання кривошипа верстатів-гойдалок є меншою за 8 об/хв. Визначено, що середньоквадратичне відхилення крутного моменту кривошипно-шківного приводу склало 9,47 кН×м, що на 33,6 % менше, ніж у традиційного балансирного приводу. За допомогою розробленої математичної моделі, у якій використано метод векторного контуру, отримано систему лінійних рівнянь для визначення залежності кута повороту φ_2 нижньої траверси, до якої кріпиться канат, та кута повороту φ_3 рухомого шківа від кута φ_1 повороту кривошипа. Встановлено, що рухомий шків змінює свій напрямок руху двічі за один оберт кривошипа виконавчого механізму, що може бути причиною пришвидшеного зносу привідного канату

Ключові слова: середньоквадратичне відхилення; свердловинна штангова насосна установка; математична модель; привід насоса; зведений момент

ISSN 1993-9973, e-ISSN 2415-332X

Vol. 25, No. 2
2025

PROSPECTING AND DEVELOPMENT OF OIL AND GAS FIELDS

https://pdogf.com.ua/en

Received: 21.07.2025. Revised: 22.10.2025. Accepted: 08.12.2025. Published: 09.01.2026.

UDC 622.245.5

DOI: 10.63341/pdogf/2.2025.48

On the selection of optimal drilling fluid formulations under HPHT constraints

Yurii Voloshyn*

PhD in Technical Sciences, Associate Professor
Ivano-Frankivsk National Technical University of Oil and Gas
76019, 15 Karpatska Str., Ivano-Frankivsk, Ukraine
https://orcid.org/0000-0002-0582-1778

Volodymyr Bohoslavets

PhD in Technical Sciences, Associate Professor
Ivano-Frankivsk National Technical University of Oil and Gas
76019, 15 Karpatska Str., Ivano-Frankivsk, Ukraine
https://orcid.org/0000-0001-9622-4065

Oleh Martsynkiv

PhD in Technical Sciences, Associate Professor
Ivano-Frankivsk National Technical University of Oil and Gas
76019, 15 Karpatska Str., Ivano-Frankivsk, Ukraine
https://orcid.org/0000-0003-4583-5944

Oleh Kutsiv

Postgraduate Student
Ivano-Frankivsk National Technical University of Oil and Gas
76019, 15 Karpatska Str., Ivano-Frankivsk, Ukraine
https://orcid.org/0009-0006-6360-2537

Bohdan Martsynkiv

Postgraduate Student
Ivano-Frankivsk National Technical University of Oil and Gas
76019, 15 Karpatska Str., Ivano-Frankivsk, Ukraine
https://orcid.org/0009-0009-6614-0130

Abstract. Drilling deep and ultra-deep wells under high-pressure/high-temperature (HPHT) conditions is a strategic pathway for expanding Ukraine's resource base and requires a scientifically grounded approach to selecting optimal drilling-fluid formulations. The objective of this research was to establish, through an in-depth analysis of international and Ukrainian HPHT well construction practices, a methodology for selecting optimal formulations of high-performance water-based, clay-free drilling fluid systems (HT-HPWBF), which integrates both the hierarchy of optimality criteria and the system's key performance indicators. A systematic review and content analysis of more than 200 publications on HT-HPWBFs were performed, the field experience from Ukrainian assets was synthesised, and a comparative analysis versus international practice was conducted. The assessment reveals that Ukraine lags behind leading HPHT regions primarily due to continued reliance on conventional KCl and biopolymer-potassium systems rather than modern HT-HPWBFs. Based on importance-impact analysis of requirements, technological constraints, and performance indicators, the study demonstrated the feasibility of constructing a hierarchical framework of core criteria for selecting optimal formulations. A three-tier optimality hierarchy comprising α-criteria (well-control and safety), β-criteria (achievement

Suggested Citation: Voloshyn, Yu., Bohoslavets, V., Martsynkiv, O., Kutsiv, O., & Martsynkiv, B. (2025). On the selection of optimal drilling fluid formulations under HPHT constraints. *Prospecting and Development of Oil and Gas Fields*, 25(2), 48-63. doi: 10.63341/pdogf/2.2025.48.

*Corresponding author

of technological objectives), and γ-criteria (environmental-economic effectiveness) was proposed. A methodology for constructing composite key performance indicators that integrate field experience, laboratory testing, and risk assessment was developed. The study substantiated the combined use of advanced analytics of historical data, real-time monitoring of fluid parameters, and key performance indicators driven decision making for formulation selection. The results can be directly applied by drilling engineers and service companies to improve the efficiency of HPHT well construction in Ukraine

Keywords: drilling mud design; indicators of efficiency; drilling mud quality index; complex analysis; clay-free systems

Introduction

The energy security and prosperity of every country depends on the level of energy supply to industry and, consequently, on the level of hydrocarbon resource development. Given the contradiction between growing global demand for energy resources and their supply, drilling deep and ultradeep wells can be a strategic step towards expanding the hydrocarbon resource base. The main problems in drilling such wells are the high pressure and high temperature (HPHT) conditions at the bottom hole. The problems of producing hydrocarbons that lie in HPHT conditions are associated with significant risks of both a geological and technical-technological nature. For successful well completion in such conditions with simultaneous mitigation of complications or emergencies, special attention should be paid to the selection of the optimal mud formula. To select the optimal formulation, the advantages and disadvantages of existing alternatives in HPHT conditions should be evaluated, taking into account the technological features of use, expert assessment of possible risks (risk assessment), economic feasibility, and environmental acceptability of each formulation in particular. The complexity of implementing drilling programs under HPHT conditions is also related to the fact that several problems of different origins (geological, technical, technological, environmental, economic, etc.) usually need to be solved simultaneously.

According to J. Zhang *et al*. (2025), high formation pressure often leads to high risks of well control loss and low penetration rates due to the need for high-density mud systems, which can lose stability when exposed to high temperatures (170-240°C) for long periods of time. As noted by B. Miikor *et al*. (2025), water-based systems are less commonly used for high-temperature wells due to the stability (in particular, thermal degradation) issues of biopolymer thickening agents, water-shale control agents, and other components of drilling fluids under such conditions. However, the practical experience of T. Hasan Hamdan *et al*. (2020) has shown that, when it is necessary to obtain high-quality logging data to assess the prospects of new fields, water-based systems are a more desirable option. In addition, as noted by the authors Y. Freschi *et al*. (2025), with the growing emphasis on minimising the impact on the surrounding environment, high-quality HT-HPWBF (High Temperature-High Performance Water Based Fluid) systems will always be a priority. This is also facilitated by the development and deployment of the principles of "sustainable development" and "green transformation" of the Industrial Revolution 4.0 in the global oil and gas industry. The oil and gas industry is increasingly using HT-HPWBF systems whose main thermostabilising components are formates (Myslyuk & Zholob, 2023), polyamines or acetates (Liu *et al*., 2020a). Such systems have both high density (without the use of barite) and good thermal stability. The choice of organic salt solutions as the basis for drilling fluids helps minimise well control problems associated with barite settling, high rheology, poor rock stability, excessive casing corrosion, etc.

The mechanisms of biopolymer degradation in solutions at high temperatures include acid-catalysed hydrolysis and redox reactions. Therefore, the thermal stability of biopolymers can often be increased (up to 180°C) in three ways: using antioxidants (polyethylene glycols, magnesium oxide, formates) that inhibit oxidative reactions and react with free hydroxyl radicals, preventing polymer degradation (Myslyuk & Zholob, 2023); using oxygen scavengers (King & Rodrigue, 2025); and modifying by grafting monomers or functional groups (Kong *et al*., 2022). In order to maintain the operational and thermal stability of water-based drilling fluids at high temperatures when using xanthan biopolymer, the authors L. Quitian-Ardila *et al*. (2024) recommend increasing its concentration in the formulation.

According to research by N. Jameel & J. Ali (2023), the problem of controlling water loss and rheological properties in water-based systems can be effectively solved by using several types of polymers simultaneously. As noted by researchers J. Sun *et al*. (2024), despite the variety of systems developed that are resistant to high formation temperatures, a number of problems still arise in their practical application, such as insufficient stability in real well conditions, the complexity of controlling rheological and filtration properties, and insufficient compatibility with formations. This situation is most likely due to the complexity of selecting the optimal concentrations of reagents for each specific application (case or well). Significant attention has been paid to the development of heat-resistant reagents and equipment capable of operating in difficult HPHT conditions, which has made it possible to overcome the main technological challenges of developing ultradeep wells. However, issues related to the selection of optimal HT-HPWBF formulations, the criteria for the effectiveness of such systems, and ways to optimise them for specific mining and geological conditions have not been sufficiently studied. The aim of the study was to develop a methodological approach to selecting optimal formulations for highly effective water-based clay-free drilling fluids for HPHT well drilling. This was based on in-depth analysis of experience,

taking into account the hierarchy of optimisation criteria and key performance indicators (KPIs) for such systems.

Materials and Methods

In accordance with the Law of Ukraine No. 4154-IX (2024), the development of mineral resources is one of the priorities. In order to improve the quality of deep and ultradeep well construction in complex mining and geological conditions, it is necessary to select the optimal drilling fluid formulations. To determine the criteria for optimality and form a system of restrictions for the main parameters of the fluids, the systematic review and content analysis of publications devoted to the selection of optimal formulations for water-based drilling fluids and their properties under HPHT conditions (more than 40 sources published in the period 2005-2025 as well as tenders from the Prozorro, n.d.) were carried out. The review covered all countries of the world, including Ukraine. The publications from peer-reviewed journals included in Scopus and Web of Since, as well as materials from the OnePetro digital library for the oil and gas industry (created and maintained by SPE) were taken into account.

To establish chronological links, trends or evolutionary changes in optimality criteria systems, all publications were grouped by year for further analysis. During the content analysis of publications, the main focus was on: the conditions in which the flushing systems were planned to be used (apart from HPHT, whether there are any other complications, such as unstable rocks, hydrogen sulphide, etc.); the objectives of developing or adapting the flushing fluid formulation; the parameters of the formulations under study; the criteria for optimality stated by experienced authors (usually practitioners); performance indicators (including KPIs) when testing formulations in both field and laboratory conditions and the methods for their development.

Based on the results of the analysis, sets of primary and secondary criteria for optimality were formed, with reference to the period of application (the degree of importance was indicated by the authors of the publications). Upon formation of the sets, a frequency assessment of the criteria was conducted and their average rank was determined for the construction of a hierarchy in the future. Based on a review of the requirements, technological limitations, and performance indicators of HT-HPWBF systems declared in publications, a hierarchical system was created. To develop recommendations for selecting a drilling fluid formulation for use in complex mining and geological conditions, a systematic and comprehensive approach was applied both at the design stage and at the subsequent stages of laboratory and industrial testing.

Important elements of the procedure for designing and selecting the optimal HT-HPWBF formulation were: assessment of predicted risks; determination of the main objectives of the formulation design; identification of the main problems and limitations imposed by HPHT conditions; formation of a list of alternative acceptable formulations in accordance with mining and geological conditions and a hierarchical system of requirements; selection of the criterion (criteria) of optimality or formation of a comprehensive indicator of the efficiency of the flushing system; implementation of the selected procedure for selecting the optimal formulation. Therefore, the paper considered the procedure for selecting optimal drilling fluids under HPHT constraints.

Results and Discussion

An analysis of publications and tenders (Prozorro, n.d.) showed that high-tech and complex HPHT wells are actively being constructed in Ukraine, and Ukrainian specialists have considerable experience in drilling such wells. Well drilling in Ukraine is steadily shifting from the normal pressure and normal temperature (NPNT) zone to the HPHT zone (Fig. 1). However, the share of modern clay-free HT-HPWBF systems in Ukraine is several times lower than in leading countries such as China or the United States.

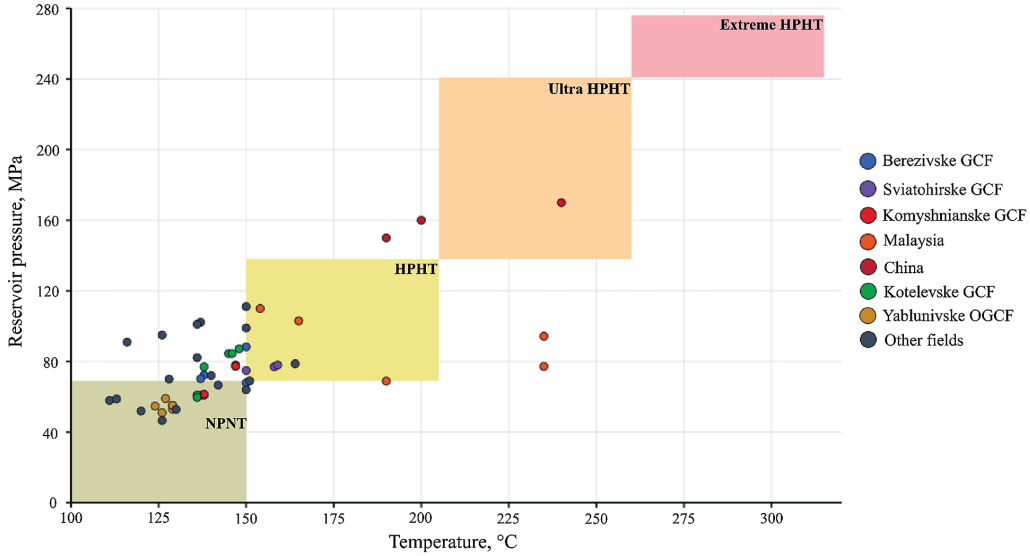

Figure 1. Comparison of HPHT well drilling trends in Ukraine with global practices

Source: created by the authors based on Prozorro (n.d.), O. Agwu *et al*. (2021), J. Zhang *et al*. (2025)

Among Ukrainian fields with HPHT conditions or conditions close to them are the Berezivske Gas Condensate Field (GCF), Shebelynske GCF, Stepove GCF, Solokhivske Oil and Gas Condensate Field (OGCF), Komyshnianske GCF, Sviatohirske GCF, etc. Although Figure 1 does not contain complete and comprehensive information on HPHT well drilling in Ukraine and worldwide, and only highlights a small part of it (available open data), it however, allows to see the general trend of lagging behind the world leaders in ultradeep well drilling (China, Malaysia, etc.). This statement applies to drilling fluids. According to the online public procurement platform Prozorro (n.d.), the most actively used fluids for HPHT drilling are chlorinated potassium-weighted HTHP solution and biopolymer-potassium HPHT solution. Although the use of these systems allows for the achievement of design depths, the total drilling time is much longer when compared to the time spent drilling with conventional HT-HPWBF systems. The increase in drilling time is associated with periods when the drilling rig or personnel are unable to perform planned productive operations due to various problems, such as waiting for the delivery of materials or specialists, or dealing with serious complications or accidents. Such time losses represent Non-Productive Time (NPT), i.e. time losses due to events or their absence, which are always officially recorded. This usually includes time lost on well control, delivery of drill string components, bits, downhole motors, cable logging, etc. In addition, during well construction, there is Invisible Lost Time (ILT), which is not always officially documented or recorded as downtime, but has a significant impact on overall work productivity and project cost. These include frequent short stops (which are not recorded as downtime due to their duration), time lost due to suboptimal decisions or lack of expertise (experience) among personnel, etc.

It should be noted that classic HT-HPWBF formulations are successfully used in Ukraine. For example, specialists from Geosynthesis Engineering used their own high-performance Biocar-TF system, which is stable at high temperatures, when drilling wells in the complex mining and geological conditions of the Semyrenkivske GCF (First utilization..., n.d.). However, the need for highly efficient clay-free HT-HPWBF systems is growing due to the trend of drilling wells over 5,500 m. In such conditions, reducing NPT and ILT during drilling by using HT-HPWBF-type drilling fluids is an important strategic decision for oil and gas companies. Another characteristic feature of the use of such systems is a significant reduction in NPT associated with loss of control over the well or stability of the wellbore (Biocar-TF biopolymer drilling..., n.d.). Since the main function of HT-HPWBF is to ensure safe working conditions while achieving maximum drilling efficiency at high bottomhole temperatures and the customer's specified consumption level, selecting the optimal formulation is a complex but crucial step in successful well drilling. To illustrate the variability of HT-HPWBF system alternatives and their component composition, Table 1 shows the characteristics of some commercial solutions developed and implemented by relevant service companies. All systems are environmentally friendly alternatives to non-aqueous-based solutions in terms of their effectiveness under HPHT conditions.

Table 1. Some commercial solutions for HT-HPWBF systems

System (Company)	Declared thermal stability, °C	Features and main components
PYRO-DRILL (Baker Hughes)	316	A highly effective system whose main components are Polydrill synthetic sulphated polymers and All-Temp and SSMA Mil-Temp interpolymers for regulating thermal stability, Chemtrol X AMPS/Aam copolymers, Kem-Seal, Pyro-Trol for controlling HPHT filtration, thickening and shale inhibition, Max-Guard™ Plus (clay inhibitor), Penetrex, Latilube™ (lubricating additives), Sulfatrol Xceed (HPHT filtration control), Max-Shield (sealing polymer).
BaraDrilN X (Halliburton)	232	A highly efficient clay-free well completion system based on synthetic polymers BDF-637 (for monovalent brines) or BDF-638 for divalent brines (CaBr2). If necessary, the system can contain corrosion inhibitors (Baracor 100) and oxygen absorbers (Oxygon™). Micromax or Mn_3O_4 can be used additionally to achieve the design densities.
BaraXtreme (Halliburton)	227	A highly efficient clay-free system based on synthetic polymer BDF-637 (BaraVis W-637), designed to control viscosity and filtration at high temperatures. The system also contains highly effective reagents that increase wellbore stability and reduce fluid loss, such as BaraFLC Nano-1 (nanocomposite suspension) and others.
VeraTherm (SLB)	205	The VeraTherm system, based on the synthetic polymer VeraVis, which is designed to regulate the rheological and filtration properties of the system, outperforms both formate and conventional polymer systems and demonstrates excellent performance at high temperatures. Depending on requirements, the system can be based on KCl, NaCl, NaBr, $CaCl_2$, $NaHCO_2$, $KHCO_2$, or $CsHCO_2$ brines.
Biocar-TF (Geosynthesis Engineering)	170	A highly efficient clay-free system based on xanthan gum, modified starch, and sodium and potassium formates. The system also contains the organo-mineral colloid Alevron, micro-marble, and other auxiliary substances.

Note: depending on drilling conditions, thermal stability can be increased or enhanced by changing the type or content of reagents; the composition of the system can be adjusted according to specific conditions or constraints

Source: created by the authors based on VeraTherm high-temperature water-based drilling fluid (n.d.), World's first application of BaraXtreme fluid in HTHP gas well (n.d.), BaraDrilN™ X fluid helps customer achieve well testing operation (n.d.), Patent No. 124224, (2020), J. Liu *et al*. (2020b)

Highly productive clay-free systems (Table 1) are based on specially developed synthetic polymers with various functional purposes that maintain their performance characteristics at the level specified in the design documentation under prolonged exposure to high temperatures. To solve the problems of controlling the filtration and rheological properties of water-based systems, the oil and gas industry most often uses supramolecular polyacrylamide, amphoteric polymers, comb-like polymers and thermo-associated polymers (Tchameni *et al*., 2025), and nanopolymers (Karakosta *et al*., 2021). The thermal stability of such synthetic polymers can be 200°C and above (Freschi *et al*., 2025). As noted by H. Shi *et al*. (2024), most water-soluble polymers degrade at temperatures of 200-240°C, which complicates the control of rheological and filtration properties at high and ultra-high temperatures.

Therefore, with increasing drilling depths, there is a need to search for new, more temperature-resistant polymers with a heat resistance limit of 260°C, such as Pyro-Trol from Baker Hughes. In order to further increase the viscosity characteristics, a small amount of clay is added to such systems (Miikor *et al*., 2025). However, according to A. Tchameni *et al*. (2025), high temperatures in the presence of clay materials (bentonite clay) in the solution formulation can cause thermally induced flocculation of clays and the formation of highly viscous gels. According to researchers S. Gautam *et al*. (2025), when developing a clay-free HPHT drilling fluid formulation, it is important to study the effect of polymer molecular weight and its distribution on the performance characteristics of the drilling fluid. This will largely solve one of the main problems of conventional water-based drilling fluids in HPHT conditions – barite ($BaSO_4$) sagging in both static and dynamic conditions, even during prolonged thermal ageing of the system.

Barite sagging can cause loss of well control (blowout), loss of fluid (due to hydraulic fracturing), problems with drill string mobility, etc. (Fakoya & Ahmed, 2023). J. Oseh *et al*. (2025) include the properties of the drilling fluid, the profile and geometry of the internal space of the well, and drilling parameters (rotation speed of the column, fluid flow rate, etc.) among the factors that most influence barite sagging. An effective measure to prevent barite sagging is to control the rheological properties of the system, among which Low Stress Yield Point (LSYP) should be noted. Another possible solution to the problem of weighting agent sagging is the correct choice of its type and particle size distribution. According to the authors, when drilling oil and gas wells in HPHT conditions, it is advisable to use nanoscale barite ($nBaSO_4$) and ilmenite ($nFeTiO_3$) due to the low susceptibility of such materials to sagging. The same opinion was expressed by researchers G. Soori *et al*. (2023), who proposed using Cerite (cerium oxide CeO_2) with a density of 6,000 kg/m^3 as a weighting agent, which would minimise the content of solid particles in the solution and, accordingly, pressure losses in the well.

According to O. Agwu *et al*. (2021), a cheaper alternative to barite in HPHT wells is manganese tetroxide (Mn_3O_4). The authors H. Mao *et al*. (2020) considered the possibility of combining barite with metal oxides, in particular iron (Fe_2O_3), and concluded that the rheological properties of HT-HPWBF largely depend on the type of weighting agents and their ratio in the formulation. Less commonly, zinc oxide (ZnO) (Ahasan *et al*., 2021; Taghdimi *et al*., 2023) or zirconium oxide (ZrO) (Medhi *et al*., 2020) are used as weighting components. Laboratory studies and computer modelling are ongoing for these nanoscale weighting agents, without widespread industrial implementation. However, other nanodispersed oxides, such as Mn_3O_4 and CuO, are considered by A. Rana *et al*. (2024) to be an important element in the development of stable HPHT system formulations. Additionally, research by A. Shokry *et al*. (2024) shows that the use of nanoscale weighting agents can reduce the thickness of the filtration crust by 40% while simultaneously reducing the rheological properties and filtration of the solution system under HPHT conditions.

To solve the problems of sagging of weighting materials with a significant content (30-50%), optimise the rheological behaviour of drilling fluids and prevent absorption under HPHT conditions, researchers H. Mao *et al*. (2020) and H. Wang *et al*. (2022) proposed the use of sealing materials with the content, size, and particle size distribution selected using the ideal packing theory. This approach reduces sagging effects, problems with Equivalent Circulating Density (ECD), and changes in formation counterpressure. Depending on the profile and design of the well, the following methods can be used to assess barite sagging (Fakoya & Ahmed, 2023): test cell method; VST test (settlement test using a rotational viscometer); VSTT test (modified VST with a thermal cup); flow contour test; dynamic sag test at a large angle. The main principle in developing new or improving existing formulations for technological fluids is to minimise costs (time, resources, expenses) in the construction of oil and gas wells while ensuring their maximum productivity. A rational approach to selecting optimal formulations for technological fluids in HPHT conditions should also include an assessment of the risks associated with extreme environments in order to minimise them while achieving maximum operational efficiency (Fig. 2).

One of the main predicted risks associated with drilling mud under HPHT conditions is loss of control over the well due to both barite sagging and unsatisfactory filtration or rheological properties of the system. Damage to the formation or loss of wellbore stability can be the result of loss of well control, but can also occur due to other situational factors. Intensive corrosion of technical columns and equipment is also one of the main predicted risks associated with drilling fluid due to the characteristics of system weighting (inorganic and organic salts) and a significant increase in the activity of components under high temperature conditions. In such circumstances, in order to ensure maximum efficiency of the well deepening process while minimising the costs and risks associated with drilling fluid, the main objectives to be achieved through the use of HT-HPWBF should be set. The main objectives of designing highly efficient drilling fluid systems for HPHT conditions are shown in Figure 3.

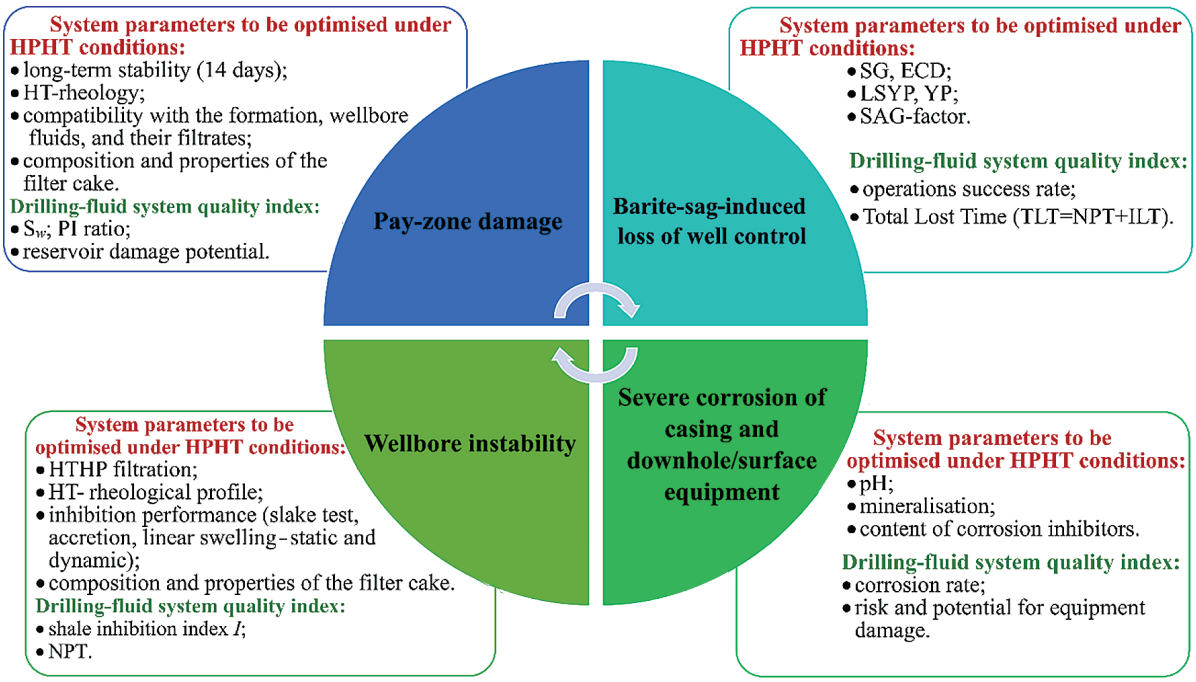

Figure 2. The main predicted risks associated with drilling fluid under HPHT conditions
Source: created by the authors based on information provided in the sources H. Mao *et al*. (2020), J. Zhang *et al*. (2025)

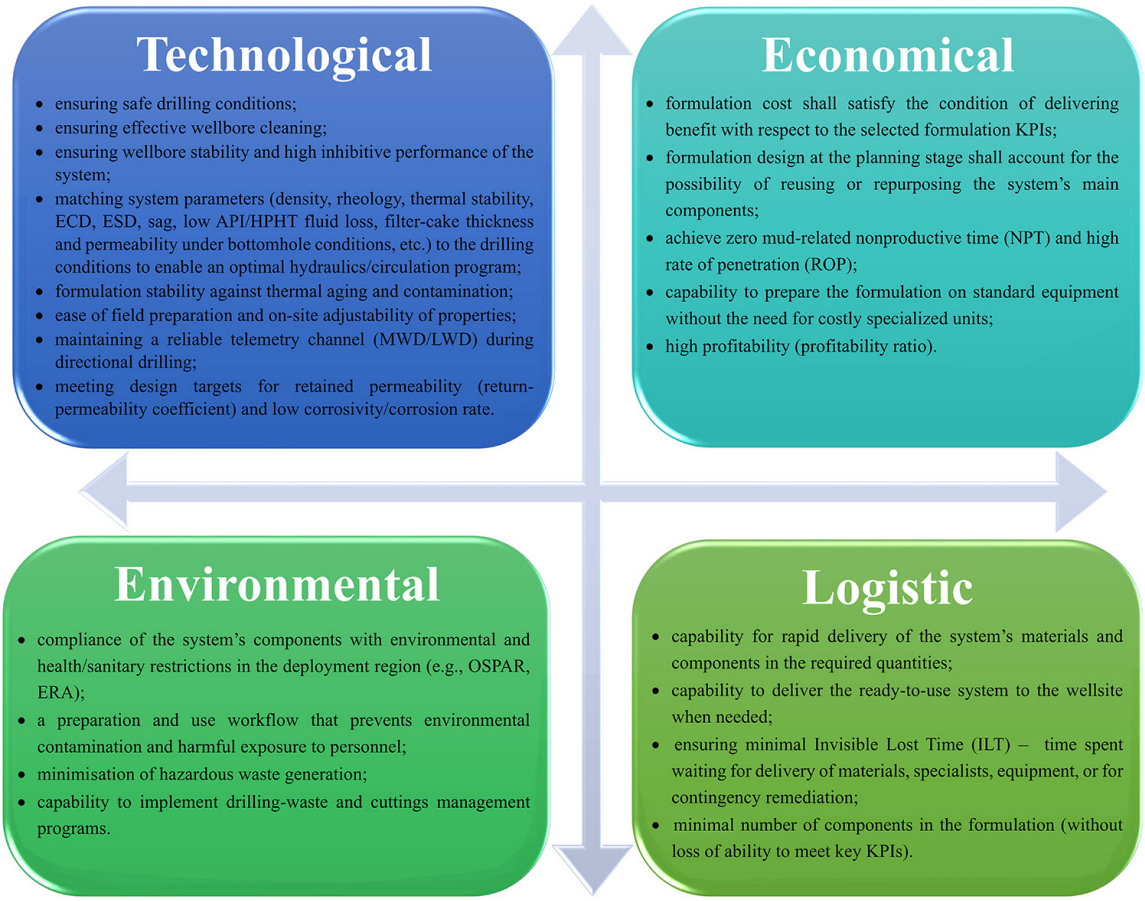

Figure 3. Objectives of designing highly efficient drilling fluid systems for HPHT conditions
Source: created by the authors based on information provided in the sources A. Morrison *et al*. (2021), C. King & K. Rodrigue (2025)

The main objectives can be divided into four groups: technological, environmental, economic and logistic. Logistic objectives are listed separately from economic ones, since in complex HPHT conditions it is important to take into account the requirements for the delivery of materials in the shortest possible time, the problems of logistics of supply and storage of large volumes of scarce materials and their qualification. The criticality and completeness of the HT-HPWBF design objectives can be determined by the customer (or authorised responsible persons) taking into account the applicable industry safety requirements and environmental restrictions in force in the region where the flushing system is to be used. The planned objectives to be achieved at the final stage of HT-HPWBF formulation development are closely related to the problems imposed by HPHT conditions (Fig. 4), requirements for drilling fluids, and criteria for selecting optimal formulations to ensure KPIs.

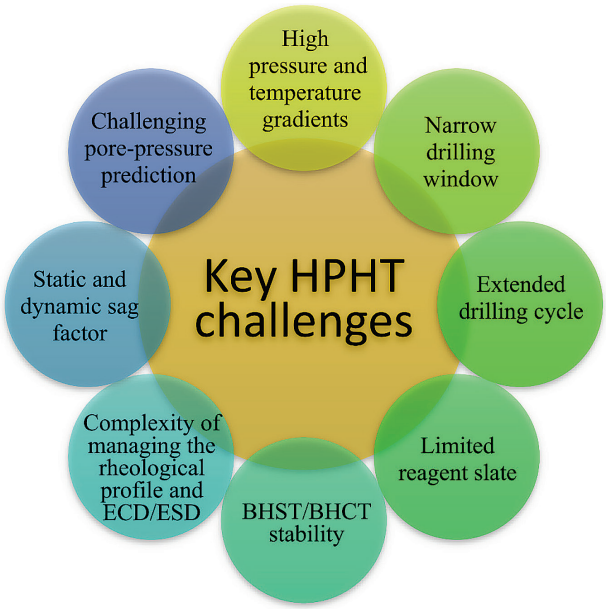

Figure 4. The main problems for drilling fluids related to HPHT conditions

Note: BHCT – Bottom Hole Circulating Temperature; BHST – Bottom Hole Static Temperature

Source: created by the authors based on information provided in the sources O. Agwu *et al*. (2021), A. Khalid *et al*. (2021), Y. Freschi *et al*. (2025)

The main problems in developing formulations for drilling fluids that must perform their functions under HPHT conditions, under technological, economic, environmental and logistical constraints, are primarily related to the limited range of acceptable materials. When selecting materials and components for highly heat-resistant formulations, it is necessary to take into account the operational, environmental, economic and logistic constraints that may arise in each specific case. The selection of drilling fluid components for high-temperature wells should be carried out in accordance with the temperature at the bottom of the well, with mandatory preliminary laboratory evaluation. Each individual component of drilling fluids has its own zero efficiency point – the temperature at which the reagents lose their productivity and effectiveness.

To develop and design a formula that is effective in HPHT conditions, regular preliminary laboratory studies must be conducted, which must include: static and dynamic ageing tests (24 and 72 hours), static and dynamic Sag Factor, including at BHST and BHCT; hot rolling for 16 hours at BHST, HPHT filtration, high-temperature rheological profile; zeta potential measurements, particle size distribution tests, etc. When optimising HPHT drilling fluid formulations, it is usually necessary to simultaneously address issues related to rheological control (rheological profile, yield point (YP), plastic viscosity (PV), LSYP, low shear rate viscosity (LSRV), etc.), filtration characteristics (application programming interface and HTHP filtration, thickness and properties of the filtration crust), as well as barite sagging. These parameters must be carefully monitored throughout the entire well construction cycle. The management of drilling fluid systems used in HPHT conditions must take into account the need to solve the problems shown in Figure 4, and also has some specific features in terms of engineering support.

According to J. Liu *et al*. (2020a; 2020b), due to the complexity of HPHT well design, extreme drilling conditions, and increased reactivity of rocks and reagents, water-based mud systems must have good inhibitory properties. In this case, the content of high-quality lubricating and antisticking additives is mandatory. This requirement is related to the need to minimise the problems of solid phase entering the mud system (Moroni *et al*., 2023). This will prevent an increase in ECD and rheological properties, prevent swelling of clayey rocks, and reduce problems associated with bit cleaning and loss of drill string mobility. As a result, when it is necessary to perform a roundtrip at significant depths, the frequency of drill string sticking and related technological downtime will decrease. With the deepening of high-temperature wells (and an increase in the temperature of the environment), the content of clay rock inhibitors should be increased and the inhibitory properties of the solution enhanced by introducing several types of inhibitors. According to X. Kong *et al*. (2022) and L. Moroni *et al*. (2023), a combination of KCl (6-12% content), amines (2-4%) and Partially Hydrolysed Polyacrylamide is effective for such purposes. According to H. Wang *et al*. (2022), polyamines are effective even at a bottomhole temperature of 235°C.

It should also be noted that water-based systems at high downhole temperatures are highly sensitive to treatment and prone to "depletion". Depending on the conditions and component composition, the "depletion" effect can manifest itself in evaporation, loss of activity, change in the pH of a particular reagent, and, accordingly, an increased need for re-treatment. Emulsifiers, wetting agents, active clay swelling inhibitors, and other surface-active substances are particularly sensitive to such depletion. Therefore, before adding any reagents to the active system, preliminary

pilot laboratory tests should be conducted. When designing a hydraulic HPHT well cleaning programme, the solution behaviour model must take into account the PVT properties of the system. Having information about changes in the state of the drilling fluid depending on pressure and temperature allows timely and correct management decisions to be made when well conditions change. The requirements for HT-HPWBF drilling fluids must ensure the safe execution of planned work, personnel safety, and the desired result under the specified HPHT constraints.

An analysis of the use of drilling fluids for HPHT conditions (Erge *et al.*, 2020; Singh *et al.*, 2024) has made it possible to identify and summarise the requirements and criteria for selecting optimal HT-HPWBF formulations. It is necessary to ensure well control and full compatibility of the system and its filtrate with formation fluids and the reservoir. For this purpose, as noted by researchers S. Deshmukh *et al.* (2021), PV, ECD, Equivalent Static Density (ESD) and Sag Factor indicators must be low (including under BHST conditions). To ensure optimal rheology and keep the slurry in suspension, the YP should be within 12-25 (pounds/100 ft^2), and the LSRV at 6 rpm should be no more than 6 units on the scale. According to researchers, an HPHT filtration index of 2-7 cm^3/30 min at temperatures up to 300°F is quite acceptable for most wells. At the same time, the formulation should be resistant to sudden changes in the temperature profile (changes in solution parameters within acceptable limits, no salt crystallisation when the solution is brought to the surface, etc.) and static ageing at high (bottomhole) temperatures. At the same time, the stability of parameters under HPHT conditions must be maintained for at least 3-7 days and even several months (King & Rodrigue, 2025; Freschi *et al.*, 2025).

Excessive requirements or too strict requirements (extremely low parameter values that are difficult to achieve in real well conditions) can lead to a significant increase in the cost of the formulation, a reduction in the number of acceptable alternative formulations, or the absence of an optimal formulation. It should also be borne in mind that formulations that are effective in laboratory testing of technical and technological properties may not be competitive in industrial testing. The reasons for this are the balance between compliance with the requirements and the specific costs of materials, transportation, preparation, and health, safety and environment (HSE). Therefore, in such cases, it is advisable to use a hierarchy of functional requirements, technological constraints and performance indicators and to select a reasonable number of them according to the circumstances. As an example, Table 2 shows a developed version of a conditional ranking of these elements according to their importance and influence. It should be noted that the assignment of a particular element in Table 2 to the corresponding level of influence may be changed in accordance with specific drilling conditions (or changes therein) by providing such a recommendation (instruction) by experts, consultants (or expert advisory systems, such as Drilling Fluid Advisor), or the customer. The information in Table 2 may be supplemented in accordance with events, new circumstances or the absence of positive results from the use of a particular formulation.

Table 2. Hierarchy of requirements, technological limitations and performance indicators of HT-HPWBF systems

Functional requirements	Technological limitations	Performance indicators
Critical		
◈ thermal stability of the system; ◈ safe and efficient well control by ensuring low LSRV and LSYP values, Sag Factor < 0.5; ◈ maximum preservation of the reservoir properties of the productive formation; ◈ compatibility with the formation, other process fluids and their filtrates; ◈ explosion, eco and fire safety of the system and its components; ◈ compatibility with well completion and development technologies; ◈ stability of properties in HPHT environment at BHST throughout the entire period of prolonged downtime (during logging, especially in exploration wells); ◈ resistance of formulation components to hydrogen sulphide aggression; ◈ resistance of the formulation to contamination (cement, brine, etc.) and inflow of formation fluids.	◈ components resistant to high temperatures in static conditions; ◈ materials resistant to CO_2 and H_2S; ◈ delivery of system components of adequate quality in sufficient quantities may be difficult or economically unviable; ◈ problems with mixing and long-term storage of system components at the drilling site.	◈ maximum well productivity index (PI ratio); ◈ permeability recovery coefficient; ◈ maximum temperature stability retention time (days); ◈ technological efficiency coefficient and minimum number of incidents related to well control and safety; ◈ cuttings carrying index (CCI); ◈ maximum well integrity (stability) retention time; ◈ recipe profitability ratio (ROI).
Important		
◈ technological efficiency in preparation and use; ◈ low corrosion activity (all forms of corrosion) and abrasive impact on casing pipes and technological equipment; ◈ high inhibitory capacity; ◈ ability to effectively transfer hydraulic power; ◈ constant rheological properties under BHST and BHCT conditions, flat rheological profile over a wide range of temperatures and pressures; ◈ thin, low-permeability filtration crust.	◈ sulphur-containing corrosion inhibitors, commonly used in halide brines, decompose to H_2S at high temperatures; ◈ some amines used for pH control and inhibitors may react with acidic gases (CO_2, H_2S) to form harmful reaction products or lose their functional properties.	◈ drilling and completion time; ◈ ensuring maximum well life; ◈ low environmental footprint and impact; ◈ high accident-free drilling rate; ◈ well life and maintenance costs.

Table 2. Continued

Functional requirements	Technological limitations	Performance indicators
Additional		
◈ thermal stability in static conditions for a long time (more than 72 hours); ◈ high retention or carrying capacity; ◈ low chloride content (<70 mg/l) to minimise the impact on logging during drilling; ◈ the ability to conduct the most comprehensive set of high-quality geophysical surveys to assess the reservoir.	◈ some components of HT-WBDF may contribute to the formation of stable foam at high temperatures; ◈ degradation of chemical reagent properties during prolonged storage in field conditions (temperature, humidity, UV radiation).	◈ minimal costs for waste management and disposal of drilling sludge; ◈ minimal environmental footprint; ◈ environmental acceptability index; ◈ logistical efficiency index; ◈ technological feasibility index.
Specific		
◈ ensuring that there is no need to introduce corrosion inhibitors; ◈ stability of the Sag Factor over a long period of time (100 hours) in the absence of circulation; ◈ absence or low content of certain components (alkanes nC15 – nC35, aromatic hydrocarbons, etc.); ◈ absence or low content of biomarkers (terpenes, steranes, etc.).	◈ if hematite (Fe_2O_3) or ilmenite ($FeTiO_3$) are used as weighting agents, there is a problem of magnetic anomalies that distort MWD/LWD results; ◈ under HPHT conditions, metal ions (Fe^{3+}, Cu^{2+}, Mn^{2+}, etc.) can catalyse the degradation of polymers and the oxidation of organic components (by a factor of 10-100); ◈ when using nanomaterials (SiO_2, Al_2O_3, etc.), there is a risk of their aggregation and migration into the environment at pH <7 or >9.	◈ minimum volume of generated sludge (especially relevant for offshore drilling); ◈ cuttings carrying capacity index; ◈ corrosion inhibitor demand; ◈ biodegradability index of formulation components; ◈ strategic security coefficient; ◈ digital integration index.

Note: Wellbore Stability Index (WSI) is a comprehensive assessment of the ability of drilling fluid to maintain the mechanical integrity of the wellbore, preventing collapses, caving and other geomechanical problems; Recipe Profitability Ratio (ROI) – the ratio of economic effect (savings from reduced NPT, increased ROP, maintained productivity) to additional costs for premium components; Technological Efficiency Ratio is an integral indicator of successful drilling without complications, taking into account ROP, wellbore quality, and the absence of sticking and absorption, the coefficient depends on the synergy of components – HPHT rheology control, HPHT filtration, clay rock inhibitors, lubricating additives, etc., which work together; Cycle Economic Efficiency (Cost per BBL) – the total cost of the solution throughout the entire drilling cycle, taking into account treatments, refills and disposal, includes initial cost, treatments (10-30% of initial cost), losses (5-15%), disposal ($20-80/m3), logistics; Logistics Efficiency Index – the ratio of the formula's performance to the complexity of its delivery, storage and preparation in the field, takes into account the number of components (optimum 5-8), shelf life, the need for special equipment, and staff qualifications; Environmental Acceptability Coefficient – an integrated assessment of the environmental impact of formulation components according to OSPAR/EPA standards, including toxicity, biodegradability, and bioaccumulation; Hole Cleaning Efficiency – the quality of sludge removal and maintenance of hole cleanliness, assessed by cavernometer and analysis of sludge on the surface, depends on the optimisation of the rheological profile (YP/PV = 0.75-1.25) and the use of additional sludge carriers (fibres, spherical particles); Preparation Technological Index – simplicity and reliability of solution preparation in field conditions, including mixing time and quality stability, depends on the solubility of components, order of introduction, the need for special conditions (temperature, pH, hydration time); Strategic Security Index – independence of the ability to prepare the required volume of solution from critical imported components and the availability of alternative sources of supply, assesses the geographical diversification of suppliers, the availability of local analogues, and strategic reserves of formulation components; Digital Integration Index – compatibility of the formulation with automatic control systems, IoT sensors, and AI optimisation, requires stable rheological signatures, predictable behaviour, and the possibility of real-time correction

Source: compiled by the authors based on T. Hasan Hamdan *et al*. (2020), A. Rana *et al*. (2024)

The hierarchy shown in Table 2 links requirements and technological constraints with performance indicators. It is impossible to prepare an optimal HT-HPWBF formulation without meeting the functional requirements, constraints and performance indicators of the critical group. If important requirements such as the technological feasibility of preparation or the formation of a thin impermeable filtration crust (or others from the table) are violated, then the use of the formulation leads to a sharp increase in both costs and risks of complications, accidents, and an increase in drilling and completion time. This, in turn, reduces the profitability of the project. The fulfilment of additional and special functional requirements and restrictions as well as the provision of appropriate performance indicators is advisable in certain cases when required by the situation at the well or by the customer. The most common performance indicators for drilling fluids are the PI ratio and the permeability recovery factor. However, other indicators such as the Strategic Security Index, Digital Integration Index, etc. are also important for better formulation.

When developing a drilling fluid formulation for specific mining and geological conditions, each individual well should be assessed in advance for potential mechanisms of contamination of the bottomhole zone and risks of oil-water emulsion formation. This step will enable the correct choice of the base of the system (type of fluid), which will then be expanded with additional reagents to give the system the necessary technological properties. It is also important to take into account the existing practical experience of using certain formulations in specific (or similar) mining and geological and thermobaric conditions as fully as possible. Such experience is not just a database, journals or archives with poorly structured data, but intelligent systems that allow the accumulated knowledge and experience to be used as quickly and efficiently as possible.

To implement the procedure for forming a list of alternative acceptable HT-HPWBF system formulations, in addition to the hierarchical system of requirements, it is necessary to select an optimality criterion or form a system of criteria according to which the selection will be made. The main criterion for the optimality of the drilling fluid was the cost per unit volume of the formulation. Although the cost of the formulation in one way or another influences the choice of the base (type) of the drilling fluid and its component composition, it cannot be the main criterion when developing a new formulation or selecting the optimal variant among those proposed. In modern conditions, it is necessary to take into account the requirements for safety and control of the well, the technological efficiency of drilling, as well as environmental and economic aspects. At the same time, it should be noted that the selection of the optimal composition of HT-HPWBF is a multi-criteria task. The number of criteria, depending on the specific case (well, customer requirements, environmental and economic, or technological constraints), can range from 3 to 6 or more.

For example, authors A. Raptanov *et al*. (2021) mentioned drilling fluid density, HPHT filtration, pH, salinity, and water phase composition as key control parameters when selecting a drilling fluid. With the accumulation of practice and experience in drilling HTHP wells, the following combinations of optimality criteria have been implemented (compatibility, thermal stability and required density conditions are preserved for all options) (Deshmukh *et al*., 2021; Morrison *et al*., 2021; King & Rodrigue, 2025): Option 1 – HTH filtration, PV, YP; Option 2 – HTH filtration, PV, YP, Sag Factor; Option 3 – HTH filtration, LSRV, LSYP, ECD, Sag Factor; Option 4 – HTH filtration, LSRV, LSYP, ECD, ESD, Sag Factor, crust friction coefficient; Option 5 – HTH filtration, filtration crust parameters (density, permeability, thickness, friction coefficient), LSRV, LSYP, ECD, ESD, Sag Factor, inhibition capacity; Option 6 – HTH filtration, filtration crust parameters (density, permeability, thickness, friction coefficient), LSRV, LSYP, ECD, ESD, Sag Factor, inhibition capacity, high-temperature rheological profile.

With the accumulation of experience in the construction of HPHT wells, the system of criteria is constantly being supplemented and complicated. For this reason, service companies strive to ensure that at least 5-12 criteria are met simultaneously when developing highly effective formulations. Although the number of such criteria may be quite significant, for the purpose of selecting the optimal HT-HPWBF formulations, they can be presented in the form of a hierarchical pyramid (Fig. 5). The system of criteria for selecting HT-HPWBF recipes is based on a three-level hierarchical structure, in which: at Level 1 α – the criteria ensure well control and safe operation (typically, Sag Factor <0.5 and LSRV at 6 rpm ⩽6 units are acceptable); at Level 2 β – criteria ensure the achievement of design technological goals (usually acceptable values are HPHT filtration 2-7 cm^3/30 min, YP 12-25 pounds/100 ft^2; the rest are determined by the conditions of well construction and/or the customer); at Level 3, the combination of γ criteria allows balancing environmental safety and economic efficiency requirements (fully determined by the conditions of well construction and the customer).

It should be noted that Figure 5 does not show all possible criteria, but only those that are most commonly used for HT-HPWBF systems. Depending on the specific drilling conditions and restrictions imposed by these conditions and/or circumstances, environmental or legal regulations, or the project budget, the number of criteria may either decrease or increase. Moreover, the level of criteria can be raised from the second and third levels to the first, or from the third to the second, but the transition of α – criteria to a lower level or β – criteria to the third level is not possible. To adapt to the specific conditions of each situation, appropriate weighting coefficients can be introduced both within levels and for all elements of the criteria pyramid. Such weighting coefficients are often used (Khosravanian & Aadnøy, 2021) to simultaneously take into account several criteria and quickly assess the effectiveness of a formulation by using various criterion combinations (linear, additive, multiplicative, Nash combination, Min-Max combination, etc.).

Each of them has both advantages and disadvantages, but in general, such convolutions are not always sufficient in practice due to: the subjectivity of weights – even a small change in coefficients gives a different “optimum”; the problem is exacerbated when the criteria are correlated; the compensatory effect – “excellent” rheology can override ”poor” ecology; scalarisation hides information about compromises: it is impossible to see how much worse/better a particular formulation is than its analogue (according to one or another individual indicator); non-linear and discrete constraints (e.g., “barite <4.2%” or “pH ⩾9”) do not lend themselves well to smooth convolution – penalties or complex transformations are required; the number of criteria is growing (more than 25 indicators, including technological, environmental, economic, HSE, specific, etc.). It does not seem realistic to set the weights correctly for such a multidimensional task. Therefore, with the development of technology and the growth of computing capabilities, the following are used as alternatives to criterion convolutions: Pareto optimisation, evolutionary multi-criteria

algorithms (NSGA-II, NSGA-III, SPEA2, PAES); machine learning methods: Gaussian Process Optimisation, Bayesian Optimisation, Random Forest; Fuzzy Logic methods: Fuzzy TOPSIS, Fuzzy AHP and many others.

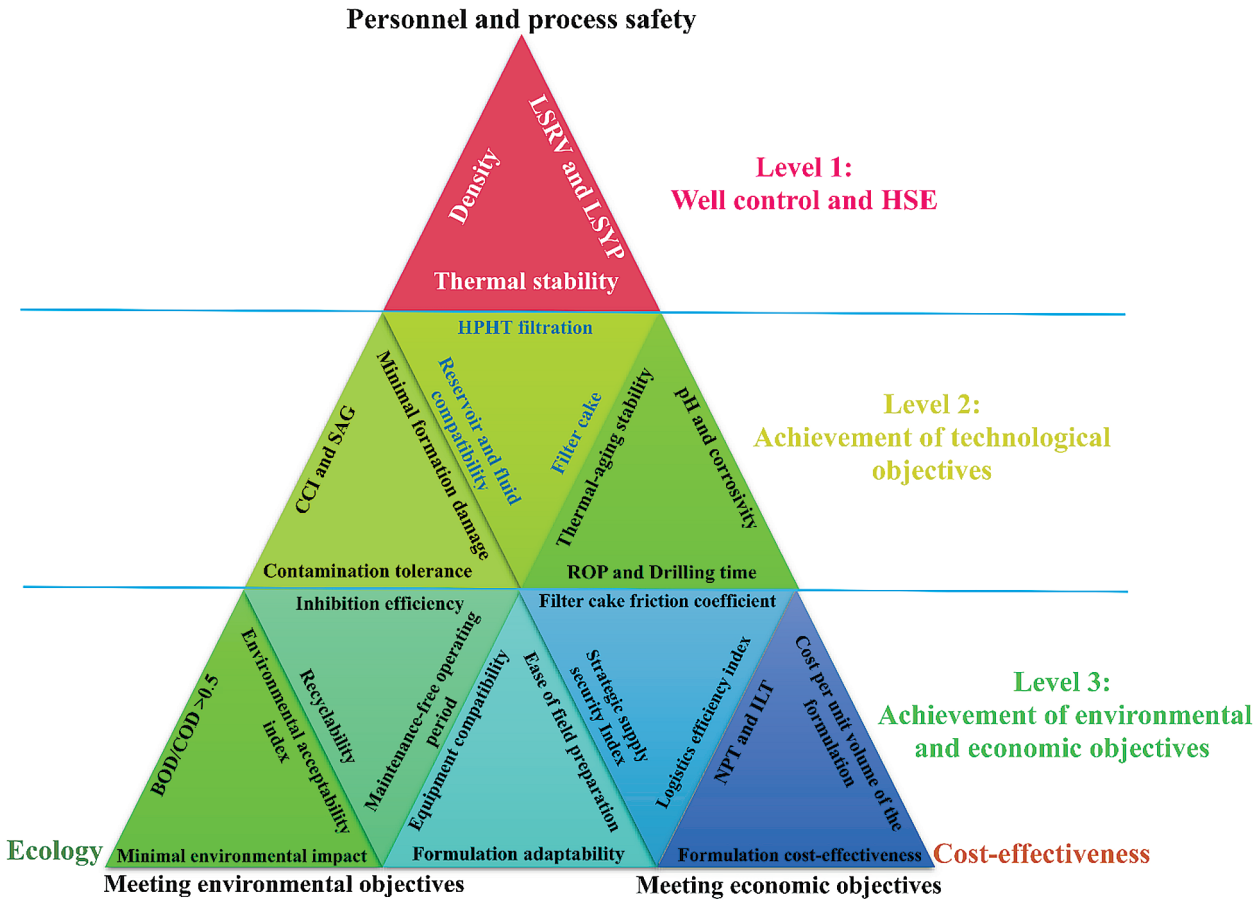

Figure 5. Illustration of the system of basic criteria for selecting HT-HPWBF formulations
Source: created by the authors

In order to make informed decisions regarding the composition of HT-HPWBF drilling fluid, it is necessary not only to identify the criteria that may influence the choice, but also to develop comprehensive KPIs that reflect the critical aspects of drilling fluid performance in terms of achieving the planned objectives. Such comprehensive KPIs provide a holistic view of the effectiveness of the formulation, taking into account the interrelationship between key parameters and performance indicators. KPIs can be developed through a weighted approach, where each individual KPI is assigned a specific weighting factor depending on its relative importance for specific drilling conditions. For example, in unstable clay formations, the weight of the clay inhibition indicator may be higher than that of the lubricity indicator. Indexing – creating an integral index by normalising and combining several KPIs. This approach provides a single numerical rating that reflects the overall effectiveness of the formulation. Matrix analysis – developing a matrix that displays the values of several core KPIs for different formulations. This allows for visual comparison and identification of optimal solutions based on trade-offs between different indicators.

The formation and correct analysis of industrial experience play a significant role in the formation of adequate predictive indicators of the effectiveness of fluid formulations used in similar or comparable drilling conditions. It should be noted that in order to form relevant KPIs, statistical, expert and big data analysis of industrial experience is performed provided that the data has been prepared in advance (systematisation, standardisation, noise component rejection, etc.). In addition to experience, i.e. accumulated knowledge and information, the proper implementation and functioning of KPIs also requires real-time monitoring and recording of flushing system parameters. Under such conditions, the actual optimisation of the formulation is carried out through laboratory testing, the design and logic of which is based on risk assessment and is adjusted in the event of significant changes in the well drilling process recorded by alert systems. This process is essentially an iterative selection of the component composition of the flushing system to achieve the design values of the system parameters, with maximum compliance with the selected optimisation criteria. Figure 6 shows the procedure for forming complex KPIs for the HT-HPWBF system.

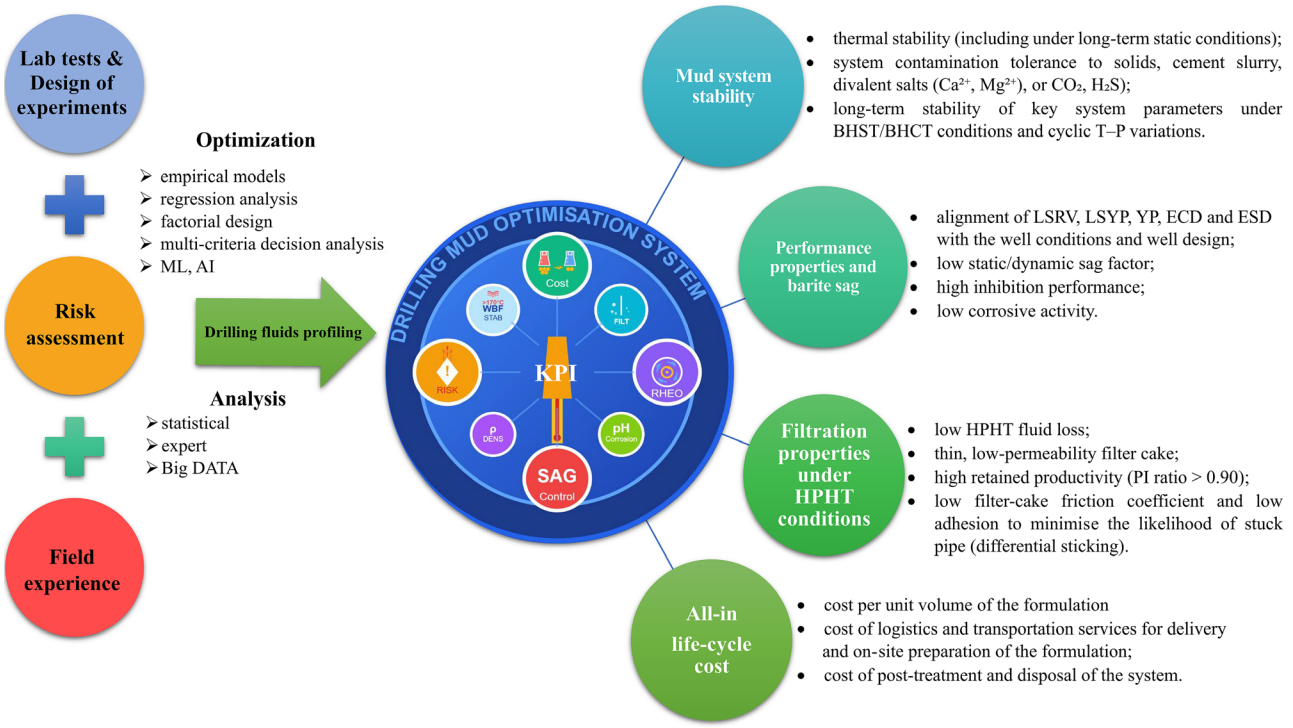

Figure 6. Formation of comprehensive KPIs for the HT-HPWBF system
Source: created by the authors

As can be seen in Figure 6, the comprehensive indicator is formed through an integrated combination of industrial experience, laboratory research, risk assessment, and drilling fluid profiling procedures. As a result, the following methodology for selecting the optimal HT-HPWBF formulation was developed: The process of researching and optimising the HT-HPWBF system involves several consecutive stages. The first stage involves collecting input data on the well and, if available, on neighbouring wells, as well as assessing technical, technological and environmental risks. In the second stage, design objectives are determined based on an analysis of key issues arising from the use of drilling fluids in HPHT conditions. The third stage involves the formation of a set of optimality criteria and their organisation into a hierarchical system, which allows the creation of a list of acceptable alternative HT-HPWBF system formulations. Finally, at the fourth stage, comprehensive KPIs are developed, which serve as the basis for the final selection of the optimal system formulation. The feasibility of using comprehensive KPIs in modern HPHT well drilling conditions is indisputable, given the increasing complexity of such projects.

For the successful application of HT-HPWBF in HTHP conditions, it is necessary to develop a set of KPIs that comprehensively reflect the suitability of the formulation. In challenging conditions of high bottomhole temperatures and pressures, to ensure maximum safety and efficiency of the drilling process, in addition to KPIs, it is recommended to simultaneously deploy and implement AI platforms for control and monitoring of the current state of well cleaning and deepening processes (such as AI-driller, Corva, etc.). The data obtained clearly correlates with the developed hierarchy of criteria. For example, indicators related to α-criteria (ensuring safe well control), such as the Sag Factor (0.45) and LSRV (5.8 units), confirm that all strict safety requirements have been met. At the same time, key technological indicators (filtration, shear stress) included in the β-criteria were achieved within the target ranges, demonstrating the high performance of the drilling fluid. Economic calculations reflecting γ criteria showed cost optimisation and high project profitability (ROI 1.6), confirming the environmental and economic efficiency of the decision.

Conclusions

The development and growth of Ukraine's oil and gas industry is closely linked to the implementation of complex high-tech projects, including drilling wells in HPHT conditions. One of the problems encountered in the implementation of these projects is the scientifically sound selection of drilling fluid systems that would ensure fast, trouble-free well drilling with proper service support. This issue is particularly relevant when selecting the optimal drilling fluid formulations under HPHT constraints. The development and service support of drilling fluid systems in complex HPHT conditions critically depends on information support and accumulated practical experience.

The study confirmed the critical importance of a scientifically sound approach to selecting optimal HT-HPWBF drilling fluid formulations for the successful implementation of deep and ultradeep well drilling projects.

An analysis of more than 200 publications and drilling experience at Ukrainian fields (Berezivske, Shebelynske, Stepove, Solokhivske GCF, etc.) revealed a significant lag behind global practice, where the thermal stability of systems reaches 316°C compared to 170-200°C in Ukraine, and the share of modern clay-free HT-HPWBF systems is several times lower than in leading countries such as China or the USA. The developed three-level hierarchical system of criteria provides a comprehensive approach to evaluating the effectiveness of formulations: α-criteria guarantee safe well control (Sag Factor <0.5, LSRV at 6 rpm ⩽6 units), β-criteria ensure the achievement of design indicators (HPHT filtration 2-7 cm^3/30 min, YP 12-25 pounds/100 ft^2), γ-criteria optimise environmental and economic efficiency (ROI >1.5, NPT reduction by 30-40%). It has been established that successful commercial systems (PYRO-DRILL, BaraDrilNX, VeraTherm) use 5-12 criteria simultaneously, providing thermal stability of 205-316°C due to the synergy of synthetic polymers, formates and nanoscale weighting agents.

The proposed methodology for forming complex KPIs integrates three key components: analysis of industrial experience (with mandatory preliminary data preparation), laboratory research (including 24-72 hour ageing tests at BHST) and dynamic risk assessment. Further research should be aimed at developing unified methodologies for forming KPIs, taking into account the specifics of Ukrainian deposits, and creating a national database of HT-HPWBF formulation efficiency to accelerate technology transfer and achieve the strategic goal of increasing Ukraine's mineral resource base.

Acknowledgements
None.

Funding
None.

Conflict of Interest
None.

References

[1] Agwu, O.E., Akpabio, J.U., Ekpenyong, M.E., Inyang, U.G., Asuquo, D.E., Eyoh, I.J., & Adeoye, O.S. (2021). A comprehensive review of laboratory, field and modelling studies on drilling mud rheology in high temperature high pressure (HTHP) conditions. *Journal of Natural Gas Science and Engineering*, 94, article number 104046. doi: 10.1016/j.jngse.2021.104046.

[2] Ahasan, M.H., Alahi Alvi, M.F., Ahmed, N., & Alam, M.S. (2021). An investigation of the effects of synthesized zinc oxide nanoparticles on the properties of water-based drilling fluid. *Petroleum Research*, 7(1), 131-137. doi: 10.1016/j.ptlrs.2021.08.003.

[3] BaraDrilN™ X fluid helps customer achieve well testing operation. (n.d.). Retrieved from https://www.halliburton.com/en/resources/baradriin-x-fluid-helps-customer-achieve-well-testing-operation.

[4] Biocar-TF biopolymer drilling fluid system was proposed. (n.d.). Retrieved from https://gse.ua/novini/1055-v-tannya-z-novim-rokom-p-dbittya-p-dsumk-v-2021-roku.html.

[5] Deshmukh, S., Motta, M.D., Prabhudesai, S., Patil, M., Kumar, Y., Mihalic, B.A., & Dey, R.S. (2021). Use of micronized weighting agents for high density completion fluids: A case study. In *IADC/SPE Asia Pacific drilling technology conference* (article number SPE-201065-MS). Yangon: SPE. doi: 10.2118/201065-MS.

[6] Erge, O., Sakaoglu, K., Sonmez, A., Bagatir, G., Dogan, H.A., Ay, A., & Gucuyener, I.H. (2020). Overview and design principles of drilling fluids systems for geothermal wells in Turkey. *Geothermics*, 88, article number 101897. doi: 10.1016/j.geothermics.2020.101897.

[7] Fakoya, M.F., & Ahmed, R. (2023). Experimental study on dynamic barite sag and effects of inclination and pipe rotation. *SPE Journal*, 29(2), 830-842. doi: 10.2118/217987-PA.

[8] First utilization of the clayless drilling mud "Biocar-TF." (2018). Retrieved from https://gse.ua/en/origins/how-it-was/806-first-utilization-of-the-clayless-drilling-mud-biocar-tf.html.

[9] Freschi, Y.L., Rincon Chavez, A.C., McCartney, R.M., Wenk, A., Manzoleloua, C., Li, D., & Derkach, E. (2025). An innovative water-based reservoir drill-in fluid solution customized to withstand the extreme thermal boundaries of the Perth Basin while minimizing formation damage. In *SPE/IADC international drilling conference and exhibition* (article number SPE-223723-MS). Amsterdam: SPE. doi: 10.2118/223723-MS.

[10] Gautam, S., Kumar, S., Kumar, A., Rajak, V.K., & Guria, C. (2025). Development of functional polymer-based clay-free HPHT drilling fluid: Effect of molecular weight and its distribution on drilling fluid performance. *Geoenergy Science and Engineering*, 246, article number 213616. doi: 10.1016/j.geoen.2024.213616.

[11] Hasan Hamdan, T., *et al*. (2020). New generation of HTHP water based drilling fluid changing conventional drilling fluids solutions. In *Abu Dhabi international petroleum exhibition & conference* (article number SPE-203439-MS). Abu Dhabi: SPE. doi: 10.2118/203439-MS.

[12] Jameel, N., & Ali, J.A. (2023). Field and experimental investigations on the effect of reservoir drill-in fluids on penetration rate and drilling cost in horizontal wells. *Gels*, 9(7), article number 510. doi: 10.3390/gels9070510.

[13] Karakosta, K., Mitropoulos, A.C., & Kyzas, G.Z. (2021). A review in nanopolymers for drilling fluids applications. *Journal of Molecular Structure*, 1227, article number 129702. doi: 10.1016/j.molstruc.2020.129702.

[14] Khalid, A., Ashraf, Q., Luqman, K., Hadj Moussa, A., Ghulam Nabi, A., & Umair, A.B. (2021). Precise bottom hole pressure management to reach target depth in a narrow windowed ultra HP-HT well: A case for automated managed pressure drilling. In *International petroleum technology conference* (article number IPTC-21410-MS). Kuala Lumpur: IPTC. doi: 10.2523/iptc-21410-MS.

[15] Khosravanian, R., & Aadnøy, B.S. (2021). *Methods for petroleum well optimization. Automation and data solutions*. Boston: Elsevier. doi: 10.1016/C2020-0-02224-3.

[16] King, C., & Rodrigue, K. (2025). Novel high temperature water-based reservoir drilling fluid to access depleted deepwater reserves. In *SPE/IADC international drilling conference and exhibition* (article number SPE-223705-MS). Amsterdam: SPE. doi: 10.2118/223705-MS.

[17] Kong, X., Chen, M., Zhang, C., Liu, Z., Jin, Y., Wang, X., Liu, M., & Li, S. (2022). Optimization of high temperature-resistant modified starch polyamine anti-collapse water-based drilling fluid system for deep shale reservoir. *Molecules*, 27(24), article number 8936. doi: 10.3390/molecules27248936.

[18] Law of Ukraine No 4154-IX "On Amendments to Certain Legislative Acts of Ukraine Regarding the Update of the Nationwide Program for the Development of the Mineral Resource Base of Ukraine for the Period Until 2030 and the Regulation of Certain Issues Concerning Minerals and Components of Strategic and Critical Importance". (2024, December). Retrieved from https://zakon.rada.gov.ua/laws/show/4154-20#Text.

[19] Liu, J., Dai, Z., Xu, K., Yang, Y., Lv, K., Huang, X., & Sun, J. (2020a). Water-based drilling fluid containing bentonite/poly (sodium 4-styrenesulfonate) composite for ultrahigh-temperature ultradeep drilling and its field performance. *SPE Journal*, 25(3), 1193-1203. doi: 10.2118/199362-PA.

[20] Liu, J., Li, G., & Xia, Y. (2020b). Technical progress on environmental-friendly, high-performance water-based drilling fluids. *Environmental and Earth Sciences Research Journal*, 7(3), 121-126. doi: 10.18280/eesrj.070305.

[21] Mao, H., Yang, Y., Zhang, H., Zheng, J., & Zhong, Y. (2020). Conceptual design and methodology for rheological control of water-based drilling fluids in ultra-high temperature and ultra-high pressure drilling applications. *Journal of Petroleum Science and Engineering*, 188, article number 106884. doi: 10.1016/j.petrol.2019.106884.

[22] Medhi, S., Chowdhury, S., Kumar, A., Gupta, D.K., Aswal, Z., & Sangwai, J.S. (2020). Zirconium oxide nanoparticle as an effective additive for non-damaging drilling fluid: A study through rheology and computational fluid dynamics investigation. *Journal of Petroleum Science and Engineering*, 187, article number 106826. doi: 10.1016/j.petrol.2019.106826.

[23] Miikor, B., Amadi, S.C., & Oriji, B.A. (2025). Performance evaluation of the types of polymers used as water-based mud viscosifiers for drilling operations in elevated temperature environment. In *SPE Nigeria annual international conference and exhibition* (article number SPE-228811-MS). Lagos: SPE. doi: 10.2118/228811-MS.

[24] Moroni, L., Fatkullin, K., & Tran Thanh, B. (2023). Evolution of a versatile HTHP water-based drilling fluid improved drilling efficiency offshore Vietnam. In *SPE/IATMI Asia Pacific oil & gas conference and exhibition* (article number SPE-215251-MS). Jakarta: SPE. doi: 10.2118/215251-MS.

[25] Morrison, A.C., King, C., & Rodrigue, K. (2021). First use of novel high temperature water-based reservoir drilling fluid to access depleted deepwater reserves. In *Abu Dhabi international petroleum exhibition & conference* (article number SPE-207825-MS). Abu Dhabi: SPE. doi: 10.2118/207825-MS.

[26] Myslyuk, M.A., & Zholob, N.R. (2023). To the assessment of thermal stability of biopolymer systems. *Journal of Hydrocarbon Power Engineering*, 10(1), 1-7. doi: 10.31471/2311-1399-2023-1(19)-1-7.

[27] Oseh, J.O., *et al*. (2025). Improvement of static and dynamic sag performance of water-based drilling mud using combined nano-barite and nano-ilmenite particles. In *SPE Nigeria annual international conference and exhibition* (article number SPE-228676-MS). Lagos: SPE. doi: 10.2118/228676-MS.

[28] Patent No. 124224. (2020). *Cement-free drilling mud*. Retrieved from https://sis.nipo.gov.ua/uk/search/detail/1608972/.

[29] Prozorro. (n.d.). *Contracts*. Retrieved from https://prozorro.gov.ua/uk/search/contracts.

[30] Quitian-Ardila, L.H., Garcia-Blanco, Y.J., Daza-Barranco, L.M., Schimicoscki, R.S., Andrade, D.E.V., & Franco, A.T. (2024). Improving the rheological and thermal stability of water-based drilling fluids by incrementing xanthan gum concentration. *Physics of Fluids*, 36, article number 103111. doi: 10.1063/5.0230214.

[31] Rana, A., Murtaza, M., Raza, A., Mahmoud, M., & Kamal, M.S. (2024). Application of high-density brines in drilling and completion fluids: Current insights and future perspectives. *Energy & Fuels*, 38(8), 6561-6578. doi: 10.1021/acs.energyfuels.3c04421.

[32] Raptanov, A.K., Ruzhenskyi, V.V., Kostiv, B.I., Myslyuk, M.A., & Charkovskyy, V.M. (2021). Analysis of the deep drilling technology in unstable formations at the Semyrenky Gas Condensate Field. *SOCAR Proceedings*, 2, 52-64. doi: 10.5510/ogp2021si200573.

[33] Shi, H., Yu, Y., Wang, Y., Ning, Z., & Luo, Z. (2024). Effect of ionic liquids with different structures on rheological properties of water-based drilling fluids and mechanism research at ultra-high temperatures. *Molecules*, 29(17), article number 4206. doi: 10.3390/molecules29174206.

[34] Shokry, A., Basfar, S., & Elkatatny, S. (2024). Evaluation of using micronized Saudi calcite in ilmenite-weighted water-based drilling fluid. *Scientific Reports*, 14, article number 12777. doi: 10.1038/s41598-024-63839-6.

[35] Singh, R., Sharma, R., & Rao, G.R. (2024). Investigation of the effects of ultra-high pressure and temperature on the rheological properties of a novel high-density clear completion fluids using magnesium bromide for applications in HPHT reservoirs. *Geomechanics and Geophysics for Geo-Energy and Geo-Resources*, 10, article number 9. doi: 10.1007/s40948-023-00724-y.

[36] Soori, G.R., Mohd Alwi, M.A., Haniff Julian, Z., Tajudin, N., Zulkifli, S.A., & Abd Rahaman, N.A. (2023). Using cerium oxide (6.0 SG) as weighting material in HTHP drilling fluids. In *Gas & oil technology showcase and conference* (article number SPE-214171-MS). Dubai: SPE. doi: 10.2118/214171-MS.

[37] Sun, J., Yang, J., Bai, Y., Lyu, K., & Liu, F. (2024). Research progress and development of deep and ultra-deep drilling fluid technology. *Petroleum Exploration and Development*, 51(4), 1022-1034. doi: 10.1016/S1876-3804(24)60522-7.

[38] Taghdimi, R., Kaffashi, B., Rasaei, M.R., Dabiri, M.-S., & Hemmati-Sarapardeh, A. (2023). Formulating a novel drilling mud using biopolymers, nanoparticles, and SDS and investigating its rheological behavior, interfacial tension, and formation damage. *Scientific Reports*, 13, article number 12080. doi: 10.1038/s41598-023-39257-5.

[39] Tchameni, A.P., Nagre, R.D., Yin, S.-M., Wang, L.-Q., Wang, X.-Y., Zhou, S.-Y., & Wang, X.-D. (2025). A thermo-associating copolymer integrated with biogenic nanosilica as a novel viscosifier in low-solid drilling fluids. *Petroleum Science*, 22(7), 2884-2904. doi: 10.1016/j.petsci.2025.04.020.

[40] VeraTherm high-temperature water-based drilling fluid. (n.d.). Retrieved from https://www.slb.com/products-and-services/innovating-in-oil-and-gas/well-construction/drilling-fluids/water-based-drilling-fluid/veratherm-high-temperature-water-based-drilling-fluid.

[41] Wang, H., Huang, H., Bi, W., Ji, G., Zhou, B., & Zhuo, L. (2022). Deep and ultra-deep oil and gas well drilling technologies: Progress and prospect. *Natural Gas Industry B*, 9(2), 141-157. doi: 10.1016/j.ngib.2021.08.019.

[42] World's first application of BaraXtreme fluid in HTHP gas well. (n.d.). Retrieved from https://www.halliburton.com/en/resources/worlds-first-application-of-baraxtreme-fluid-in-hthp-gas-well.

[43] Zhang, J., Wang, H., Ji, G., Cui, M., Chen, L., Li, W., & Liu, L. (2025). Technologies and achievements for drilling and completion of onshore deep and ultra-deep wells in China. In *International petroleum technology conference* (article number IPTC-24918-MS). Beijing: IPTC. doi: 10.2523/IPTC-24918-MS.

До питання вибору оптимальних рецептур бурових розчинів в умовах HPHT обмежень

Юрій Волошин
Кандидат технічних наук, доцент
Івано-Франківський національний технічний університет нафти і газу
76019, вул. Карпатська, 15, м. Івано-Франківськ, Україна
https://orcid.org/0000-0002-0582-1778

Володимир Богославець
Кандидат технічних наук, доцент
Івано-Франківський національний технічний університет нафти і газу
76019, вул. Карпатська, 15, м. Івано-Франківськ, Україна
https://orcid.org/0000-0001-9622-4065

Олег Марцинків
Кандидат технічних наук, доцент
Івано-Франківський національний технічний університет нафти і газу
76019, вул. Карпатська, 15, м. Івано-Франківськ, Україна
https://orcid.org/0000-0003-4583-5944

Олег Куців
Аспірант
Івано-Франківський національний технічний університет нафти і газу
76019, вул. Карпатська, 15, м. Івано-Франківськ, Україна
https://orcid.org/0009-0006-6360-2537

Богдан Марцинків
Аспірант
Івано-Франківський національний технічний університет нафти і газу
76019, вул. Карпатська, 15, м. Івано-Франківськ, Україна
https://orcid.org/0009-0009-6614-0130

Анотація. Буріння глибоких та надглибоких свердловин в умовах високих пластових тисків і температур (HPHT) є стратегічним напрямом розвитку мінерально-сировинної бази України, що потребує науково обґрунтованого підходу до вибору оптимальних рецептур бурових розчинів. Метою дослідження було формування на основі глибокого аналізу практики спорудження HPHT-свердловин методології вибору оптимальних рецептур високопродуктивних безглинистих систем бурових розчинів на водній основі (HT-HPWBF), яка б одночасно враховувала ієрархію критеріїв оптимальності і ключові показники ефективності системи. Проведено систематичний огляд та контент-аналіз понад 200 публікацій щодо застосування HT-HPWBF систем, узагальнено досвід використання таких систем на українських родовищах та виконано порівняльний аналіз з міжнародною практикою. Встановлено відставання України від світових лідерів у бурінні HPHT-свердловин переважно через використання традиційних хлоркалієвих та біополімер-калієвих систем замість сучасних HT-HPWBF. На основі аналізу важливості та впливовості вимог, технологічних обмежень і показників ефективності систем HT-HPWBF показано можливість формування ієрархічної системи основних критеріїв для вибору оптимальних рецептур. Розроблено тирівневу ієрархічну систему критеріїв оптимальності, що включає α-критерії контролю свердловини, β-критерії досягнення технологічних цілей та γ-критерії еколого-економічної ефективності. Запропоновано методологію формування комплексних ключових показників ефективності, що інтегрує промисловий досвід, лабораторні дослідження та оцінку ризиків. Обґрунтовано доцільність одночасного використання процедур інтелектуального аналізу історичних даних, моніторингу параметрів у режимі реального часу та впровадження ключових показників ефективності для вибору оптимальних рецептур. Результати дослідження можуть бути використані інженерами-технологами бурових підприємств та сервісних компаній для підвищення ефективності буріння HPHT-свердловин в Україні

Ключові слова: проєктування промивальної системи; індекс якості промивальної системи; критерії вибору; комплексний аналіз; безглинисті системи

ISSN 1993-9973, e-ISSN 2415-332X

Vol. 25, No. 2
2025

PROSPECTING AND DEVELOPMENT OF OIL AND GAS FIELDS

https://pdogf.com.ua/en

Received: 07.05.2025. Revised: 30.09.2025. Accepted: 08.12.2025. Published: 09.01.2026.

UDC 622.24.622.2

DOI: 10.63341/pdogf/2.2025.64

Advanced analytical methods for evaluating technological indicators in sand-prone wells

Shahin Ismayilov

PhD in Technical Sciences, Associate Professor
Azerbaijan State Oil and Industry University
AZ1010, 20 Azadliq Ave., Baku, Azerbaijan
https://orcid.org/0000-0002-9558-4701

Zaur Mirzayev*

Postgraduate Student
Azerbaijan State Oil and Industry University
AZ1010, 20 Azadliq Ave., Baku, Azerbaijan
https://orcid.org/0009-0003-9066-3114

Vusal Iskenderov

Postgraduate Student
Azerbaijan State Oil and Industry University
AZ1010, 20 Azadliq Ave., Baku, Azerbaijan
https://orcid.org/0009-0009-6626-5136

Nijat Ismayilov

Postgraduate Student
Azerbaijan State Oil and Industry University
AZ1010, 20 Azadliq Ave., Baku, Azerbaijan
https://orcid.org/0009-0009-4453-0461

Abstract. The aim of the study was to identify key technological indicators affecting productivity and the risk of sand production in the operation of sand-bearing wells at an offshore field. The methodology included field and laboratory studies of 32 production wells of various geometries, conducted from January 2024 to June 2025. Parameters such as flow rate, temperature gradient, bottomhole and formation pressure, and vibration frequency were monitored using digital sensors and processed using dimensionality reduction and machine learning methods. The results showed significant differences between vertical and horizontal wells: with an average flow rate of 74.71 m^3/day, vertical wells had a productivity coefficient of 11.01 m^3/day·MPa, while horizontal wells had a productivity coefficient of 22.56 m^3/day·MPa at a flow rate of 66.10 m^3/day. The principal component method revealed the greatest significance of the temperature gradient and flow rate (load coefficients of 0.667), as well as the decisive role of vibration activity in the formation of unstable modes (coefficient of 0.851), defined in this study as operational regimes exhibiting rapid changes in flow rate and pressure variance exceeding 15% within a 24-hour period. The calculated Spearman's coefficient ($\rho = 0.88$, $p < 0.0001$) between temperature fluctuations and productivity changes confirmed the direct influence of thermodynamics on filtration processes. Among the predictive models, XGBoost demonstrated the best regression accuracy (RMSE = 3.45; MAPE = 8.23%; $R^2 = 0.91$). However, to assess the risk of sand production as a classification task, additional metrics were calculated: F1-score = 0.91, AUC = 0.94, Precision = 0.88, Recall = 0.93, confirming the model's suitability for this purpose. The practical significance of the results obtained lies in the possibility of using the developed approaches by

Suggested Citation: Ismayilov, Sh., Mirzayev, Z., Iskenderov, V., & Ismayilov, N. (2025). Advanced analytical methods for evaluating technological indicators in sand-prone wells. *Prospecting and Development of Oil and Gas Fields*, 25(2), 64-74. doi: 10.63341/pdogf/2.2025.64.

*Corresponding author

technological monitoring services, design organisations, and field operators to build intelligent control systems aimed at reducing accidents, increasing production stability, and optimising the operating modes of sand-bearing reservoirs

Keywords: filtration stability; vibration intensity; temperature gradient; sampling modes; geomechanical risks; predictive algorithms

Introduction

Ensuring stable and safe operation of sand-bearing wells in offshore fields remains one of the key challenges for the modern oil and gas industry. Sand production leads to intensive equipment wear, reduced flow rates, premature well decommissioning, and, in some cases, emergencies requiring costly interventions. This problem is particularly acute in offshore production, where technical access to wells is limited and restoration work is associated with high costs and risks. Not all wells are equally susceptible to sand production: its intensity depends on a variety of factors, including wellbore geometry, formation and bottomhole pressures, temperature conditions, and vibration characteristics. Despite the active development of digital monitoring and forecasting technologies, engineering practice still lacks comprehensive approaches that allow these parameters to be considered simultaneously, identify their interrelationships, and assess their impact on well productivity and stability. In this context, the need to develop improved analytical methods for assessing technological indicators in sand-bearing reservoirs is of paramount importance.

An important feature of sand-bearing well operation is the influence of multicomponent factors on the stability of filtration processes. Studies have shown that unstable heat and mass transfer in the bottomhole zone can intensify reservoir decompaction processes and, as a result, provoke sand production. S. Alkhasli *et al*. (2022), analysing temperature gradients in deepwater wells, found that temperature fluctuations of more than 5°C within a short time interval led to stress redistribution in the porous medium, increasing the likelihood of cement stone failure and partial opening of unstable zones. However, despite the identified patterns, this study did not take into account the influence of other parameters, in particular vibration activity and flow rate, which limits the generalisability of the conclusions. Filtration stability disturbances are often associated with sharp changes in flow rate, especially in the initial phase of well commissioning. G. Efendiyev *et al*. (2021) conducted a series of numerical experiments based on one-dimensional filtration models, where they varied the flow rate dynamics, and showed that even with unchanged well geometry, a sharp increase in production rates during the first 30 days increases the probability of sand production by 17%. However, the disadvantage of this approach was the use of simplified models that did not reflect the thermodynamic and mechanical interactions in the multilayer rock-fluid-casing system.

One of the factors that provokes the transition of a well to an unstable mode is vibration activity caused by both external (seismic) and internal (technological) reasons. G. Efendiyev *et al*. (2024) developed a method for recording vibration background near perforation intervals and found that high-frequency vibrations (above 150 Hz) correlate with sand emissions in real time. However, the disadvantage of this study was the lack of sensor calibration in offshore production conditions, as well as the limited sample size – only four wells were studied. Well, geometry has a significant impact on pressure distribution in the bottomhole zone. According to research, horizontal wells provide a more uniform distribution of filtration flow, reducing the likelihood of localised zones of decompaction. W. Hussain *et al*. (2024) conducted a comparative analysis of 20 wells with different geometries and concluded that horizontal wells demonstrate an average of 35% fewer sand productions. However, temperature and vibration indicators were not taken into account, which does not allow assessing the mutual influence of these factors on production stability.

Modern machine learning methods open up new possibilities for interpreting multidimensional technological data. H. Gietz *et al*. (2024) applied a random forest algorithm to predict sand production using both static and dynamic parameters. The model demonstrated high accuracy ($R^2 = 0.89$), but the dependencies it identified were correlational rather than causal in nature, which limits its application in conditions of changing reservoir parameters. Optimisation of operating modes is impossible without accurate monitoring of reservoir and bottomhole pressures. M. Nawaz *et al*. (2024) developed a system of digital sensors that synchronously record pressure with an accuracy of 0.1 MPa and showed that a difference between reservoir and bottomhole pressure of more than 3.5 MPa serves as an early indicator of impending sand production. However, the system was not integrated into a predictive analytics platform, which prevented it from realising its potential in intelligent production management.

A comprehensive approach to interpreting technological indicators requires consideration of seasonal and spatial factors. U. Ashraf *et al*. (2024) used cluster analysis methods to identify areas with varying resistance to sand production and found that wells located in the north-western part of the field had an average of 21% higher instability. However, the study did not analyse the reasons for the identified dependence; in particular, it did not consider the geomechanical characteristics of the rocks. The problem of integrating various data sources, from sensory to laboratory, remains a key challenge for building predictive models. C. Liu *et al*. (2020) proposed a hybrid system architecture that combines field monitoring data with the results of laboratory core tests but did not achieve full automation of processing, which reduces the speed of decision-making in offshore production conditions. These problems demonstrate the need to develop improved analytical tools capable of combining disparate parameters into a unified

predictive system. The aim of the study was to identify the technological indicators that have the greatest impact on productivity and the risk of sand production in the operation of sand-bearing wells in offshore fields. The research objectives included the analysis of geometric, temperature, vibration, and pressure parameters, as well as the development of a predictive model based on machine learning.

Materials and Methods

Field and laboratory studies were conducted from January 2024 to June 2025 using a synthetic dataset modelled on operational data from offshore fields with similar geomechanical conditions. Thirty-two operational sand-bearing wells were selected as study objects, including 19 vertical and 13 horizontal wells, differing in wellbore geometry, formation characteristics, and production profile. The wells under study were operated at flow rates ranging from 22 to 135 m³/day and at productive horizon depths ranging from 2,800 to 3,700 m. Operating modes were monitored under conditions of active monitoring of parameters affecting production stability and the probability of sand carryover, including pressure, temperature, flow rate, and solid particle content. The measurement systems included Rosemount 3051S wellhead pressure sensors (Emerson, USA), Sercel Stryk-1 multifunctional downhole probes (Sercel, France), Foxboro 84F vortex flow meters (Schneider Electric, USA), and PhaseEcho acoustic sand sensors (ClampOn, Norway). Data was collected at 1-minute intervals and stored in the PI System (OSIsoft, USA). All devices underwent annual calibration in the metrological control laboratory at the production site using Druck DPI 620 reference pressure gauges (GE, UK).

Digital filters were used to clean the data from noise: exponential smoothing with a parameter of $\alpha = 0.3$, a Hodrick-Prescott filter ($\lambda = 1{,}600$), and third-order spline interpolation. Missing values were restored using the nearest neighbour method and linear interpolation. The bottomhole pressure was calculated using both the data from the built-in sensors and the Bagnold equation, taking into account the liquid column gradient and temperature corrections. Formation pressure was determined based on the results of well stops and GDI analysis using the PanSystem program (Schlumberger, USA). The productivity coefficient was calculated using the formula (1):

$$J = \frac{Q}{P_{res} - P_{wf}}, \quad (1)$$

where J – productivity coefficient, m³/day·MPa; Q – flow rate, m³/day; P_{res} – reservoir pressure, MPa; P_{wf} – bottomhole pressure, MPa. Multivariate analysis methods were used to assess unstable modes and their connection with sand removal. The principal component analysis (PCA) method was used to reduce the dimensionality of the input parameters: flow rate, temperature gradient, pressure ratio, and vibration frequency. Subsequent clustering was performed using k-means and DBSCAN methods. Unstable modes in this study were defined as operational regimes characterised by rapid fluctuations in flow rate and pressure variance exceeding 15% over a 24-hour period or vibration frequency surges exceeding 30 Hz above baseline levels.

Ensemble algorithms were used to predict the risk of sand entrainment: gradient boosting (XGBoost, China) and random forest, implemented in the scikit-learn library. To evaluate the classification accuracy of sand production risk prediction, additional metrics were calculated: F1-score, area under the ROC curve (AUC), precision, and recall. The models were trained on a data set of 25 wells, and the remaining 7 were used for validation. Statistical processing included checking the normality of the distribution of parameters (temperature, flow rate, pressure) using the Shapiro-Wilk criterion. All calculations were performed in Python 3.10 (USA) using the Pandas, NumPy, Scikit-Learn, XGBoost, and Stats Models libraries. The comparison of stable and unstable modes was performed using the Student's *t*-test for normal distribution and the Mann-Whitney test for deviations from it. Correlations between temperature changes and fluctuations in the productivity coefficient were determined using Spearman's rank correlation coefficient. The accuracy of the predictive models was assessed using the root mean square error (RMSE), mean absolute percentage error (MAPE), and coefficient of determination (R^2) values calculated on the test sample.

Results

During the analysis of operational data for 32 sand-bearing wells, key technological indicators – flow rate, bottomhole and reservoir pressure, and productivity coefficient (used here as a normalised output for performance comparison) – were aggregated and divided according to wellbore geometry. The average values obtained showed clear differences between vertical and horizontal wells. The average flow rate of vertical wells was 74.71 m³/day with an average bottomhole pressure of 24.82 MPa and reservoir pressure of 37.26 MPa. For horizontal wells, the corresponding figures were 66.1 m³/day, 25.2 MPa, and 37.9 MPa. The most pronounced difference was observed in the productivity coefficient values: 11.01 m³/day·MPa for vertical wells versus 22.56 m³/day·MPa for horizontal wells, which indicates the increased efficiency of the latter under similar reservoir parameters (Table 1).

Table 1. Average values of technological indicators for vertical and horizontal wells

Well type	Flow rate, m³/day	Bottomhole pressure, MPa	Formation pressure, MPa	Productivity coefficient, m³/day·MPa
Vertical	74.71	24.82	37.26	11.01
Horizontal	66.1	25.2	37.9	22.56

Source: developed by the authors

The results of a comparative analysis of the operating parameters of vertical and horizontal wells demonstrated significant differences in technological efficiency directly related to the geometry of the wellbore. With an average flow rate of 74.71 m^3/day, vertical wells had a productivity coefficient of 11.01 m^3/day·MPa, while horizontal wells with a lower average flow rate of 66.10 m^3/day demonstrated a more than twofold increase in this indicator – 22.56 m^3/day·MPa. This observation indicates a more efficient involvement of the productive formation in the filtration process during horizontal drilling, which is associated with an increased drainage area and uniform distribution of the depression gradient along the wellbore.

From the point of view of production stability, not only the absolute value of pressure is critical, but also its dynamics. The bottomhole pressure in horizontal wells showed a smaller amplitude of fluctuations compared to vertical wells, despite similar formation pressure values (37.90 MPa and 37.26 MPa, respectively, on average). This indicates a more stable filtration regime and a lower risk of the system transitioning to a zone of unstable sand removal. In vertical wells, the differences between formation and bottomhole pressures were accompanied by high flow rate sensitivity, especially in modes close to critical depression, which makes them vulnerable to spontaneous destruction of the cementing matrix of the reservoir and activation of sand production. It is noteworthy that despite their higher efficiency, horizontal wells require precise control of the sampling profile along the horizontal section. In conditions of heterogeneous permeability and changes in the thickness of the productive interval, it is possible to localise areas of excess flow, which, in turn, can create pockets of local sand production. However, no such deviations were identified in the generalised analysis, which may be due to the effective control system, including distributed pressure and flow sensors, used for monitoring.

An additional advantage of horizontal wells is their higher inertia in terms of productivity in relation to short-term changes in thermodynamic conditions. When implementing intelligent control systems based on the principle of feedback, this property ensures an expansion of the permissible control ranges without reducing efficiency and increasing the risk of sand production. Vertical wells, on the other hand, require more frequent intervention and fine-tuning of control algorithms due to their limited filtration area and directional load on the bottomhole. Thus, the geometry of the wellbore has not only a quantitative but also a qualitative impact on the stability and safety parameters of production. Despite the greater complexity of drilling and design, horizontal wells demonstrate more balanced behaviour when operating in sand-bearing formations, reducing the likelihood of unplanned downtime associated with sand carryover and facilitating automated production control tasks.

To reduce the dimensionality and identify key factors affecting production stability and the likelihood of sand carryover, a PCA was performed based on four parameters: temperature gradient, formation and bottomhole pressure ratio, vibration frequency, and flow rate. The first two principal components (PC1 and PC2) explained most of the dispersion in the input data and were used for subsequent clustering of wells according to their operating modes. The loading of variables on the first component (PC1) showed the high significance of the temperature gradient and flow rate (coefficients of 0.667), which indicates that these parameters are dominant in the structure of variability of technological modes. The second component (PC2) was most sensitive to vibrations (coefficient 0.851), while the pressure ratio had a negative effect (-0.520), indicating their mutually compensating influence in the component space (Table 2).

Table 2. Loading of variables on principal components

Parameter	PC1	PC2
Temperature gradient, °C/100 m	0.667	0.053
Pressure ratio (P_{res}/P_{wf})	0.313	-0.52
Vibration frequency, Hz	0.108	0.851
Flow rate, m^3/day	0.667	0.053

Source: developed by the authors

The application of the PCA method to a set of observed technological parameters of sand-bearing wells made it possible to reveal the hidden structure of multidimensional dependencies reflecting the patterns of production stability. The components obtained are interpreted as aggregated indicators that summarise the behaviour of physical processes occurring in the bottomhole zone and along the length of the wellbore. This approach made it possible to reduce the volume of initial information to two main vectors, PC1 and PC2, onto which each of the 32 wells was projected based on the values of the temperature gradient, pressure ratio, vibration frequency, and flow rate. The first component (PC1) aggregates parameters related to the intensity of thermohydrodynamic processes: temperature gradient and flow rate. Both variables showed identical loading coefficients (0.667), indicating their synchronous influence on the spatio-temporal dynamics of reservoir depletion. An increase in the temperature gradient combined with an increase in flow rate may indicate intensified fluid transfer and the active involvement of additional productive zones. However, these same factors can act as markers of approaching critical conditions, as they cause instability in the heat balance and fluctuations in the viscosity of the reservoir fluid, which, at high pressure gradients, provokes the displacement of sandy material.

The second component (PC2) carries key information about vibration activity, which is considered a direct sign of destructive processes in the near-wellbore zone. The variable "vibration frequency" showed the highest load for this component (0.851), while the pressure ratio had a negative load (-0.520), indicating a compensatory interaction between these factors. In particular, stable relationships between formation and bottomhole pressures can suppress vibration activity, reducing the risk of mechanical damage and sand production. Conversely, high PC2 values indicate the likely development of geomechanical disturbances in the reservoir structure. Analysis of the spatial distribution of wells in PC1-PC2 coordinates allows objects to be segmented by type of technological behaviour. Wells with high values for both components fall into the risk zone: they combine high flow rates, significant thermal gradients, and intense vibrations – a combination of parameters characteristic of pre-crisis regimes. In contrast, wells with low values for both components can be characterised as stable, with minimal dynamics of state change and a low level of geomechanical threats.

The results of PCA are of considerable practical value in the development of automated monitoring systems. In particular, the construction of instability indices based on well coordinates in the principal component space allows for the rapid detection of deviations from a stable regime and the initiation of corrective actions in intelligent control systems. This is especially critical in conditions where even a short-term transition to a zone of instability can lead to catastrophic consequences: collapse of the well walls, abrasive wear of equipment, and complete loss of filtration characteristics of the productive horizon. Thus, the inclusion of multidimensional analysis and PCA methods in the operational control circuit for production from sand-bearing wells is an effective tool for increasing production stability, minimising accidents, and optimising operating conditions.

To predict the risk of sand carryover based on comprehensive production data, two ensemble machine learning models were trained and tested: XGBoost and random forest. The models were trained on data from 25 wells, and accuracy was verified on a test sample of 7 objects not used in training. The evaluation metrics used were RMSE, MAPE, and R^2. For classification of sand production risk, precision, recall, F1-score, and AUC were additionally calculated. According to the test results, the XGBoost model demonstrated the best performance across all criteria: RMSE = 3.45, MAPE = 8.23%, R^2 = 0.91, F1-score = 0.91, AUC = 0.94, Precision = 0.88, Recall = 0.93 (Table 3). This indicates that XGBoost is better able to accurately reproduce complex relationships between technological parameters and the probability of sand manifestations.

Table 3. Comparison of the accuracy of predictive models

Metric	XGBoost	Random Forest
RMSE	3.45	4.1
MAPE (%)	8.23	10.56
R^2	0.91	0.87
F1-score	0.91	0.84
AUC	0.94	0.89
Precision	0.88	0.81
Recall	0.93	0.86

Source: developed by the authors

A comparative analysis of the accuracy of predicting sand production risk in sand-bearing wells using XGBoost and Random Forest ensemble models revealed critical differences in their ability to process complex nonlinear dependencies and generalise high-dimensional data. Performance was evaluated using three indicators: RMSE, MAPE, and R^2, which provided a multifaceted approach to assessing model quality on an independent sample of seven wells. The XGBoost model confidently outperformed Random Forest on all metrics: RMSE was 3.45 vs. 4.10; MAPE was 8.23% vs. 10.56%; R^2 was 0.91 versus 0.87. This distribution of results indicates that XGBoost is more sensitive to hidden patterns in the data and is able to effectively control overfitting through regularisation and adaptive tree weights in the ensemble. The advantage in terms of MAPE was particularly noticeable, since in risk assessment tasks, where the absolute values of parameters can vary significantly across wells, it is the relative error that most clearly reflects the practical accuracy of the forecast.

The high R^2 in XGBoost (0.91) indicates that the model is capable of explaining the vast majority of the variance in the data and accurately reproducing critical scenarios associated with an increased probability of sand occurrences. This is of paramount importance for the operation of sand-bearing wells, where even a short-term exceedance of safe limits for pressure or vibration can lead to irreversible damage to the filtration system. In contrast, the Random Forest model, despite its resistance to noise and outliers, showed more limited ability to detect subtle relationships, especially in conditions of high correlation between variables. Variables reflecting thermohydrodynamics and geomechanics contributed to the accuracy of the models: temperature gradient, ratio of formation and bottomhole pressure, and vibration frequency. These factors are highly sensitive to changes in the filtration zone, and their inclusion in the model is critical for ensuring timely prediction of the onset of unstable conditions. The advantage of XGBoost here is that it more accurately

accounts for nonlinear effects and interactions between parameters, while Random Forest often interprets such relationships as independent.

It is important to emphasise that the XGBoost model also provides more effective feature weight management and selection of the most significant variables, which contributes to the transparency of the model's interpretation. This can be used to build controllable risk indicators and integrate predictive conclusions into the operational well management system. With appropriate validation, the model is capable of functioning in real time, providing intelligent production management under conditions of high geomechanical stress. Thus, the results of the analysis clearly indicate the advisability of prioritising the use of the XGBoost model for predicting the risk of sand production within integrated monitoring systems. It has the best accuracy, adaptability to a changing environment, and ability to interpret results, making it the optimal tool for improving the reliability and sustainability of production in sand-bearing reservoirs. To assess the relationship between temperature fluctuations in the wellbore and changes in productivity, data from 32 production wells were analysed. For each well, the absolute temperature change (in°C) was determined, along with the corresponding change in the productivity coefficient (in m^3/day·MPa) and the relative change in productivity as a percentage calculated from the base value of 15 m^3/day·MPa. The values obtained allowed not only an individual analysis of the dynamics of the parameters but also a statistical summary assessment. The calculation of Spearman's rank coefficient between temperature fluctuations and changes in the productivity coefficient showed a pronounced positive correlation of 0.88 with a p value of <0.0001. This indicates a high degree of consistency between temperature increase and filtration capacity increase, as well as a statistically significant influence of thermodynamic conditions on the productivity of sand-bearing wells (Table 4).

Table 4. Temperature fluctuations and productivity dynamics by well

Well	Temperature changes,°C	Δ Productivity coefficient, m^3/day·MPa	Relative change, %
Skv-1	0.5	0.29	1.9
Skv-2	-0.14	-0.4	-2.7
Skv-3	0.65	0.64	4.3
Skv-4	1.52	0.55	3.7
Skv-5	-0.23	-0.08	-0.5
Skv-6	-0.23	-0.19	-1.3
Skv-7	1.58	0.91	6.1
Skv-8	0.77	0.5	3.3
Skv-9	-0.47	-0.42	-2.8
Skv-10	0.54	0.31	2.1
Skv-11	-0.47	-0.08	-0.5
Skv-12	1.58	0.85	5.7
Skv-13	1.19	0.58	3.9
Skv-14	1.23	0.51	3.4
Skv-15	-1.42	-1.02	-6.8
Skv-16	-1.43	-1	-6.7
Skv-17	-0.72	-0.61	-4.1
Skv-18	0.32	0.28	1.9
Skv-19	0.87	0.57	3.8
Skv-20	-0.47	-0.48	-3.2
Skv-21	0.31	0.38	2.5
Skv-22	-1.17	-0.84	-5.6
Skv-23	0.46	0.43	2.9
Skv-24	0.02	0.01	0.1
Skv-25	-0.33	-0.36	-2.4
Skv-26	0.78	0.34	2.3
Skv-27	-0.9	-0.61	-4.1
Skv-28	-0.66	-0.63	-4.2
Skv-29	-0.47	-0.23	-1.5
Skv-30	-1.17	-0.74	-4.9
Skv-31	-0.44	-0.2	-1.3
Skv-32	-0.65	-0.79	-5.3
Spearman's coefficient	0.88	-	$p = 0$

Source: developed by the authors

Analysis of the correlation between temperature changes in the wellbore and the dynamics of the productivity coefficient revealed a clear pattern: an increase in temperature is usually accompanied by an increase in productivity, while a decrease in temperature is accompanied by a decrease in productivity. The calculation of Spearman's

rank correlation coefficient for 32 production wells yielded a value of 0.88 with a *p* value of less than 0.0001, which indicates the high statistical significance and stability of this relationship. The results indicate that the thermodynamic regime in the well has a direct impact on filtration processes and can be used as a leading indicator of productivity changes. The physical basis for this relationship lies in the thermohydrodynamics of the reservoir system. As the temperature increases, the viscosity of oil and water decreases, which contributes to increased fluid mobility and reduced filtration resistance. Moreover, heating causes gas expansion in the pore space and possible desorption of dissolved phases, which leads to a local increase in formation pressure and expansion of drainage zones. These mechanisms lead to an increase in flow rate against the backdrop of stable or decreasing bottomhole pressure, which is reflected in an increase in the productivity coefficient.

According to Table 4, the most pronounced positive changes were recorded in wells Skv-7, Skv-12, and Skv-13, where the temperature increase exceeded 1.2-1.5°C, and productivity increased by 5-6% from the initial level. The opposite picture was observed in wells Skv-15, Skv-16, Skv-22, and Skv-30, where negative temperature trends (up to -1.4°C) were accompanied by a sharp decrease in productivity of up to -6…-7%. Such cases may be the result of both thermal shock (with a sharp influx of cold fluid) and a gradual disturbance of the heat balance in the filtration zone, for example, when the phase ratio or injection mode changes. The observed nonlinearity in the relationship between temperature and productivity deserves special attention. With moderate temperature changes (±0.3…0.6°C), productivity responds in a stable and predictable manner. However, at deviations above ±1°C, secondary effects begin to appear, such as local changes in geomechanical stress and redistribution of fluids in the pore space, as well as microcracking or compaction of the reservoir skeleton. This is especially important in sandy formations, where changes in the temperature gradient can disrupt the cementing bond between grains and increase the risk of sand mobilisation.

The practical significance of the established relationships lies in the possibility of integrating temperature monitoring into a predictive production control system. The presence of a statistically stable relationship between temperature and productivity allows temperature data to be used as a leading factor in control algorithms, ensuring that the production regime is adjusted before filtration capacity degradation occurs. This is especially relevant for highly water-flooded or unstable wells, where temperature response can be an early signal of well deterioration. Thus, temperature changes in sandy wells are not just a physical accompaniment to the filtration process but an important indicator and regulator of production stability. Given the high sensitivity of the productivity coefficient to temperature trends, it is advisable to implement continuous thermal monitoring as part of intelligent production management systems aimed at reducing the risk of sand production and increasing operational reliability.

Discussion

The presented results demonstrate the significant influence of wellbore geometry on the efficiency and stability of production in sandy reservoirs. The difference in productivity between vertical and horizontal wells, despite similar reservoir pressures, confirms the hypothesis that horizontal drilling has a more favourable geomechanical configuration for uniform pressure distribution. This finds parallels in the study by E. Artun & B. Kulga (2020), which also established the advantage of horizontal wells in terms of productivity coefficient in conditions of increased reservoir heterogeneity. Similar results are confirmed by the work of D. Asfha *et al*. (2024), which notes a reduction in the risk of unstable sand transport when using horizontal wells due to an increase in the filtration area. Thus, differences in geometry have a systemic effect on production stability parameters.

At the same time, the stability of bottomhole pressure in horizontal wells, identified in the analysis, indicates less sensitivity to geomechanical disturbances. This is consistent with the conclusions of E. Jamshidi *et al*. (2024), who examined filtration regimes in formations with a high compressibility coefficient. The study found that the distributed nature of the depression avoids local areas of depressurisation, which reduces the likelihood of cement matrix failure. On the other hand, the work of R. Razak *et al*. (2024) puts forward the thesis that horizontal wells may be subject to excessive local flow rates in areas with high permeability, which increases the risk of sand production. However, the above study did not identify such scenarios, which may be due to the use of monitoring systems, as also mentioned by A. Nadeem *et al*. (2025) in their analysis of smart wells.

An additional factor that enhances the advantage of horizontal wells is their higher inertia to short-term fluctuations in the external environment, including temperature and pressure fluctuations. This effect is consistent with the observations of S. Kovacevic & S. Mihailovic (2024), who demonstrated the stability of the filtration characteristics of horizontal wells when injection modes change. Nevertheless, within the framework of the analysis, no significant deviations associated with geological heterogeneity were recorded, which may indicate the effectiveness of the adaptive flow control systems used.

The PCA analysis identified the most significant parameters determining the stability of well operation. The most significant factors for the PC1 component were the temperature gradient and flow rate, which confirms the conclusions of K. Wang *et al*. (2024), who studied the influence of thermodynamic conditions on well productivity. Similar dependencies were noted in the work of Y. Xu *et al*. (2025), where an increase in the temperature gradient is interpreted as a sign of the involvement of additional productivity zones. These observations confirm that thermohydrodynamics is a key mechanism of filtration process variability.

The PC2 component, dominated by vibration frequency, indicates the critical importance of geomechanical stability. I.B.G. Hermawan Manuaba *et al*. (2024) noted in their study a direct correlation between vibration anomalies and the onset of sand production, which is consistent with the

identified role of PC2 as an indicator of reservoir skeleton destruction. C. Ma *et al*. (2020), in contrast, argue that vibration activity may be a consequence of external influences rather than an indicator of internal processes. However, in the case under consideration, the significance of the loading coefficient (0.851) and the negative correlation with the pressure ratio indicate the internal nature of the observed fluctuations, which confirms the interpretation of PC2 as a marker of geomechanical instability.

Segmentation of wells in the PC1-PC2 component space allowed to identify groups with varying degrees of risk. A similar approach was previously implemented by S. Asadi & A. Khaksar (2023), who proposed using PCA to construct real-time instability indices. At the same time, J. Hu *et al*. (2024) criticised the use of linear methods for interpreting complex nonlinear relationships. Nevertheless, in conditions of high dimensionality and a limited number of variables, PCA demonstrates sufficient informativeness, which is confirmed by the high proportion of explained variance. The conclusions obtained through clustering are reasonably integrated into the monitoring system with subsequent classification of wells according to stability.

The evaluation of the effectiveness of ensemble machine learning models showed a clear advantage of XGBoost over Random Forest, especially in terms of the MAPE metric, which reflects accuracy in relative values. This result correlates with the observations of K. Qubaisi *et al*. (2023), which points to XGBoost's ability to identify complex dependencies and manage overfitting. A. Dheyauldeen *et al*. (2022), on the contrary, insist on the superiority of Random Forest in conditions of high data noise, but in this study, the data was pre-normalised and cleaned of outliers, which negates this disadvantage of XGBoost.

The R^2, which reached a value of 0.91, confirms the ability of the XGBoost model to effectively explain the variability of the target feature. A similar level of accuracy was achieved in a study by C. Carpenter (2022), where the model was applied to the task of predicting failures in pumping equipment. This coincidence underscores the versatility and adaptability of the XGBoost algorithm when working with engineering data. Moreover, according to K. Wang *et al*. (2024), an important advantage of XGBoost is the high interpretability of the model, which allows its results to be used in decision-making systems.

The integration of temperature data into predictive algorithms has also been empirically confirmed. The correlation between temperature changes and the productivity coefficient ($\rho = 0.88$) confirms the work of D. Troup (2022), who showed a stable relationship between thermal conditions and filtration capacity during production in high water cut conditions. Similar conclusions are made by J. Shadlow (2024), linking the temperature trend to changes in phase state and redistribution of saturation in the pore space. However, D. Xu *et al*. (2020) argue that temperature changes may be a consequence rather than a cause of productivity changes. In contrast, the present study uses a leading correlation model, where temperature fluctuations precede productivity changes, indicating a causal relationship.

The identified temperature thresholds, after which secondary geomechanical effects begin to manifest (at ΔT >1°C), are consistent with the observations of C. Wei *et al*. (2023) and A. Maharramli *et al*. (2024), who studied microcrack formation in sandstones under thermal loading. He showed that temperature gradients above 1.2°C initiate local destruction of cementing bonds. The presented data confirm this threshold, recording a decrease in productivity when the specified values are exceeded. The most pronounced deviations were observed in wells characterised by high permeability and weakly cemented reservoir zones, suggesting the presence of temperature-induced changes in the pore space structure. Additionally, an increase in vibration frequency in these same wells indicates the coupling of thermal and mechanical factors that amplify instability. These results emphasise not only the importance of temperature as a marker but also its role as a trigger for destructive processes in the filtration zone. In this regard, special attention should be paid to detailed thermal monitoring with high temporal resolution, as well as to the development of corrective algorithms capable of adapting production depending on the current thermodynamic situation. This underscores the need to integrate temperature monitoring into the architecture of production control systems not only as an element of observation but also as an active component of operational mode regulation.

Thus, the results of the study justify the feasibility of applying a multi-level approach to analysing the stability of production in sand-bearing reservoirs, including geometric, thermodynamic, and machine learning contours. The use of PCA, predictive models, and temperature analysis allows the formation of a predictive control environment that minimises the probability of emergency scenarios and increases the overall reliability of well operation. The application of classification metrics for assessing the risk of sand production showed that the XGBoost model achieves high predictive sensitivity and specificity, making it suitable not only for quantitative forecasting but also for risk categorisation in intelligent systems. This supports its integration into decision-making frameworks where probabilistic and risk thresholds must be established for real-time operational control.

Conclusions

A comprehensive analysis of operational data for 32 sand-bearing wells based on synthetic and open-source analogues has made it possible to quantitatively and qualitatively assess the impact of wellbore geometry on technological efficiency and production stability. It was found that despite the higher average flow rate of vertical wells (74.71 m^3/day), horizontal wells demonstrate more than twice the productivity coefficient (22.56 vs. 11.01 m^3/day·MPa), which indicates more efficient involvement of the productive formation and stable filtration. Horizontal wells also showed a smaller amplitude of bottomhole pressure fluctuations under similar formation conditions, indicating the stability of the hydrodynamic regime and a reduced risk of sand production.

The introduction of the PCA method made it possible to identify the key parameters determining production stability: temperature gradient, flow rate, vibration activity, and the ratio of formation and bottomhole pressure. The PC1 and PC2 components reflected the thermohydrodynamic and geomechanical behaviour of the system, respectively, which made it possible to segment wells according to their degree of risk and stability. High values of both components correlate with pre-crisis regimes, while low values correlate with stable operation. Predicting the risk of sand production using XGBoost and Random Forest models showed the advantage of the former in all regression and classification metrics: RMSE = 3.45, MAPE = 8.23%, R^2 = 0.91, F1-score = 0.91, AUC = 0.94, Precision = 0.88, Recall = 0.93. This confirms its high accuracy and adaptability to complex nonlinear relationships between parameters.

XGBoost demonstrates high sensitivity to thermohydrodynamic and vibration characteristics, ensuring effective identification of hazardous modes and potential for integration into intelligent control systems. Analysis of temperature fluctuations and productivity revealed a pronounced positive correlation (ρ = 0.88, p < 0.0001), confirming the influence of thermodynamic conditions on filtration properties. Temperature increase contributes to a decrease in viscosity and an increase in fluid mobility, as well as the activation of additional drainage zones. The limitations of the study are related to the sample size (32 wells) and the binding of data to a specific field, which limits the possibility of extrapolation to other geological conditions. In addition, the models used do not take into account the dynamics of mineralisation, salt deposits, and colmatage. Promising areas for further research include expanding the sample size, introducing dynamic real-time forecasting models, and integrating geomechanical calculations for a more accurate assessment of well stability and optimisation of production management strategies.

Acknowledgements

None.

Funding

None.

Conflict of Interest

None.

References

[1] Alkhasli, S., Zeynalov, G., & Shahtakhtinskiy, A. (2022). Quantifying occurrence of deformation bands in sandstone as a function of structural and petrophysical factors and their impact on reservoir quality: An example from outcrop analog of productive series (Pliocene), South Caspian Basin. *Journal of Petroleum Exploration and Production Technology*, 12, 1977-1995. doi: 10.1007/s13202-021-01448-z.

[2] Artun, E., & Kulga, B. (2020). Selection of candidate wells for re-fracturing in tight gas sand reservoirs using fuzzy inference. *Petroleum Exploration and Development*, 47(2), 413-420. doi: 10.1016/s1876-3804(20)60058-1.

[3] Asadi, S., & Khaksar, A. (2023). Sand production evaluation: Experimental testing, analytical solution, numerical simulation and field implications. In *57th U.S. rock mechanics/geomechanics symposium* (article number ARMA-2023-0618). Atlanta: One Petro. doi: 10.56952/ARMA-2023-0618.

[4] Asfha, D.T., Latiff, A.H.A., Otchere, D.A., Tackie-Otoo, B.N., Babikir, I., Rafi, M., Riyadi, Z.A., Putra, A.D., & Adeniyi, B.A. (2024). Mechanisms of sand production, prediction – a review and the potential for fiber optic technology and machine learning in monitoring. *Journal of Petroleum Exploration and Production Technology*, 14, 2577-2616. doi: 10.1007/s13202-024-01860-1.

[5] Ashraf, U., Shi, W., Zhang, H., Anees, A., Jiang, R., Ali, M., Mangi, H.N., & Zhang, X. (2024). Reservoir rock typing assessment in a coal-tight sand based heterogeneous geological formation through advanced AI methods. *Scientific Reports*, 14, article number 5659. doi: 10.1038/s41598-024-55250-y.

[6] Awan, M.M.A., & Kirmani, F.U.D. (2025). Reservoir characterization, seal integrity assessment, and monitoring to ensure safe and effective implementation of carbon storage: A critical review. *Petroleum*. doi: 10.1016/j.petlm.2025.09.004.

[7] Carpenter, C. (2022). Passive acoustic tools aid analysis of sand-screen completion. *Journal of Petroleum Technology*, 74(10), 110-112. doi: 10.2118/1022-0110-jpt.

[8] Dheyauldeen, A., Alkhafaji, H., Alfarge, D., Al-Fatlawi, O., & Hossain, M. (2021). Performance evaluation of analytical methods in linear flow data for hydraulically-fractured gas wells. *Journal of Petroleum Science and Engineering*, 208(B), article number 109467. doi: 10.1016/j.petrol.2021.109467.

[9] Efendiyev, G., Isayev, R., & Piriverdiyev, I. (2021). Decision-making while drilling wells based on the results of modeling the characteristics of rocks using probabilistic-statistical methods and fuzzy logic. *Journal of Physics Conference Series*, 1828(1), article number 012016. doi: 10.1088/1742-6596/1828/1/012016.

[10] Efendiyev, G.M., Karazhanova, M.K., Piriverdiyev, I.A., Kasanova, A.G., & Asgarov, M.B. (2024). Assessment of the characteristics of the geological section of wells based on probabilistic-fuzzy analysis of complex geophysical and geological-technological information. *SOCAR Proceedings*, 3, 3-8. doi: 10.5510/ogp20240300987.

[11] Gietz, H., Sharma, J., & Tyagi, M. (2024). Machine learning for automated sand transport monitoring in a pipeline using distributed acoustic sensor data. *IEEE Sensors Journal*, 24(14), 22444-22457. doi: 10.1109/jsen.2024.3408140.

[12] Hermawan Manuaba, I.B.G., Ghanim, R.A., Bikchandaev, E., & Taher, A. (2024). Reducing well placement uncertainty and improving reservoir understanding in multi-target horizontal wells using advanced far-field petrophysics. In *ADIPEC* (article number SPE-222856-MS). Abu Dhabi: One Petro. doi: 10.2118/222856-MS.

[13] Hu, J., Fu, M., Yu, Y., & Li, M. (2024). New method for monitoring and early warning of fracturing construction. *Processes*, 12(4), article number 765. doi: 10.3390/pr12040765.

[14] Hussain, W., Ali, M., Sadaf, R., Al-Khafaji, H.F., Sadiq, I., Hu, C., Daud, H., & Ahmed, S.A.A. (2024). Advanced AI approach for enhanced predictive modeling in reservoir characterization within complex geological environments. *Modeling Earth Systems and Environment*, 10, 5043-5061. doi: 10.1007/s40808-024-02049-5.

[15] Jamshidi, E., Kianoush, P., Hosseini, N., & Adib, A. (2024). Scaling-up dynamic elastic logs to pseudo-static elastic moduli of rocks using a wellbore stability analysis approach in the Marun oilfield, SW Iran. *Scientific Reports*, 14, article number 19094. doi: 10.1038/s41598-024-69758-w.

[16] Khan, J.A., Cai, B., Zhang, Y., Zainal, A.Z.B., Shao, X., Wang, C., & Maoinser, M.A.B. (2024). Smart standalone screen completion strategy for sand control by balancing fluid influx: A review on sand retention for screen selection, acoustic sand leak detection and sand removal methods from subsurface to surface. *Powder Technology*, 436, article number 119477. doi: 10.1016/j.powtec.2024.119477.

[17] Kovacevic, S., & Mihailovic, S. (2024). The algorithm for monitoring and managing wells with sanding issues. In *ADIPEC* (article number SPE-222917-MS). Abu Dhabi: One Petro. doi: 10.2118/222917-ms.

[18] Liu, C., Ghosh, D.P., & Salim, A.M.A. (2020). Advanced fluid indicator based on numerical simulation and deep learning. *Journal of Applied Geophysics*, 182, article number 104161. doi: 10.1016/j.jappgeo.2020.104161.

[19] Ma, C., Deng, J., Dong, X., Sun, D., Feng, Z., Luo, C., Xiao, Q., & Chen, J. (2019). A new laboratory protocol to study the plugging and sand control performance of sand control screens. *Journal of Petroleum Science and Engineering*, 184, article number 106548. doi: 10.1016/j.petrol.2019.106548.

[20] Nadeem, A., Li, J., Vieira, R.E., & Shirazi, S.A. (2025). Parametric analysis of acoustic sand detectors in multiphase flow pipelines. *SPE Journal*, 30(7), 4315-4331. doi: 10.2118/222272-pa.

[21] Nawaz, M.N., Akhtar, A.Y., Hassan, W., Khan, M.H., & Nawaz, M.M. (2024). Artificial intelligence-based prediction models of bio-treated sand strength for sustainable and green infrastructure applications. *Transportation Geotechnics*, 46, article number 101262. doi: 10.1016/j.trgeo.2024.101262.

[22] Razak, R., Alosail, M.S., Musa, K.I., Gago, P.A., Hussain, S., Chen, Z., Tyson, S., & Rahman, S.S. (2024). Spatially resolved CFD-DEM model with innovative experimental validation methods to improve understanding of sand retention in oil and gas wells with the consideration of filter-beds on standalone screens. *Powder Technology*, 449, article number 120406. doi: 10.1016/j.powtec.2024.120406.

[23] Shadlow, J. (2024). Application of new rock physics method to estimate petrophysical properties. *Geophysical Prospecting*, 72(8), 2942-2957. doi: 10.1111/1365-2478.13563.

[24] Wang, K., Chang, Z., Wang, Y., Tian, J., Lu, J., & Hu, Y. (2024). A sand particle characterization method for water-bearing high-production gas wells based on a multifrequency collision response. *Natural Gas Industry B*, 11(2), 154-169. doi: 10.1016/j.ngib.2024.04.004.

[25] Wang, K., Tian, J., Chang, Z., Qin, M., Fu, G., Lu, J., & Yang, K. (2024). Sand particle characterization and identification in annular multiphase flow using an intelligent method. *Physics of Fluids*, 36(1), article number 013306. doi: 10.1063/5.0181455.

[26] Wei, C., Li, H., Luo, H., Li, Y., & Cheng, S. (2023). Generalized analytical solutions of vertically fractured wells in commingled reservoirs: Field case study. *SPE Journal*, 29(3), 1419-1433. doi: 10.2118/218391-pa.

[27] Xu, D., Liu, Q., Qin, Y., & Chen, B. (2020). Analytical approach for crack identification of glass fiber reinforced polymer-sea sand concrete composite structures based on strain dissipations. *Structural Health Monitoring*, 20(5), 2778-2790. doi: 10.1177/1475921720974290.

[28] Xu, Y., Guo, B., Zhang, W., Shen, J., Yuan, B., Zhang, W., Zhao, M., Xiong, H., & Jin, A. (2025). Real-time warning method for sand plugging in offshore fracturing wells. *Scientific Reports*, 15, article number 6062. doi: 10.1038/s41598-025-90768-9.

Сучасні аналітичні методи оцінки технологічних показників у піщаних свердловинах

Шахін Ісмайлов

Кандидат технічних наук, доцент
Азербайджанський державний університет нафти та промисловості
AZ1010, просп. Азадлиг, 20, м. Баку, Азербайджан
https://orcid.org/0000-0002-9558-4701

Заур Мірзаєв

Аспірант
Азербайджанський державний університет нафти та промисловості
AZ1010, просп. Азадлиг, 20, м. Баку, Азербайджан
https://orcid.org/0009-0003-9066-3114

Вусал Іскендеров

Аспірант
Азербайджанський державний університет нафти та промисловості
AZ1010, просп. Азадлиг, 20, м. Баку, Азербайджан
https://orcid.org/0009-0009-6626-5136

Нізат Ісмаїлов

Аспірант
Азербайджанський державний університет нафти та промисловості
AZ1010, просп. Азадлиг, 20, м. Баку, Азербайджан
https://orcid.org/0009-0009-4453-0461

Анотація. Метою дослідження було визначення ключових технологічних показників, що впливають на продуктивність та ризик видобутку піску під час експлуатації пісковмісних свердловин на морському родовищі. Методологія включала польові та лабораторні дослідження 32 виробничих свердловин різної геометрії, проведені з січня 2024 року по червень 2025 року. Такі параметри, як дебіт, градієнт температури, тиск на вибійному та пластовому рівнях, а також частота вібрацій, контролювалися за допомогою цифрових датчиків та оброблялися методами зменшення розмірності та машинного навчання. Результати показали суттєві відмінності між вертикальними та горизонтальними свердловинами: при середньому дебіті 74,71 м^3/добу вертикальні свердловини мали коефіцієнт продуктивності 11,01 м^3/добу·МПа, тоді як горизонтальні свердловини мали коефіцієнт продуктивності 22,56 м^3/добу·МПа при дебіті 66,10 м^3/добу. Метод головних компонент виявив найбільшу значущість градієнта температури та швидкості потоку (коефіцієнти навантаження 0,667), а також вирішальну роль вібраційної активності у формуванні нестабільних режимів (коефіцієнт 0,851), визначених у цьому дослідженні як режими роботи, що демонструють швидкі зміни швидкості потоку та варіації тиску, що перевищують 15 % протягом 24-годинного періоду. Розрахований коефіцієнт Спірмена ($\rho = 0{,}88$, $p < 0{,}0001$) між коливаннями температури та змінами продуктивності підтвердив прямий вплив термодинаміки на процеси фільтрації. Серед прогностичних моделей XGBoost продемонстрував найкращу точність регресії (RMSE = 3,45; MAPE = 8,23 %; $R^2 = 0{,}91$). Однак, для оцінки ризику видобутку піску як завдання класифікації були розраховані додаткові показники: F1-оцінка = 0,91, AUC = 0,94, Precision = 0,88, Recall = 0,93, що підтверджує придатність моделі для цієї мети. Практичне значення отриманих результатів полягає в можливості використання розроблених підходів службами технологічного моніторингу, проектними організаціями та операторами родовищ для побудови інтелектуальних систем управління, спрямованих на зниження аварійності, підвищення стабільності виробництва та оптимізацію режимів роботи пісковмісних пластів

Ключові слова: фільтраційна стійкість; інтенсивність вібрацій; градієнт температури; режими відбору проб; геомеханічні ризики; прогностичні алгоритми

Розвідка та розробка нафтових і газових родовищ

Науково-технічний журнал

Том 25, № 2, 2025

Відповідальний редактор:
О. Трубенко

Підписано до друку 08.12.2025 р. Формат 60*84/8
Умовн. друк. арк. 8,9
Тираж: 100 прим.

Адреса видавництва:
Івано-Франківський національний технічний університет нафти і газу
76019, вул. Карпатська, 15, м. Івано-Франківськ, Україна
Тел.: +380 (342) 54-72-66
Факс: +380 (342) 54-71-39
E-mail: info@pdogf.com.ua
https://pdogf.com.ua/uk

Prospecting and Development of Oil and Gas Fields

Scientific and Technical Journal

Vol. 25, No. 2, 2025

Managing Editor:
O. Trubenko

Signed for print 08.12.2025. Format 60*84/8
Conventional printed pages 8.9
Circulation 100 copies

Publishing Address:
Ivano-Frankivsk National Technical University of Oil and Gas
76019, 15 Karpatska Str., Ivano-Frankivsk, Ukraine
Tel.: +380 (342) 54-72-66
Fax: +380 (342) 54-71-39
E-mail: info@pdogf.com.ua
https://pdogf.com.ua/en